# Genetic Analysis of Innate Immunity and Its Contribution to Disease Resistance in the Brassicaceae Family

**Hicret Aslı YALÇIN**

Thesis submitted to the University of East Anglia for the degree of Doctor of Philosophy

John Innes Centre

July 2020

© This copy of the thesis has been supplied on condition that anyone who consults it is understood to recognise that its copyright rests with the author and that use of any information derived there-from must be in accordance with current UK Copyright Law. In addition, any quotation or extract must include full attribution.

***Abstract***

Brassicas are important crops susceptible to significant losses caused by disease. Breeding resistant lines can mitigate the effects of pathogens. The first layer of active defence in plants is based on the perception of pathogen- (or microbe-) associated molecular patterns (PAMPs/MAMPs) leading to PAMP-triggered immunity (PTI). In this study I studied the response to various PAMPs including Necrosis & Ethylene-inducing peptide 1-like proteins (NLPs) in 3 different plant species from Brassicaceae.

This PhD research investigates the immune system of Brassicas in different aspects, and how it is contributing to quantitative disease resistance (QDR). I developed a segregating population from a cross between two NLP responsive and non-responsive *Brassica napus* accessions and revealed that recognition of NLP induces the resistance against *Botrytis cinerea. In silico* mapping of the region associated with NLP-recognition on *B. napus* genome was accomplished with an improved BSA pipeline and the most significant peak was identified on chromosome A04 spread over a 2.5Mbp region. KASP markers were designed and tested on $F_2$ individuals of the BSA population to narrow down the region and to reduce the number of the candidate genes. I identified 4 KASP markers tightly linked to the phenotype. I also genetically mapped the locus responsible for high NLP-induced ROS burst, and show that *BnaBSK1.A01* is involved in modulating the NLP response, and further supported by functional tests of the gene in *A. thaliana*.

The genetic tolerance under drought stress conditions is another agronomically important trait for the changing climate conditions in the world. The effect of environmental conditions, including drought stress, on the PTI responses of the plants observed quite a lot during the study. To investigate the effect of abiotic stress conditions, I optimised reproducible drought stress conditions to enable further mapping of induced QTL on *Brassica oleracea* genome and design and RNA-Seq experiment to reveal underlying genes. As a result, I showed that drought stress induces both PTI and disease resistance against *B. cinerea* in *B. oleracea*. The work will provide new insight into crop improvement, enabling more reliable QDR for controlling Brassica diseases to be developed.

***Table of contents***

*“I send you as sparks,*
*you should come back as flames.”*

*Mustafa Kemal ATATÜRK*

***Acknowledgement***

This PhD gave me the possibility to change my life, meet with amazing people, and learn lessons that will never leave me through my life. I am grateful to each person who supported me during these years.

Firstly, I would like to thank my primary supervisor Chris Ridout for his endless patience and continuous support even though there were more than 2000 miles between us while writing this thesis. Chris, I am very thankful for you for being amazingly strong and raising me up in all circumstances. I would like to also thank my secondary supervisors Lars Østergaard and Judith Irwin for their support and valuable contributions through my PhD. Thank you for trusting me and encouraging me, Judith. I would like also to thank my committee members Rachel Wells and Eleri Tudor for their valuable discussions in my committee meetings which I looked forward to having each time thanks to them. Rachel, thank you, your support was beyond the committee, it was at any time and in any condition. I would like to also thank Peter Walley for running the QTL mapping analysis and his encouragement. One who deserves the most thanks is Ricardo Humberto Ramírez González. His endless support, answering all my questions with patience, teaching all the things were infinitely valuable. Ricardo, thanks for trusting me and I am more than happy if I could make you and my family feel proud of me.

I was lucky that I supervised an amazing student, Emma Verbeek, who contributed to phenotyping studies of the BSA population. Besides all, I had an amazing group that adds meaning to each day of my PhD. I have lots of moments with you all which will make me smile whenever I remember. I am so glad to have you all; Catherine Jacott, Abraham Gómez-Gutiérrez, and Rachel Burns. Special thanks to Catherine for reviewing my thesis and her endless guidance, and Rachel for your contribution to my gene expression analysis.

I would like to thank horticultural services for making all this research possible. Special thanks to Lesley Philips, Damian Alger and Catherine Taylor for their being always helpful and taking care of my plants. I would like to also thank Burkhard Steuernagel from Scientific Computing for his valuable discussions through all my projects.

Most importantly, I am aware that this PhD would not be possible with the support from my lovely family, my partner Hakkı Onur Ercan, my road friend and sister Laura Haag, and my beloved friend Şadiye Hayta. I have so many feelings about your support and no words would be enough to describe how thankful I am.

Lastly, I am grateful to The Scientific and Technological Research Council of Turkey (TÜBİTAK) and the British Council for funding my PhD with the Newton-Katip Çelebi Fund.

## *Abbreviations*

| | |
|---|---|
| ABA | Abscisic acid |
| ATP | Adenosine Triphosphate |
| BAK1 | BRASSINOSTEROID INSENSITIVE 1 (BR1)-ASSOCIATED RECEPTOR KINASE 1 |
| BcNEP1 | *Botrytis cinerea* Necrosis and Ethylene Protein 1 |
| BcNEP2 | *Botrytis cinerea* Necrosis and Ethylene Protein 2 |
| BFR | Bulk frequency ratio |
| bp | Base pair |
| BR | Brassinosteroid |
| BSA | Bulk segregant analysis |
| BSK1 | BR-SIGNALING KINASE1 |
| cDNA | Complementary DNA |
| CER | Controlled environment rooms |
| cM | Centimorgan |
| DAMP | Damage-associated molecular patterns |
| DNA | Deoxyribonucleic acid |
| dpi | Days post-infection |
| Elf18 | 18 amino acids elongation factor |
| ET | Ethylene |
| ETI | Effector-triggered immunity |
| ETS | Effector triggered susceptibility |
| Flg22 | 22 amino acids flagellin peptide |
| GWAS | Genome wide association studies |
| HaNLP3 | *Hyaloperonospora arabidopsis* NLP3 |
| hpi | Hours post-infection |
| JA | Jasmonic acid |
| JAR1 | Jasmonic acid-amido synthetase |
| LRR | Leucine-rich repeat |
| MAMP | Microbe associated molecular patterns |
| MAPK | Mitogen-activated protein kinase |
| MQM | Multiple QTL model |
| NLP | Necrosis and ethylene inducing-like peptide |
| Ogs | Oligogalacturonides |
| PAMP | Pathogen associated molecular patterns |
| PCR | Polymerase chain reaction |
| PRR | Pattern recognition receptor |
| PTI | PAMP-triggered immunity |
| QDR | Quantitative disease resistance |
| qRT-PCR | Quantitative reverse transcription PCR |

| | |
|---|---|
| QTL | Quantitative trait loci |
| RLCK | Receptor like cytoplasmic kinase |
| RLK | Receptor like kinase |
| RLP | Receptor like protein |
| RLP23 | Receptor-like protein 23 |
| RNA | Ribonucleic acid |
| ROS | Reactive oxygen species |
| SA | Salicylic acid |
| SNP | Single nucleotide polymorphism |
| SOBIR1 | SUPPRESSOR OF BRASSINOSTEROID INSENSITIVE 1 (BRI1)-ASSOCIATED KINASE (BAK1)-INTERACTING RECEPTOR KINASE 1 |
| WGT | Whole-genome triplication |
| WRKY33 | WRKY Transcription factor 33 |
| wt | Wild type |

***File formats***

| | |
|---|---|
| *vcf* | Variant Call Format (https://samtools.github.io/hts-specs/VCFv4.2.pdf) |
| *sam* | Sequence Alignment/Map format (https://samtools.github.io/hts-specs/SAMv1.pdf) |
| *bam* | Binary Alignment Map format (https://samtools.github.io/hts-specs/SAMv1.pdf) |

# CHAPTER 1

## Introduction

Plant diseases cause significant losses to farmers, with an average of 26% of worldwide crop production affected by pre-harvest pests and pathogens, which threatens food security (Alexandratos & Bruinsma, 2012; OERKE, 2006; Savary, Ficke, Aubertot, & Hollier, 2012). Plant diseases can be controlled by using chemical pesticides or fungicides. Although these are effective in preventing invasive pathogens, these chemicals have long-term detrimental effects on soil and water reserves, and their use is discouraged. Disease resistance enables the control of pathogens without the harmful effects of chemicals. Genetically resistant varieties are therefore important to support sustainable agriculture in which chemical use is reduced to protect the environment (Dangl et al., 2013; Piquerez et al., 2014). However, pathogens can evolve to overcome resistance leading to 'break down', which is also a threat to crop production. Increasing the knowledge of the underlying mechanisms of plant-pathogen interactions will improve effective control with reduced pesticide usage and enable more durable resistance to be developed.

Since ancient times plants have been exposed to pathogens, and both pathogens and plants have evolved molecular mechanisms to enhance their fitness. Increasing the understanding of underlying plant-pathogen interaction mechanisms can lead to improved breeding strategies for disease resistant varieties. Recently, many studies have been conducted to understand innate immunity in plants and how this can be incorporated into breeding strategies to make resistance more efficient and durable (Ellis, Lagudah, Spielmeyer, & Dodds, 2014; Schwessinger, Bart, Krasileva, & Coaker, 2015, Boutrot & Zipfel, 2017). Fundamental studies, which have been carried out by using model species such as *Arabidopsis thaliana,* have helped to improve understanding of immunity in plants.

### 1.1. Plant immune system

Plant immunity is considered to have two different levels first described in the Zig-Zag model (Dodds & Rathjen, 2010; Jones & Dangl, 2006). The first level is usually described as Pathogen Associated Molecular Pattern (PAMP) or Microbe Associated Molecular Pattern (MAMP) triggered immunity (PTI/MTI) (here after referred to as as PAMPs, as in this study, it is in the context of pathogenicity) whereas the second level is known as Effector-triggered immunity (ETI). The zig-zag model provided a useful conceptual framework to understand the immune system of plants, although nowadays, it is considered to have a number of limitations, including absence of environmental context, being qualitative, being limited in the molecular scope of the interactions, in physical scale and in time-scale (Pritchard & Birch, 2014).

The first level of the plant immune response is called PAMP-triggered immunity (PTI). PTI is based on first recognition of Pathogen Associated Molecular Patterns (PAMPs) or Microbe Associated Molecular Patterns (MAMPs), which are highly conserved through the diverse taxa of pathogens since those molecular patterns are essential for life. Recognition of PAMPs is achieved with transmembrane pattern recognition receptors (PRRs) on the plant cell plasma membrane (Couto & Zipfel, 2016; Zipfel, 2014). Also, host-derived damage-associated molecular patterns (DAMPs),

endogenous signals released during infection, are recognized by PRRs (Dodds & Rathjen, 2010). PRRs are particularly encoded by receptor-like kinase (RLK) and receptor-like protein (RLP) genes. After recognition of the PAMPs, a signalling cascade is initiated to activate defence response to invasive pathogens (Boller & Felix, 2009; Zipfel et al., 2004). PTI responses include a variety of changes at the cellular level on plant cells related to defence, such as; rapid mitogen activated protein kinase (MAPK) phosphorylation, $Ca^{2+}$ influx, production of reactive oxidative species (ROS burst) and induced transcriptional changes of genes. Other changes include cell wall reinforcement by callose deposition, phytoalexin accumulation, plasma membrane ion fluxes, and can be used to quantify PAMP responsiveness (Simon R Lloyd et al., 2014).

At the beginning of the second level of immunity, successful invasive pathogens deliver effectors, previously described as avirulence (Avr) molecules through the plant cells in order to interfere with the PTI triggered signalling cascade and to enhance microbial fitness (Lo Presti et al., 2015). Transmission of effector molecules into plants causes Effector Triggered Susceptibility (ETS). Nucleotide-binding site leucine-rich repeat (NB-LRR) proteins, which are encoded by *R* genes, recognize these effector molecules inside the cell, induce the Effector Triggered Immunity (ETI) (Stotz et al., 2014; Takken et al., 2006; Wu et al., 2014). This R/Avr (also termed as `gene-for-gene resistance`) recognition results in strong immunity and resistance and is associated with a hypersensitive response (HR) at the infection site of the plant (Flor, 1971). It has been recently suggested that, as all these mechanisms evolved in pathogens through interfering with the PTI mediated defence responses, main evolutionary purpose of the ETI is potentiating the PTI. My PhD research focusses on PAMP-triggered immunity which I describe in more detail here.

### 1.1.1. PTI signalling pathway and its components

#### 1.1.1.1. Pattern Recognition Receptors (PRRs)

The two most widely studied PRRs are FLAGELLIN SENSING 2 (FLS2) and EF-Tu RECEPTOR (EFR) which recognise flg22 (a 22 amino acid peptide fragment from the bacterial flagellum) and elf18 (an 18 amino acid peptide from bacterial Elongation Factor-Tu) respectively. Both PRRs are found in *Arabidopsis thaliana* and belong to leucine-rich repeat receptor-like kinase family XII (LRR-RLKs) (Gómez-Gómez & Boller, 2000; Zipfel et al., 2006). After investigation of different flagellin epitopes recognized by different PRRs, FLAGELLIN SENSING 3 (FLS3) was identified as receptor-like kinase which detects flgII-28 (Hind et al., 2016). In rice, CHITIN ELICITOR BINDING PROTEIN (CEBiP), a type of lysin motif (LysM) domain-containing receptor-like protein (RLP), recognises chitin and CHITIN ELICITOR RECEPTOR KINASE (CERK1), a type of RLK, is required to initiate the PTI response to recognition of chitin by CEBiP (Kaku et al., 2006; Miya et al., 2007). The leucine-rich repeat receptor protein (LRR-RP) RLP23 was recently identified in *A. thaliana* as a receptor for nlp20, a PAMP used in my investigation and described in more detail later (Bae et al., 2006; Bi et al., 2014; Oome et al., 2014).

In addition to recognition of PAMPs, damage-associated molecular patterns (DAMPs) are recognized by particular receptors. In *A. thaliana*, oligogalacturonides (OGs) found in the plant cell wall are released after infection of a pathogen. Released OGs are recognized by WALL-ASSOCIATED KINASE1 (WAK1), and this recognition triggers the defence responses (Brutus et al., 2010). Other important DAMP types are plant-derived ATPs that are released after infections through wounds. By mutant screening studies in *Arabidopsis thaliana*, DOESN'T RESPOND TO NUCLEOTIDES (DORN1), a lectin-RLK, the first discovered plant receptor for extracellular ATP, was found to have detected those ATPs at the extracellular space and initiate the immune signalling cascade (Choi, Tanaka, Cao, et al., 2014; Choi, Tanaka, Liang, et al., 2014).

#### 1.1.1.2. Co-receptors - Receptor-Like Cytoplasmic Kinases

Receptor-like cytoplasmic kinases (RLCKs) are related to but distinct from RKs because they lack the extracellular domain or ectodomain (Lehti-Shiu et al., 2009). They have important regulatory roles in major functions of the plant; abiotic/biotic stress responses, growth, defence responses, and reproduction. RLCKs have specific roles in PTI signalling pathway and are mostly regulated by their associated PRRs. Their phosphorylation is critical for their activation and functional diversification (Majhi et al., 2019).

Brassinosteroid hormones (BRs) play critical roles in a variety of developmental processes such as; stem and root growth, and flower and fruit developments. BRs also have been involved in plant responses to abiotic stress. BRASSINOSTEROID INSENSITIVE 1 (BR1)-ASSOCIATED RECEPTOR KINASE (BAK1) is a leucine-rich repeat receptor-like kinase that has important role in BR signalling mechanism in higher plants. In addition, BAK1 has a critical role in PTI signalling as a positive regulator for multiple PRRs in *A. thaliana* and is required in innate plant immunity for FLS2 mediated ROS burst as co-receptor(Chinchilla et al., 2007; Macho & Zipfel, 2014). BAK1 is believed to have role in trade-off between plant growth and immunity because it is required as a co-receptor for ligand binding for both steroid hormones to BR1 and required for perception of PAMPs such as flg22 binding to FLS2 (Chinchilla et al., 2009; Z.-Y. Wang, 2012). With related studies to reveal this trade-off between both signalling events, BR treatment has been found to enhance disease resistance in rice and tobacco. However, the mechanisms by which BAK1 acts as a common element for growth and defence are largely unknown (Bajguz & Hayat, 2009; Z.-Y. Wang, 2012).

BAK1 belongs to the SOMATIC-EMBRYOGENESIS RECEPTOR-LIKE KINASE (SERK) family. In addition to BAK1, BAK1-LIKE1/SERK4 (BKK1/SERK4) was found to have a positive regulatory role in plant innate immunity. With co-immunoprecipitation and mass spectrometry analyses, it was shown that heteromerization of EFR and FLS2 with BAK1/BKK1 cooperatively provide a high level response to elf18 and flg22 (Roux

et al., 2011). In contrast to BAK1, LRR receptor-like kinase (LRR-RLK) SUPPRESSOR OF BRASSINOSTEROID INSENSITIVE 1 (BRI1)-ASSOCIATED KINASE (BAK1)-INTERACTING RECEPTOR KINASE 1 (SOBIR1) is a positive regulator of PRRs as co-receptor especially for RLPs (Liebrand et al., 2014).

Another important co-receptor with a role in plant immunity is BR-SIGNALING KINASE1 (BSK1), a type of receptor-like cytoplasmic kinase with a membrane localization signal. When the localization signal of BSK1 is modified by mutation, plants become susceptible to multiple pathogens indicating that the co-receptor has a regulatory function in plant immunity. To investigate the function of BSK1 in disease resistance, Arabidopsis *edr2* (*enhanced disease resistance 2*) mutant was used (H. Shi, Yan, et al., 2013). Mutations in Enhanced Disease Resistance region lead to increased resistance to powdery mildew disease (*Golovinomyces cichoracerum*) (Frye & Innes, 1998; Tang et al., 2005, 2006; Vorwerk et al., 2007). A *bsk1-1*/*edr2* mutant was obtained by mutagenesis by screening in the *edr2* background in *A. thaliana*. In related disease resistance assays, it was found that; *bsk1-1* mutation suppressed the *edr2*-mediated resistance, and *bsk1-1* single mutant displays enhanced susceptibility to a variety of pathogens such as *G. cichoracearum*, *Pseudomonas syringae*, and *Hyaloperonospora arabidopsidis*. Also, with related experiments, it was shown that BSK1 and FLS2 physically associates, and this association is significantly required for ROS burst response. With all of these results, it is clearly suggested that BSK1 is a key component in BR signalling and plant immunity as a positive regulator of defence responses (H. Shi, Shen, et al., 2013).

### 1.1.2. Reactive Oxygen Species (ROS) production

Reactive oxygen species are extremely reactive reduced oxygen molecules that have major roles in various plant developmental and immune signalling mechanisms. The main reactive oxygen species produced by the plant cells intracellularly or within organelles are superoxide ($\cdot O_2^-$), hydroxyl radical ($\cdot OH$), and hydrogen peroxide ($H_2O_2$) (Tripathy & Oelmüller, 2012). ROS are produced via different mechanisms in response to distinct stimuli such as pathogen infection, environmental stress, and polar growth (Mittler, 2017). For instance, as an important redox signalling molecule, hydrogen peroxide has a role in plant developmental processes as well as its role in stress response (Xia et al., 2015). Recent research showed that $H_2O_2$ induces the oxidization of the master regulator transcription factor in BR signalling pathway, BRASSINAZOLE-RESISTANT1 (BZR1). This modification of BZR1 enhances its interaction between various regulators involved in auxin-signalling and light-signalling pathways (Y. Tian et al., 2018).

In higher plants, NADPH oxidases, a family of RESPIRATORY BURST HOMOLOGs (RHOBs), are responsible for apoplastic ROS burst due to pathogen recognition. This type of production is most widely studied because of its vital role in plant immunity (Qi et al., 2017). RHOBD was identified as a protein interacting with BIK1 (BOTRYTIS-INDUCED KINASE 1), FLS2 and EFR with protein pull-down and mass spectrometry methods. RHOBD phosphorylation directly by BIK1 is necessary for the FLS2 and EFR related downstream ROS burst. BIK1 phosphorylation is defined as the priming event for RHOBD, and other signalling components such as calcium-binding and phosphatidic acid-binding regulate the full activation of the protein (Kadota et al., 2015).

Reactive Oxygen species are toxic, and the ROS burst could potentially be a defensive weapon against invasive pathogens. However, pathogens evolved various effectors to suppress the apoplastic ROS burst, which will occur immediately after the perception of the PAMP motif (Jwa & Hwang, 2017). As well as being toxic, the ROS burst is important in plant immunity due to its priming effect on many immune

signalling mechanisms, such as cell wall reinforcement via enhancing the callose deposition (Daudi et al., 2012) and the triggering of systemic acquired resistance against *P. syringae* pv.*tomato* DC3000 in *A. thaliana* (S. Tian et al., 2016).

### 1.1.3. PTI contribution to Quantitative Disease Resistance (QDR)

Quantitative disease resistance (QDR) is a particular type of disease resistance controlled by multiple genes with smaller effects and explained as a reduction in disease (e.g. also known as basal resistance) in contrast to qualitative disease resistance leading to complete resistance (e.g. specific recognition of pathogen effectors or their targets). Incorporating the R-genes into cultivars is relatively easy when compared to obtaining cultivars with QDR. Although *R*-gene mediated resistance has those advantages along with a stronger and more rapid response to the pathogens, this high level of specificity means that it can be easily defeated by pathogens. The invasive pathogens can adapt by evolving new, slightly modified, effector molecules that are no longer recognised by the corresponding R protein (Zhang et al., 2016). However, in comparison to qualitative resistance, each QDR locus has smaller effects on resistance, this leads to low selection pressure on pathogens. Therefore, QDR is considered to be more durable. (Poland et al., 2009). Increasing evidence suggests that PTI could be a component of QDR (Boyd et al., 2013).

To investigate the QTL for QDR, natural variation between species is the most widely used approach. To support the breeding of *Pseudomonas syringae* pv. tomato (*Pst*) resistant tomato (*Solanum lycopersicum* L.) cultivars, a study was carried out to identify the variation of immunity associated-traits between heirloom tomato lines (also called heritage varieties) in response to flg22 and flgII-28 and csp22 (Felix & Boller, 2003). In comparison to other PAMP responses, variation in csp22 responses of RG-PtoS and *Solanum habrochaites,* a type of wild relative of tomato, were observed between $F_1$ and $F_2$ generations. The results illustrate how a mapping population can be created by using natural variation among these lines and used to identify underlying QDR loci (Veluchamy et al., 2014).

Natural variation in disease resistance between citrus species and the *Xcc*-derived PAMP (*Xanthomonas citri* ssp. citri, *Xcc*) was investigated in another study to reveal PTI mechanisms in citrus canker disease. Results showed that in resistant cultivars Xflg22 induces strong PTI response, and PTI has a crucial role in resistance mechanisms to citrus canker disease(Q. Shi et al., 2015).

In maize, a high-resolution map-based cloning approach was used and the location of *Htn1*, which is believed to have a role in QDR to Northern corn leaf blight (NCLB) caused by *Exserohilum turcicum*. A resistance locus on chromosome 8 was identified and delimited to a 131.7-kb physical interval. Three candidate genes were defined in the Htn1 locus, two wall-associated RLKs (ZmWAK-RLK1 & ZmWAKRLK2), and one wall-associated RLP (ZmWAKRLP1). Also, TILLING (target-induced local lesions in genomes), in the same study, suggested the involvement of PTI in QDR. This study provides the basis for future studies to investigate the role of wall-associated receptor-like kinase family in QDR of the crop species (Hurni et al., 2015).

All of these studies above and many others in literature increasingly support the idea that PTI is contributing to the QDR. Importantly, methods to quantify PTI can be quite high-throughput and so could potentially be used for screening large populations. If there is a good correlation between PTI and QDR, this could enable more rapid identification of QDR in crop species. Using developed quantification methods (such as; MAPK phosphorylation, $Ca^{2+}$ influx, oxidative burst (ROS changes), cell wall reinforcement by callose deposition, phytoalexin accumulation, plasma membrane ion fluxes and induced transcriptional changes defence-related genes), some of which are already developed in our group (Simon R Lloyd et al., 2014), can provide a relatively fast and high-throughput way to quantify QDR in agronomically important crop species.

### 1.1.4. Effects of hormones and environmental stress on plant immunity

Plants are living in dynamic environments and need some plasticity to adapt these dynamic interactions with the physical changes in the living conditions and their interplay with various microorganisms. The regulation of the adaptation is mostly regulated by plant hormones. As well as their vital role in stress response, plant hormones have a role in major living functions such as growth and development, and reproduction (Bürger & Chory, 2019).

Two main systemic immune responses are playing roles in plant immunity against phytopathogens. The hormone salicylic acid (SA) controls systemic acquired resistance (SAR) (Conrath, 2006), which activates defences against biotrophic pathogens. In contrast, jasmonic acid (JA) directs the defence against necrotrophic pathogens via induced systemic resistance (ISR) (Choudhary et al., 2007).

JA-signalling pathway is one of the most well-studied phytohormone pathways due to its function in regulating the abiotic and biotic responses and also plant growth and development (Wasternack, 2007). JA driven responses require endogenous bioactive form of JA molecule, Jasmonoyl-L-isoleucine (JAIle), which is produced by the JA AMIDO SYNTHASE (JAR1) enzyme via conjugating JA with L-Ile (Fonseca et al., 2009). Several studies were used *Arabidopsis jar1* mutant line as JA-insensitive mutant to reveal the function of the JA-signallnig pathway on plant major living functions (Laurie-Berry et al., 2006; Pieterse et al., 1998; Staswick et al., 2002). Additionally, *JAR1* gene were used as JA-related marker gene to track and validate the activation of the pathway (Hickman et al., 2017; Kammerhofer et al., 2015).

Both of these systemic immune responses are proven to be antagonistic to each other. Thus, they need to be fine-tuned by the plant for an effective defence system. This adjustment is maintained by other plant hormones such as abscisic acid (ABA) (Finkelstein, 2013), Brassinosteroid (BRs) (Nolan et al., 2020), ethylene (ET) (Iqbal et al., 2017), auxin (AUX) (Yunde Zhao, 2010) and gibberellins (GAs) (Davière & Achard, 2013).

Abiotic stress tolerance is mediated by ABA in evolutionarily conserved mechanisms (Finkelstein, 2013). Increasing activation of ABA due to abiotic stress conditions causes suppression in SA-regulated defence responses (Yasuda et al., 2008). This suppression mechanism is regulated by various pathways, including transcriptional regulation. It is proven in a recent study that, ABA-triggered immune suppression to biotrophic *P. syringae* in *A. thaliana* requires ABA RESPONSIVE ELEMENT (ABRE) BINDING PROTEIN (ARBE) transcription factors (TFs) which are regulating ABA-mediated transcriptional changes (Berens et al., 2019).

Another transcription factor with a role in suppression of SAR is WRKY33, which interacts specifically with the WRKY factor-binding sites (W boxes (5'-TTGAC[CT]-3')), required in defence responses against the necrotrophs *A. brassicicola* and *Botrytis. cinerea* (Zheng et al., 2006). In *wrky33* mutant plants, after *B. cinerea* infection, there was an increase in activation of the SA-mediated responses. Thus, the working hypothesis is that the WRKY33 suppresses the SA-mediated responses and prevents the antagonistic effect of SA pathway against the JA-mediated defence responses (Birkenbihl et al., 2012).

The evolutionary purpose of the regulation between the ABA and SA-mediated pathways is proposed to be a mechanism for prioritizing abiotic stress response over biotic stress responses (Berens et al., 2019). Also, the antagonistic relationship between the SA and JA-mediated immune responses provides a mechanism for regulating immunity against pathogens according to the nature of the microbe (Ton et al., 2002). Although these cross-talk mechanisms could maximize the plant fitness, it has been proven that pathogens can manipulate those specific mechanisms to suppress the targeted systemic resistance by mimicking or manipulating the balance between them (Bürger & Chory, 2019).

## 1.2. The Brassicaceae family

The focus of this PhD research is in the immune system and its involvement in disease resistance. The investigations are carried out in Brassica crop species, specifically *B. napus* and *B. oleracea*. In this section, I describe the nature of these species, relevant to the study. The Brassicaceae is a large family, including 338 genera and more than 3709 species (Schmidt et al., 2001). This family of the plant kingdom includes economically important species that are used for edible vegetable oil such as *B. napus* (Oilseed rape or Canola), *B. rapa* (Turnip)*, B. juncea* (Black mustard)*, B. carinata* (Abyssinian mustard). According to the FAOSTAT (http://faostat.fao.org/), only in the UK and Northern Ireland 2,012,000-ton rapeseed was produced as the 9$^{th}$ great producer in the world in 2018. Besides the vegetable oil production, agronomically important cultivars are included in this family mostly in *B. oleracea* species such as cauliflower, broccoli, and cabbages. As well as being economically and agronomically important, the genetic, metabolic, and morphological diversity of the Brassica family has been widely studied (Schmidt, Acarkan, & Boivin, 2001).

### 1.2.1. Polyploidy and Genetics

All Brassica crop species have undergone an extra whole-genome triplication (WGT) event, estimated to have occurred between 9–15 million years ago, and ~28 million years ago (Lukens et al., 2004; Lysak et al., 2005). Approximately 7500 years ago, the allopolyploid Oilseed rape (*Brassica napus* L.) genome was formed with a hybridization between *B. rapa* (A genome) and *B. oleracea* (C genome) chromosomes which is also followed by chromosome doubling (Chalhoub et al., 2014). Both of the ancestor Brassica species for the A and C genomes were derived from a hexaploid ancestor, clearly revealed by investigating their extensively triplicated genomes. The interactions and the evolutionary processes of the brassica species have been summarised by the 'Triangle of U' (Figure 1.1) (Cheng et al., 2015). Within the Brassicaceae family, *A. thaliana* and Brassica diverged from a common ancestor 14-24 million years ago(Koch et al., 2000). Therefore, *A. thaliana* is thought to have

multiple orthologs (retaining the same function) in the *B. napus* genome. Also, based on the evolutionary relationship between the *B. rapa* and *B. oleracea*, each gene of the A genome has a corresponding gene on C genome in Brassicas (Parkin et al., 2005).

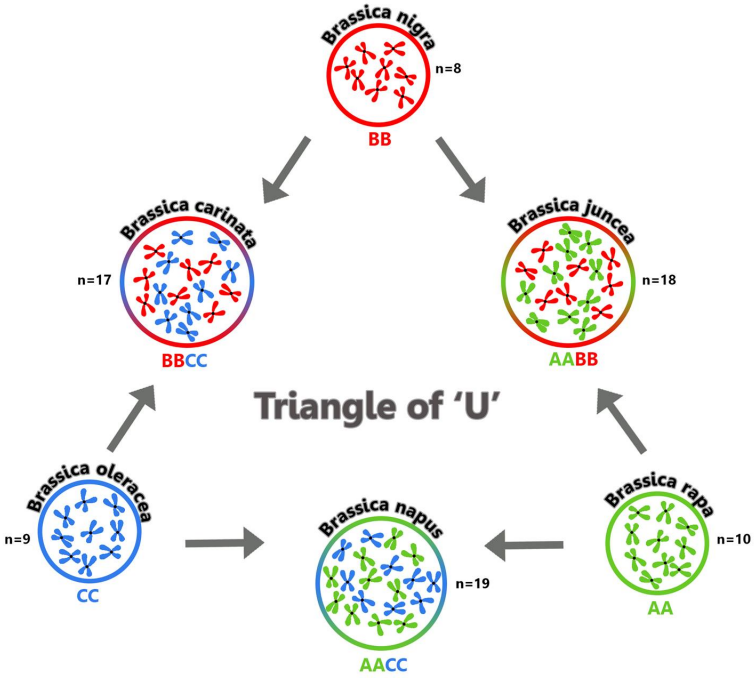


**Figure 1.1.** Triangle of `U` theory, shows the evolutionary relations between diploid brassicas and the evolution of the *B. napus* as a result of allopolyploid hybridization between *B. oleracea* & *B. rapa* (Cheng et al., 2015).

The genome of *B. rapa*, which is one of the ancestors of *B.napus* A genome, has been published (X. X. Wang et al., 2011) and a high-density single nucleotide polymorphism (SNP) linkage map has been developed (Bancroft et al., 2011). Also, computational methodology development has been done for the qualification of transcript abundance in polyploids, by using the mRNA-seq data, which provides apportioning of transcript abundance to A and C genomes (Higgins et al., 2012).

#### 1.2.1.1. Genome-Wide Association Studies (GWAS)

With increasing improvements in RNA-seq technologies together with advancements in computational methods, mRNA sequencing has become widely-used in brassicas. Using the unigene reference of Higgins et al., (2012) with transcriptome sequencing data of a *B.napus* diversity set (84 diverse *B.napus* lines), a large scale Genome-Wide Association Study (GWAS) of glucosinolate content of the seeds was performed (Harper et al., 2012). The SNP reference was based on mRNA sequences, which also enabled quantification of each transcript (unigene) abundance. The study showed that associations between the transcriptomic data and phenotypic traits for each diverse accessions could be obtained in order to identify novel loci where the transcription directly correlated with the trait. This developed method is termed as "Associative Transcriptomics" and clearly reveals that even with minimal genomic resources, it is possible to identify and score molecular markers for interesting traits by using RNA-seq data from a diverse population.

In recent years, GWAS has been popular to use for the identification of genetic loci for agronomically important traits in rapeseed, such as yield, seed quality and flowering time (Lun Li et al., 2015; Liu et al., 2016; Lu et al., 2017). Studies that investigate the quantitative and qualitative disease resistance locus have also been undertaken with GWAS. Harsh Raman and Rosy Raman with their colleagues carried out a study to identify loci associated with resistance to *L. maculans* in canola. They could define new genomic loci contributing to resistance of *B. napus* to *L. maculans* (Raman et al., 2016). In another study, GWAS was used to reveal new loci for resistance to clubroot disease caused by *Plasmodiophora brassicae Woronin* in *B. napus*. Success in the identification of those novel QTL shows the strong ability of GWAS to define the responsible regions for important traits (Lixia Li et al., 2016).

Another study was undertaken for the identification of new loci for controlling the resistance against the Stem Rot disease caused by the fungus *Sclerotinia sclerotiorum*. By using Illumina 60K Brassica SNP array, GWAS analysis of 347 accessions was performed to reveal the pathogenesis-related genes. Besides the

GWAS analysis, transcriptome sequencing of five highly resistant and susceptible *B. napus* lines was completed. In both SNP-trait association and transcriptome sequencing analysis, 24 genes were found as disease resistance-related (Wei et al., 2016).

#### 1.2.1.2. Bulk Segregant Analysis (BSA)

Bulk segregant analysis (BSA) is a technique used for identifying the genetic markers for specific target loci responsible for interesting traits (Michelmore et al., 1991). There are main advantageous using BSA technique such as, being much faster as even usage of heterozygous plants are enough to map the corresponded region and, using bulked samples for sequencing is lowering the cost and labour. In this technique, resolution of the mapping is dependent on some factors such as covering recombinations in that region with an appropriate number of individuals and increasing the marker density (C. Zou et al., 2016). The method is very flexible that any segregating population can be used as any NGS-enabled protocol can be applied to create the genetic map, such as RNA-Seq (Trick et al., 2012) or whole-genome re-sequencing (Tudor et al., 2020). Already various agronomically important traits were investigated within different crop species like *Oryza sativa, Triticum aestivum L.* and *B. napus* with this analysis (Ramirez-Gonzalez, Segovia, et al., 2015; Takagi et al., 2013; Trick et al., 2012; Tudor et al., 2020; H. Wang et al., 2016).

The BSA method consists of creating pools from a segregating population with contrasting phenotypes. Pools are created via bulking the DNA/RNA of individuals coming from the population. The results from Next Generation Sequencing (NGS) are used to identify polymorphisms between the bulks. The observations of the allelic region associated to the trait of interest is enriched in the bulk with the same phenotype as the parental line (C. Zou et al., 2016). To measure the relative enrichment of the corresponding parental allele in the appropriate bulk, each SNP is scored with their corresponding Bulk Frequency Ratio (BFR). The scoring is made by calculating the ratio between the frequency of each informative base at each SNP position of the non-responsive and responsive bulk (Figure 1.2) (Trick et al., 2012).

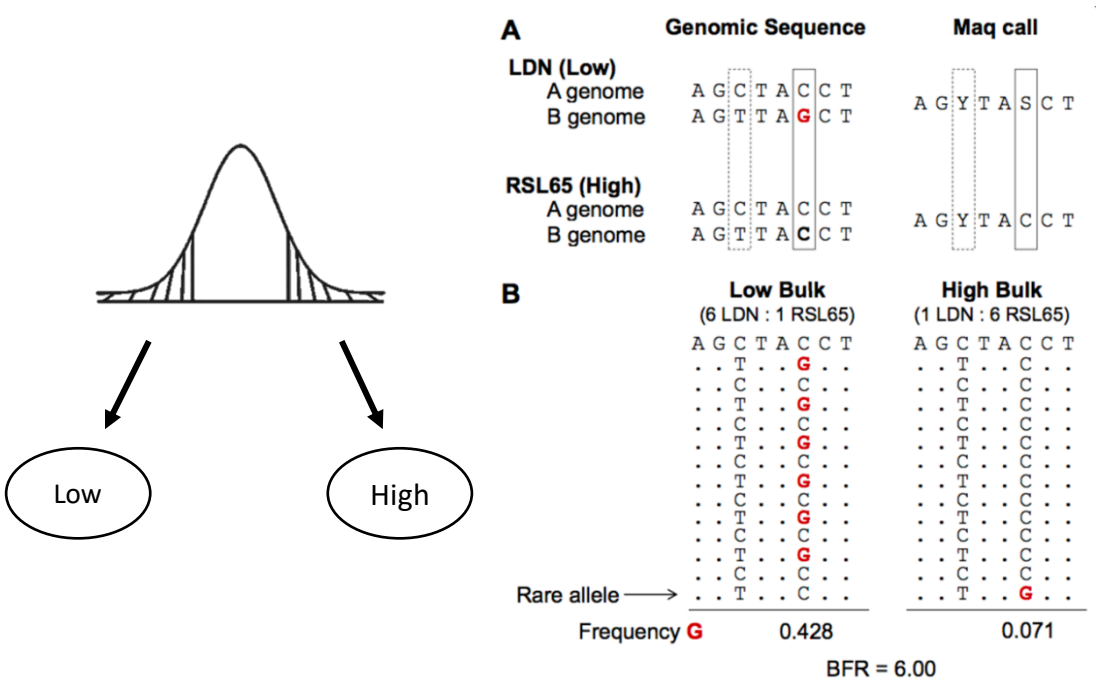


**Figure 1.2** An illustration for explaining the calculation of the Bulk Frequency ratio of an example SNP from Trick et al., 2012. On the left panel, selection of extremes in an example population according to their phenotypic segregation displayed as "Low" and "High" bulks. On the right panel, as described in Trick et al., 2012, (A) a homoeologous SNP between A & B genome is represented. (B) The composition of the alleles for an SNP which is closely linked to the interested trait in the Low and the High bulks.

One of the most recent BSA study was conducted by Tudor and her colleagues in the *B. napus* genome. In order to reveal the determinative region for vernalisation requirement, distinct phenotypical varieties, Cabriolet and Darmor, were used to create the segregating population according to their flowering time. A major QTL was defined at a 10Mbp region on chromosome A02, which includes orthologues of *AtFLC* (*FLOWERING LOCUS C* (*BnaFLC.A02*) and *AtFT* (*FLOWERING LOCUS T* (*BnaFT.A02*) successfully (Tudor et al., 2020).

### 1.2.2. Diseases affecting Brassicas

Various types of pathogens are affecting the crop yield in Brassicaceae by causing severe diseases. Most devastating diseases are stem canker by *Leptosphaeria maculans* (Howlett et al., 2001) and light leaf spot by *Pyrenopeziza brassicae* (Oxley & Walters, 2012). Another important pathogen is *Sclerotinia sclerotiorum,* which causes Sclerotinia stem rot (Khot et al., 2011). This pathogen is genetically closely related to *Botrytis cinerea* (Amselem et al., 2011) which is also a major necrotrophic pathogen of vegetable crops such as *B. oleracea* cultivars (Williamson et al., 2007).

*Botrytis cinerea* is a phytopathogenic fungus that has necrotrophic lifestyle and over 200 hosts in mainly dicotyledonous plants worldwide. The symptoms in plant tissues can be summarised as water soaking of parenchyma tissues and a rapid appearance of grey masses of conidia on the infected area. *B. cinerea* can produce sclerotia within dying host tissues, a type of reproductive structure that can survive in soil for many years and which germinate to produce conidiophores and multinucleate conidia. As well as the sclerotia, mycelium can also survive in the dead plant tissue and serve as inoculum to start infection by producing conidia (Amselem et al., 2011; Williamson et al., 2007). *B. cinerea* is a well-studied model for molecular studies of necrotrophic fungi through its huge number of hosts and effective adaptation abilities to various fungicides due to its genomic plasticity. In this PhD investigation, *B. cinerea* used not only as a model necrotrophic phytopathogen but also because there were well-established quantifying methods which easy quantification for high-throughput experiments. Two strains of *B. cinerea* were used in this PhD study; B05.10 as wild type and B05.10-derived mutant ΔBcatrB4. This mutant strain has a specific mutation in *BcatrB*, an ATP-binding cassette (ABC) transporter gene, which have role in exporting exogenous toxic materials such as antibiotics (H. Schoonbeek et al., 2002), fungicides and plant defence compounds (Del Sorbo et al., 2000; Vermeulen et al., 2001), such as camalexin. This mutant strain can start the infection as effective as B05.10 at 10-24 hpi, however at 48 hpi the effect of the mutation could be observed. It has been proved that, this mutation cause loss of virulence on plants producing camalexin, which is a type of early immune response and functions as a phytoalexin

(Glawischnig, 2007). As ΔBcatrB4 is not able to export the camalexin out efficiently, the penetration and *in planta* growth of the mutant strain was observed as weaker when compared with wild type strain (Stefanato et al., 2009).

#### 1.2.2.1. Necrosis- and ethylene-inducing peptide 1 (Nep1)-like proteins (NLPs)

As a PAMP molecule, *Botrytis cinerea* Necrosis and Ethylene Protein 2 (BcNEP2) was used in this study. BcNEP2 is a member of the superfamily of NLPs, which are widely found in bacteria, fungi, and oomycetes. In a recent study, 1794 NLP homologues were identified in 497 species, in which 80% of the NLPs were carrying signalling peptide (SP), which allows the protein to be secreted to the extracellular environment (Seidl & Van den Ackerveken, 2019). As NLPs are present in three kingdoms of microbial life, they occur in a broader range of organisms than any other PAMP molecule. Many NLP-bearing organisms have plant pathogenic lifestyle, but they are also present in taxa with other lifestyles, suggesting the role of NLPs are not limited to pathogen virulence on plants (Bhatti et al., 2017; Tekaia & Latgé, 2005).

NLPs have two main activities, first the cytotoxicity by triggering the necrosis, and the second immunogenicity via stimulating the immunity-associated defences in dicotyledonous plants. According to some research studies, NLPs have been found as vital for microbial virulence of necrotrophic microorganisms. NLPs are expressed in pathogens at specific phases of the infection. Cytotoxic NLP is expressed not early in the infection phase but later when the pathogen is switching from the biotrophic phase to the necrotrophic phase in hemibiotrophic organisms (Irieda et al., 2014). Comparative RNA-seq analyses of the *L. maculans* isolate D5 at four different time points after inoculation on both susceptible and resistant *B. napus* cultivars (Topas-DH16516 and introgression line Topas-Rlm2) have shown that, Nep1-like protein (NPP1, gene_11090) in *L. maculans* was highly expressed at the $7^{th}$ and $11^{th}$ day post-infection (Sonah et al., 2016).

In the previous studies, *Bcnep1* and *Bcnep2* mutants of the *B. cinerea* were created in order to reveal the effect of those genes on the virulence of the pathogen. Both of the mutant strains were not significantly different from the virulence of the wild type strain (Cuesta Arenas et al., 2010). On the other hand, in a recent study, it has been shown that silencing of BcNEP2 in *B. cinerea* and its corresponding homologue SsNEP2 in *S. sclerotiorum* by dsRNA resulted in significant reduction in lesion size in *B. napus* from related pathogen. Although there was no correlation between the effects of the silencing on the lesion sizes, it was still concluded that these dsRNA targets could be used as a controlling agent for both of the pathogens (McLoughlin et al., 2018).

The identical structural properties of NLPs from different taxonomic microorganisms cause both plasma membrane permeabilization and cytolysis and restore bacterial virulence. An NLP-deficient rot bacterium *Pectobacterium carotovorum* strain had been transformed with two different $NLP_{Pya}$ or $NLP_{Pp}$-encoding sequences (*Pythium aphanidermatum* & *Phytophthora parasitica*) and a clear induction of virulence (30%-40%) was observed (Ottmann et al., 2009). Also, the virulence level of *Verticillium dahlia* was reduced on different host plants by individual deletion of two different NLP genes(Santhanam et al., 2013). Also, in another study, researchers showed that the 24 amino acid fragment of *Hyaloperonospora arabidopsis* NLP3 (HaNLP3) in the central region of the protein act as a PAMP by triggering the plant defence responses (Oome et al., 2014). So, it is suggested that recognition of NLPs can require other processing factors because the recognized peptide fragment is predicted not to be surface exposed, but located on the inside of the protein. As the filtrated mature protein from the *Fusarium oxysporim* f. sp. *erythroyli* culture was found to be starting from amino acid position 32 (Bailey, 1995), one of those processing factors is suggested to be the post-translational modifications that the protein undergoes by secreted fungal proteases.

A peptide fragment of 10–25 aa from the conserved region inside of the HaNLP3 protein is, in most cases, sufficient for triggering PTI as PAMP motif. This was demonstrated by Albert and her colleagues who investigated the protein complex,

which mediates the NLP-triggered immunity by using 20 amino-acid fragment long recognition region of the NLP (nlp20). In *Arabidopsis*, the leucine-rich repeat receptor protein RLP23 recognises NLPs and forms a constitutive complex with the LRR receptor kinase SOBIR1 in a ligand-independent way and also recruits a second LRR receptor kinase, BAK1, into complex upon ligand binding (Albert et al., 2015).

A limited number of studies on NLP-recognition have been conducted with crop species. One example is in cultivated lettuce (*L.sativa* cv. Olof), which recognizes the nlp24-PAMP motif, triggering the immune responses and decreasing the disease susceptibility to *Bremia lactucae* (Böhm et al., 2014). Interestingly, in that study, no RLP23 homologue was found to be present in the Lettuce genome. Additionally, it was shown that *L. sativa* cv. Olof has broader recognition of the NLP peptides than *A. thaliana* leading to the hypothesis that another version/type of a PRR is responsible for NLP-recognition (Raaymakers, 2018).

Another study indicated a perception mechanism different from RLP23 might be operating in *Cucurbitaceae* cultivars. The cytotoxic NLP1 molecule, which is expressed by *Colletotrichum orbiculare* during the switch phase to necrotrophy, was used. Transgenic *C. orbiculare* lines constitutively expressing NLP1 and a truncated variant lacking the PAMP motif were created, and disease assays were conducted on various *Cucurbitaceae* cultivars - cucumber, melon, winter melon, and long melon. Interestingly, the plants were highly resistant to the transgenic pathogen which constitutively expressed both the full-length and the truncated NLP1 proteins. Subsequently, it was found that carboxy-terminal 32 amino acid of NLP1 is recognized by *Cucurbitaceae* cultivars through a different mechanism than RLP23 (Azmi et al., 2018; Irieda et al., 2014).

### 1.3. Aims & Objectives

The aims of the study were to investigate the importance and the contribution of PAMP-triggered immunity in QDR and genetically map the regions responsible for regulating the PTI of the Brassicas, to functionally test candidate genes with a role in PTI and QDR, and to advance knowledge on how environmental stress affects PTI.

In order to cover all aspects above, the objectives were as below;

1. To understand how NLP-recognition contributes to QDR against *B. cinerea* in *B. napus* via high throughput phenotyping assays followed with statistical analysis using $F_2$ individuals from the segregating population (Chapter 3).

2. To define the loci and the candidate genes having a role in recognition of the NLPs and NLP-induced ROS burst in *B. napus* using specifically created segregating population in Bulk segregant analysis (Chapter 4).

3. To test the function of the candidate gene *BSK1* in NLP-induced ROS burst and disease resistance against *B. cinerea* by mutants and gene expression assays in *A. thaliana* (Chapter 5).

4. To investigate further and genetically map the regions controlling the effect of abiotic stress on PTI and disease resistance against the *B. cinerea* in *B. oleracea* genome through stress treatments and high-throughput phenotyping assays by using DH mapping population (Chapter 6)

# CHAPTER 2

## Materials & Methods

### 2.1. Plant material

*Brassica napus*, *Brassica oleracea*, and *Arabidopsis thaliana* plants were used in this study. Growth conditions specific to each project and plant material can be found under section 2 .2.

#### 2.1.1. *Arabidopsis thaliana bsk1-1* mutants

*Arabidopsis bsk1-1* mutant seeds and Col-0, used as wild type, were kindly obtained from Prof. Dingzhong Tang, Chinese Academy of Sciences, Institute of Genetics and Developmental Biology. This mutant line was identified from an Ethyl methanesulfonate (EMS) mutagenized *edr2* population (Nie et al., 2011).

#### 2.1.1.1. Genotyping of *bsk1-1* mutants

*A. thaliana* leaves were used for DNA isolation. The leaf samples were sent to the Genotyping platform service, John Innes Centre, and the isolation process completed by Richard Goram with DNeasy® Plant kit (Qiagen) used according to the manufacturer's protocol. All *A. thaliana* samples were verified to contain the *bsk1-1* mutation using a Cleaved Amplified Polymorphic Sequence (CAPS) marker with primers designed to detect the presence of mutations (H. Shi, Shen, et al., 2013) (Table 2.1). Polymerase Chain Reaction (PCR) was conducted by using Taq DNA Polymerase (Qiagen) in a final reaction volume of 25 µl with 2.5 µl of the diluted genomic DNA (50 ng), 0.5 µM from each primer pairs, 0.2X polymerase buffer, 0.5 units Taq polymerase, 0.5 mM dNTPs and water to 25 µl. The optimized PCR programme had an initial denaturation step at 96 °C for 3 minutes with a Touchdown PCR protocol followed as 11 cycles of 94 °C for 30 seconds, 68 °C to 58 °C for 30 seconds and 72 °C for 2 minutes. Then, it was followed with a PCR protocol beginning with 34 cycles of 94 °C for 30 seconds, 59 °C for 30 seconds, 72 °C for 2 minutes and ending with a final elongation at 72 °C for 5 minutes. To visualize the cloned PCR products, 6X loading dye added to PCR samples before loading onto an agarose gel containing ethidium bromide.

**Table 2.1** Primer sequences used for genotyping *bsk1-1* mutation on *A. thaliana.*

| **Primer Name** | **Sequence** |
|---|---|
| *bsk1-1*_R | GGTTATGGTTAAAGCCAGATTTG |
| *bsk1-1*_F | GCATAGTAAGTAGCATAGACTTGGC |

Digestion mix was prepared directly for each PCR sample produced from each sample DNA according to the manufacturer's protocol. The mix contained; 15 µl of PCR product, 20 units of restriction enzyme BsuRI (HaeIII) from New England Biolabs (NEB), 2 µl of 10X Buffer R, and 13 µl of water. Prepared mixes were incubated at 37 °C for 2 hours. After digestion, 15 µl of digested fragments were run on an 2.4% Agarose gel (9.6 gr Agarose, 400 ml 1X TRIS/acetic acid/EDTA (TAE), 8 µl Ethidium Bromide). 100bp DNA Ladder (NEB #B7025) was used as a reference in the Agarose gel. DNA bands visualized by using AlphaImager EP system.

### 2.1.2. *Brassica oleracea* ssp *alboglabra* (A12DHd) and *B. oleracea* ssp *italica* (Green Duke GDDH33) biparental population

A biparental mapping population of *Brassica oleracea* ssp *alboglabra* (A12DHd) and *B. oleracea* ssp *italica* (Green Duke GDDH33) was produced by Bohuon *et al.,* in order to create an RFLP (restriction fragment length polymorphism) map of *B. oleracea* (Bohuon et al., 1996). Seventy-six double haploid genotypes derived from A12DHd and GDDH33 population and both parental lines were kindly made available from Penny Hundleby and Judith Irwin (JIC, Norwich, UK) (Sparrow et al., 2004). Substitution Lines (SLs) of A12 were kindly provided by Dr Graham Teakle, (Warwick HRI, Coventry UK).

### 2.1.3. *Brassica napus* accessions

Tapidor, Ningyou1, N02D-1952, and Ningyou7 were obtained from *B. napus* diversity set available in Brassica Germplasm Collection Resource Unit at the John Innes Centre. The origin, crop type, and the source of the accessions are summarised in Table 2.2.

**Table 2.2** Details of the *B. napus* accessions used in this study.

| Accession name | Crop type | Origin | Source |
|---|---|---|---|
| Ningyou1 | Semi-winter oilseed rape | China | OCRI, Wuhan |
| Tapidor | Winter oilseed rape | France | UKVGB, Warwick |
| N02D-1952 | Spring oilseed rape | Australia | UKVGB, Warwick |
| Ningyou7 | Semi-winter oilseed rape | China | OCRI, Wuhan |

#### 2.1.3.1. Cross fertilizations

Reciprocal crosses between Tapidor, Ningyou1, N02D-1952, and Ningyou7 were generated by manual crossing. In total 12 different crosses were obtained (Table 2.3). Flower buds that were still closed were selected for crossing to prevent self-pollination. Flower buds were emasculated by leaving the stigma out and hand-pollinating with other accessions' anthers. After manual crossing, the pollinated buds were labelled and covered with bags. The seed pods produced were harvested, threshed, and packed separately.

**Table 2.3** Parental information for 12 crosses generated by using four *B. napus* (Tapidor, Ningyou1, N02D-1952, and Ningyou7) accessions.

| Female ♀ | Male ♂ |
|---|---|
| Ningyou1 | N02D-1952 |
| Ningyou1 | Ningyou7 |
| Ningyou1 | Tapidor |
| Ningyou7 | Tapidor |
| Ningyou7 | N02D-1952 |
| Ningyou7 | Ningyou1 |
| Tapidor | Ningyou7 |
| Tapidor | N02D-1952 |
| Tapidor | Ningyou1 |
| N02D-1952 | Ningyou1 |
| N02D-1952 | Tapidor |
| N02D-1952 | Ningyou7 |

**Table 2.4** Primer sequences used for control and genotyping of $F_2$ plants in Ningyou1 x Ningyou7 population.

| Primer Name | Sequence |
|---|---|
| Saskatoon_sR12095_F | GCTGCGAGGAAATCAGAGTC |
| Saskatoon_sR12095_R | TACACACTTGATCGCGCTTC |
| Bn_FAD2_Sel1+2_F | GTCTCCTCCCTCCAAAAAGT |
| Bn_FAD2_grp13'UTR-R | CAAGACGACCAGAGACAGC |

### 2.1.3.2. Genotyping of heterozygous $F_1$ plants

Five seeds from each $F_1$ seed pack were sown for further use. Leaf samples from each $F_1$ plant were used for DNA isolation. Samples were collected and frozen before being sent to the Genotyping platform service, John Innes Centre. The isolation process was performed by Richard Goram with a DNeasy® Plant kit (Qiagen) according to the manufacturer's protocol. Publicly available microsatellite markers (http://www.brassica.info/resource/markers/ssr-exchange.php) were used to detect polymorphic markers between the parental accessions. The sequences of the microsatellite markers and a control primer set (FAD2) were kindly supplied by Rachel Wells (Wells et al., 2014). The sR12095-Saskatoon marker defined polymorphism between the parental accessions as the primer pair amplified different bands for each parent (Table 2.4).

Amplification of sR12095-Saskatoon primer product;

Polymerase Chain Reaction (PCR) was conducted by using AmpliTaq Gold™ DNA Polymerase (ThermoFisher) in a final reaction volume of 20 µl with 2 µl of the diluted genomic DNA (100 ng), 0.5 µM from each primer pairs, 2 µl PCR buffer, 1 units AmpliTaq Gold™ DNA Polymerase (5 u/µl), 2.5 mM dNTPs and water to 20 µl. The optimized PCR programme had an initial denaturation step at 94 °C for 10 minutes with a PCR protocol followed as 8 cycles of 94 °C for 15 seconds, 50 °C for 15 seconds and 72 °C for 30 seconds. Then, it was followed with a PCR protocol beginning with 32 cycles of 94 °C for 15 seconds, 50 °C for 15 seconds, 72 °C for 30 seconds and ending with a final cool down at 8 °C.

Amplification of FAD2 primer set product;

AmpliTaq Gold™ DNA Polymerase (ThermoFisher) was used in a final reaction volume of 20 µl with 2 µl of the diluted genomic DNA (100 ng), 0.5 µM from each primer pairs, 2 µl PCR buffer, 1 units AmpliTaq Gold™ DNA Polymerase (5 u/µl), 2.6 mM dNTPs and water to 20 µl. The optimized PCR programme had an initial denaturation step at 94 °C for 5 minutes with a PCR protocol

followed as 35 cycles of 94 °C for 30 seconds, 57 °C for 30 seconds and 72 °C for 1 minute. Then, it was followed with a final extension with 72 °C for 10 minutes and ended with a final cool down at 12 °C.

To visualize the amplified PCR products, 6X loading dye was added to PCR products before loading onto an agarose gel containing ethidium bromide. To visualize the amplified fragments, 15 µl of PCR products were run on a 3.0% Agarose gel (12 gr Agarose, 400ml 1X TRIS/acetic acid/EDTA (TAE), 8 µl Ethidium Bromide). 100bp DNA Ladder (NEB #B7025) and 1kb DNA Ladder (NEB #B7025) were used as a reference in the Agarose gel. DNA bands visualized by using AlphaImager EP system.

#### 2.1.3.3. Creation of $F_2$ segregant population

After microsatellite marker screening of the $F_1$ individual crosses, plants identified as genotypically homozygous were discarded. Plants confirmed as successfully crossed with a heterozygous genotype were selfed to investigate possible segregation in $F_2$ individual plants. Ningyou1 (responsive to NLP) and Ningyou7 (non-responsive to NLP) were used to create the main segregating population by self-pollination of the NLP-responsive and genotypically heterozygote $F_1$ plants. In total 960 $F_2$ seeds from four different seed packs were sown and grown under Controlled Environment Room (CER) conditions, as described in section 2.2.2. The sowings were carried out in four different batches - each week ~240 seeds were sown from five independent $F_1$ plants of Ningyou1 and Ningyou7 crosses (Table 2.5).

**Table 2.5** Four seed packs belong to Ningyou1 and Ningyou7 parents were sown to grow each individual $F_2$ plants to further use in the Bulk-segregant Analysis.

| Sowing date | Seed Pack | Quantity |
|---|---|---|
| 03/05/2018 | Nin7xNin1-1 | 230 |
| 10/05/2018 | Nin1xNin7-2 | 240 |
| 24/05/2018 | Nin7xNin1-1 | 235 |
| 31/05/2018 | Nin7xNin1-2 | 220 |

## 2.2. Plant growth conditions

### 2.2.1. *Arabidopsis thaliana*

*Arabidopsis thaliana* plants were sown in *A. thaliana* mix soil in 24-cell trays. Seeds were stratified by leaving in the dark for two days at 4-5 °C. Trays were covered with a transparent plastic lid to increase the humidity for the first 1-2 weeks. After stratification, plants were grown at 20-22 °C / 18-20 °C day / night and 70% relative humidity under a 10 hours light and 14 hours dark cycle in a walk-in cabinet. Plants were grown for 5-6 weeks before phenotyping further.

### 2.2.2. *Brassica napus*

Parental lines and $F_1$ plants were sown in Levington F2 with Grit and grown in a lit glasshouse with a 16-hour photoperiod at 18 °C / 12 °C day / night temperatures until they were ready to harvest the seeds (~6 months). Glasshouse grown plants were maintained by Catherine Taylor from Field & Horticultural Services, John Innes Centre. $F_2$ plants were grown under Controlled Environment Rooms (CERs) conditions; at 22 °C and 70% relative humidity under a 10 hours light and 14 hours dark cycle. The seeds were sown in Levington F2 with grit and grown for 4-5 weeks for sampling and phenotyping.

### 2.2.3. *Brassica oleracea*

Seventy-six double haploid genotypes derived from A12DHd and GDDH33 population, including thirteen Substitution Lines (SLs) (Ramsay et al., 1996) and both parental lines (A12 & GD) were grown under Controlled Environment Room (CER) conditions as described in the section for *B. napus* (section 2.2.2). The Control group was grown under normal watering conditions for 6 weeks. (~20 ml water every day).

#### 2.2.3.1. Drought stress conditions

The stress conditions causing induction in ROS response of AG1012 line from A12DHd and GDDH33 population were not defined. To define the stress conditions, different growing conditions with various temperatures and watering regimes were tested (Table 2.6).

**Table 2.6** Different temperature and watering regime treatments to 4 weeks old A12, Green Duke, and AG1012 for 2 weeks.

| Temperature | Water |
|---|---|
| 6 °C | Drought |
| 6 °C | High humidity |
| 21 °C | Control |
| 21 °C | Drought |
| 27 °C | High humidity |
| 27 °C | Drought |

Abiotic stress was applied to the drought stress group of plants after 4 weeks of growth under normal watering conditions. The stress was applied for 2 weeks by watering them only with 5 ml water on Monday, Wednesday, and Friday. To allow normal stabbing to sample the leaf tissue, all plants in the drought stress group were rehydrated by full watering a day before the phenotyping and sampling.

## 2.3. Reactive Oxygen Species (ROS) Assay

### 2.3.1. Detection of oxidative burst

This Luminol/peroxidase based assay was carried out to measure the Reactive Oxygen Species (ROS) produced as PAMP response in plant samples. 4mm leaf discs from *B. napus* (3rd leaf), *B. oleracea* (3rd leaf), or *A. thaliana* plants were taken using a tissue sampler and incubated in 200 µl of sterile water in a 96-well plate for overnight at room temperature in dark conditions. The water was drained and replaced by 100 µl solution containing; 0.2 nM luminol at 34 mg/l, horseradish peroxidase (HRP) at 20 mg/l, and the selected PAMP at concentrations of 50 nM, 10 nM or 2 nM. The luminescence was recorded over a 40-minute period and displayed as photon production quantitated as relative light units (RLUs) over this period. Luminol and HRP were obtained from Sigma. Emitted photons were counted using a Varioskan Flash plate reader (ThermoFisher Scientific, Waltham, MA, USA).

### 2.3.2. Pathogen Associated Molecular Pattern (PAMP) Peptides

Peptides of flg22 (22 amino acid long flagellin fragment; QRLSTGSRINSAKDDAAGLQIA) and elf18 (the first 18 amino acids at the N-terminus of bacterial elongation factor Tu; Ac-SKEKFERTKPHVNVGTIG) peptides were ordered from Peptron (http://www.peptron.co.kr, Korea) dissolved in sterile $H_2O$ at 10 mM. BcNEP2 (Botrytis cinerea Necrosis and Ethylene-inducing protein 2; AIMYSWYMPKDEPSTGIGHRHDWE) were supplied from Genscript (www.genscript.com) at 87.5% purity and dissolved in DMSO at 10 mM. Chitin (NA-COS-Y) was provided by Yaizu Suisankagaku Industry CO (Yaizu, Japan) and suspended in sterile $H_2O$ (100 g/l) and autoclaved before use. Flg22, elf18, BcNEP2 were aliquoted to 100 µM in H2O and stored at -20 °C before use.

## 2.4. *Botrytis cinerea* disease assays

### 2.4.1. Maintaining *Botrytis cinerea* isolates

*Botrytis cinerea* strain B05.10 and the camalexin sensitive mutant ΔBcatrB4 strain in the same background was kindly provided by Henk-jan Schoonbeek (John Innes Centre, Norwich, UK). All *B. cinerea* strains were grown on 1/5 Potato Dextrose Agar (PDA) or on MEYAA plates including; Malt Extract Agar (MEYA, OXOID# CM0059) at 30 g / l with Yeast extract at 2g/l and Agar (FORMEDIUM) at 5 g / l at 21 °C with no selection. *B. cinerea* plates were grown at least for 2 weeks before collecting the spores for inoculations.

### 2.4.2. Collecting *B. cinerea* spores

After 2 weeks of growth in a growth cabinet at 21 °C, a matt of aerial hyphae was becoming clearly visible on the *B. cinerea* plates. 15 ml water with 0.05% tween 80 was used to scrape the spores from the plate with the help of an L-shaped spreader. After collecting the solution, glass wool was placed in 5 ml pipette tips for use as a filter to prevent the mycelium from mixing with the spores in the solution. After collection, spore concentration was measured by using a haemocytometer and adjusted to $2.5x10^7$; the spores were then stored at 4 °C. Fresh spores were collected less than 3 days before each experiment.

### 2.4.3. *Botrytis cinerea* inoculation

#### 2.4.3.1. Inoculation of *B. napus* and *B. oleracea* plants

One day prior to the inoculation of *B. napus* and *B. oleracea* leaf discs, 200 µl from *B. cinerea* spores with $2.5x10^6$ spores/ml concentration were spread on 1/5 PDA plates and grown at 21 °C with no selection. One day prior to *B. cinerea* inoculation, 22 mm width leaf discs were cut from each individual *B. napus* and *B. oleracea* plants using a cork-borer the $4^{th}$ leaf being used in most cases. Up to 16 technical replicates were placed on water agar plates in square Petri dishes and left in the dark overnight. The next day, the leaf discs were inoculated with 4 mm diameter *B. cinerea* plugs. Only B05.10(wt) strain was used for disease assay with *B. napus* and *B. oleracea* plants. Plates with inoculated leaf discs were incubated in the growth cabinet at 21 °C. The lesion size was measured after 3 days with a digital caliper (Figure 2.1).

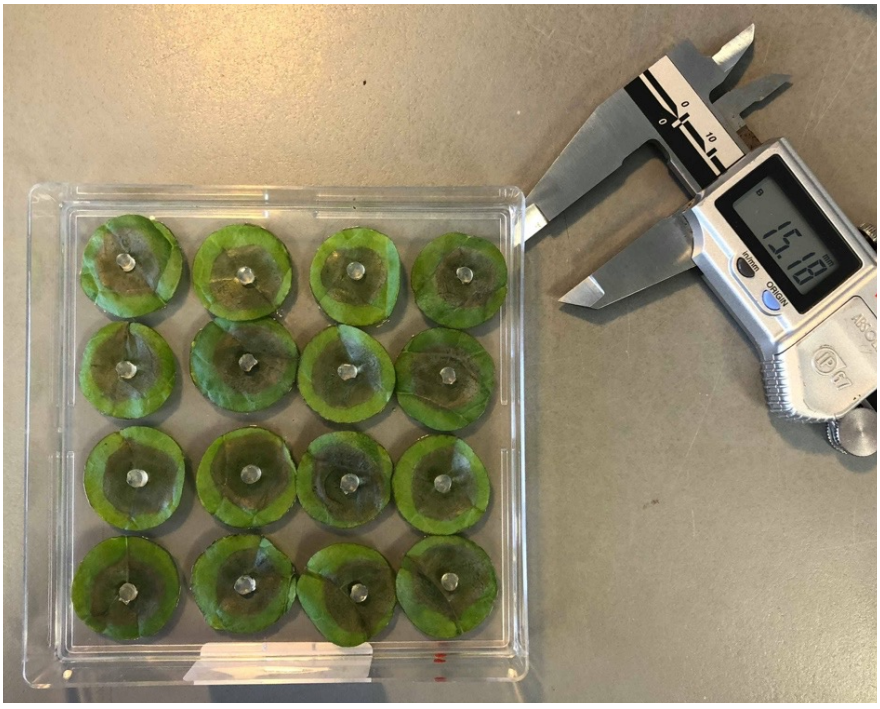

**Figure 2.1** *B. cinerea* inoculated six-week-old *B. oleracea* leaf discs. The plate was photographed after 3 days of inoculation.

#### 2.4.3.2. Inoculation of *A. thaliana* plants

Prior to inoculation of *A. thaliana* plants, *B. cinerea* spores were diluted to obtain $2.5x10^5$ spores/ml concentration in 1⁄2 PDB solution and left in room temperature for 90 minutes on a shaker. Whole plants in 24-cell trays were used for the assay, 5 µL droplets from the spore solution were placed on selected 5-6 leaves of one of the plants. B05.10 strain and ΔBcatrB4 strain could be placed on the same leaf at the same time; one on the upside left and one on the downside right of the adaxial leaf surface. Then to create a stable humidity environment for the plants, the trays were carefully covered with plastic lids and sealed with parafilm. The sealed trays were then placed in a growth cabinet at 21°C. The lesion size was measured after 3 days with a digital caliper (Figure 2.2).

**Figure 2.2** *B. cinerea* inoculated five-week-old *A. thaliana* plant. The plant was photographed after 3 days of inoculation.

## 2.5. Quantification of Gene Expression (*A. thaliana*)

### 2.5.1. PAMP pre-treatment

5-week old Col-0 and *bsk1-1* mutant *A. thaliana* plants were grown as described in section 1.2.1. For PAMP treatment, 100 nM BcNEP2 was dissolved in water with 0.01% DMSO prepared and injected to at least 6 leaves of individual plants from the Treatment group. Plants belonging to the control (Mock) group were injected with Mock solution (Water with 0.01% DMSO). Each leaf was injected with ~200 µl solution using a 1 ml syringe. Samples were collected at different time points; 0h, 12h, and 24h. Mock or 100 nM BcNEP2 treated leaf samples were frozen in -80 °C using liquid nitrogen. Additionally, for no-Treatment, samples were collected from 3 Col-0 and 3 *bsk1-1* plants. At least 3 biological replicates were performed for each treatment. 3 technical replicates were used from each biological replicate.

### 2.5.2. RNA isolation

In total, sixty-six frozen samples were carefully ground into a fine powder using liquid Nitrogen in mortar and pestles. RNA was extracted with the RNeasy® plant mini kit (QIAGEN) according to the manufacturer's protocol. After isolation, each isolated RNA sample was treated with DNAse to remove the DNA. TURBO DNA-*free*™ kit (INVITROGEN) was used according to the manufacturer's protocol.

### 2.5.3. Complementary DNA (cDNA) synthesis

To synthesize the cDNA, SuperScript IV™ Reverse Transcriptase (INVITROGEN) was used according to the manufacturer's protocol. The reaction volume was adjusted to 20 µl with 1 µg of DNase-treated RNA in it.

### 2.5.4. Quantitative Reverse Transcription Polymerase Chain Reaction (qRT-PCR)

Primers used in this study were designed using Primer3Plus software (Untergasser et al., 2007). At least two primer pairs were designed for each gene of interest. Primers were ordered from Sigma and amplification efficiencies of each primer pairs were tested with a cDNA dilution series. Only primer pairs with amplification efficiencies over 90-100% were selected for qRT-PCR analysis. Sequences of the primers used are shown in Table 2.7. Melting curve analysis was used for each primer pair to determine their specificity. A LightCycler LC480 system was used to complete all the qRT-PCR analyses, which were carried out in 384-well plates. Each of the reactions was performed with 12 µl reaction mix containing 1:20 diluted cDNA. SYBR® Green JumpStart™ Taq from Sigma-Aldrich was used according to the manufacturer's protocol. The qRT-PCR programme was 96 °C for 4 minutes, followed by 45 cycles at 94 °C for 19 seconds, 60 °C for 19 seconds and 72 °C for 22 seconds. cycle threshold (CT) values were used to determine the relative transcript levels according to the 2ΔCT method using ACTIN as a reference (H. Shi, Shen, et al., 2013). To calculate the fold induction, transcript levels of the genes in BcNEP2-treated samples were compared with Mock treated controls.

**Table 2.7** Primer sequences used in *A. thaliana* qRT-PCR analysis.

| Primer Name | Sequence | Author / Reference |
|---|---|---|
| Tang_ACTIN_F | TCTCCCGCTATGTATGTCGCC | H. Shi et al., 2013 |
| Tang_ACTIN_R | GTCACGTCCAGCAAGGTCAAGA | H. Shi et al., 2013 |
| RT_BSK1_F | TGAGAAAGCCCCAAATCTTGT | Yalcin: This study |
| RT_BSK1_R | ATGCTTCTTCCGCAAATTGTT | Yalcin: This study |
| RT_RLP23_F | TTGGTCTCTTGAAGGCACTGA | Yalcin: This study |
| RT_RLP23_R | AACGAAATGCTCCCTAGTCCA | Yalcin: This study |
| RT_WRKY33_F | GGAAAGGGGACAATGAAACAA | Yalcin: This study |
| RT_WRKY33_R | CGACTTTCTGGCCGTATTTTC | Yalcin: This study |
| RT_JAR1_F | TTACGCGGGTGATCTACCTCT | Yalcin: This study |
| RT_JAR1_R | AACCGGTTTCTCCTCTCCTTC | Yalcin: This study |

## 2.6. Genomic studies

### 2.6.1. Bulk Segregant Analysis (BSA)

#### 2.6.1.1. Experimental design - the creation of the pools

BcNEP2-induced ROS response data from the $F_2$ population was normally distributed. Extremes from the tails of the normal distribution representing ~5% of the population were selected to create the pools. The number of the lines selected was based on the calculation of 5% of 747 NLP-responder lines, which equaled 37. Therefore, 30 lines were selected per each pool. The phenotypic characteristics of the pools created are shown in Table 2.8.

**Table 2.8**: The phenotypical features of the selected individuals from $F_2$ population for the BSA pools.

| Phenotype | Pool1 | Pool2 | Pool3 | Pool4 |
|---|---|---|---|---|
| Magnitude of flg22-induced ROS response | Low | High | Low | High |
| BcNEP2 recognition (-/+) | - | - | + | + |
| Magnitude of BcNEP2-induced ROS response | - | - | Low | High |

**Note:** Individual $F_2$ plants were selected based on their magnitude of BcNEP2- and flg22-induced ROS reponses and their ability to recognize BcNEP2 molecule. "Low" PAMP-induced ROS response is stating individuals with ROS response lower than 1.0E5 RLU. "High" PAMP-induced ROS response is stating individuals with ROS response higher than 8.0E5 RLU. - Classification of the individual plants according to their ability to recognize BcNEP2 molecule states as "-" for blind individual plants and "+" for the responders.

#### 2.6.1.2. High quality DNA isolation for Illumina sequencing

In order to isolate high-quality DNA from the *B. napus* leaf tissues 'DNA preparation from Brassica for Illumina Sequencing' was used, the protocol being kindly supplied by Rachel Wells. Leaf tissue from each individual $F_2$ plant was collected and frozen at -80 °C using liquid Nitrogen. The samples were kept in -70 °C freezer until the isolation step. 0.05 g leaf samples from each selected line were bulked during the grinding step to create the DNA pools. To ensure the same quantity of samples used for each pool and the parental samples, in total 1.5g of leaf sample from Ningyou1 and Ningyou7 was used for DNA isolation.

Reagents used in this DNA isolation method;

***Nuclei Extraction Buffer (NEB)***

*10 mM TRIS-HCl (pH:9.5)*

*10 mM EDTA (pH:8.0)*

*100 mM KCl*

*500 mM Sucrose*

*4 mM Spermidine*

*1 mM Spermine*

*0.1% β-mercaptoethanol*

***Lysis Buffer***

*10% Triton-x*

*90% Nuclei Extraction Buffer*

***CTAB Extraction Buffer***

*100 mM TRIS-HCl (pH:7.5)*

*0.7 M NaCl*

*10 mM EDTA (pH:8.0)*

*%1 CTAB (adjusted in this study, originally in SOP; 0.1%)*

*%1 β-mercaptoethanol*

*3M NaAc*

*Chloroform/Isoamyl Alcohol (24:1)*

*Phenol/Chloroform/Isoamyl Alcohol (24:23:1)*

*Proteinase K (10 µg/µl)*

*RNase A (10 µg/µl)*

*RNase T1 (1000u/µl)*

Leaf tissues were ground to a fine powder by using mortars and pestles in liquid Nitrogen. Ground tissue was added to a 50 ml Falcon tube containing 40 ml ice-cold NEB. The tubes were vortexed until the ground tissue was evenly distributed. Homogenised tissue then filtered through two layers of Miracloth (Calbiochem) in a funnel to a new 50 ml Falcon tube. Then, 8 ml Lysis buffer were added, and tubes were kept on ice for 2 minutes. After that, the tubes were centrifuged at 1000 rcf for 20 minutes at 4 °C in order to obtain the nuclei as a pellet. The supernatant was removed and discarded. The pellet was resuspended in pre-warmed 3 ml CTAB Buffer and incubated at 60 °C water bath for 30 minutes. After incubation, an equal volume of Chloroform/Isoamyl Alcohol was added to lyse the sample and rotated in a cold room (5 °C) for 10 minutes. The sample was centrifuged at 1000 rcf for 10 minutes at 4 °C. The aqueous phase was removed, then 0.15 µl RNase T1 and 15 µl RNase A were added to the sample tube and incubated in a water bath at 37 °C for 45 minutes. Then, 30 µl of Proteinase K was added to a 3ml solution, and the sample was incubated further at 37 °C for 45 minutes. An equal volume of Phenol/Chloroform/Isoamyl Alcohol was added to the sample tube and mixed by inverting the tube for ~20 times. The sample was then centrifuged at 1000 rcf for 10 minutes, and the supernatant was retained. The treatment with Phenol/Chloroform/Isoamyl Alcohol was repeated. To ensure the high purity of the isolated DNA, further treatment with Chloroform/Isoamyl Alcohol was performed by adding to the lysed sample, rotating in a cold room (5 °C) for 10 minutes and centrifuging at 1000 rcf for 10 minutes. DNA was precipitated by adding 10% 3M NaAc and 3X volume of 100% Ethanol to each tube, after which the DNA spindles became visible. The sample tubes were centrifuged gently, and the ethanol was removed. The pellet was air-dried and gently resuspended in 50 µl $H_2O$. The final DNA concentration was measured using a Nanodrop and DNA samples were run on 1% Agarose gel to visualize any possible degradation.

#### 2.6.1.3. Sequencing

The prepared DNA samples were sent to Novogene (Cambridge, UK) following the company's recommendations. With a sequencing plan of 40x coverage for each sample, 350bp insert DNA library was used for sequencing of the bulked pools and parents, and 150-bp paired-end reads were generated with Illumina sequencing.

#### 2.6.1.4. Data analysis

All the code used in this PhD study is available on the github repository: https://github.com/hicretyalcin/BSA_Brassica_napus.

##### 2.6.1.4.1. Quality control of sequenced reads

The quality of the sequencing results was evaluated with FastQC v0.11.8 (https://www.bioinformatics.babraham.ac.uk/projects/fastqc/).

##### 2.6.1.4.2. Alignment of the reads

150-bp paired-end reads from each sequenced sample generating 40X coverage were aligned to *B. napus* reference genome Darmor-*bzh* (https://wwwdev.genoscope.cns.fr/brassicanapus/data/) using *bwa* v0.7.1(H. Li & Durbin, 2010). From each alignment, a corresponding SAM file was created. Then, SAM files converted to BAM files using *samtools* v1.9 (H. Li et al., 2009). The converted BAM files were sorted, the duplicates were removed and all bam files containing data from the same pool where merged in a single BAM file.

#### 2.6.1.4.3. INDELs and SNP-calling

After indexing all the BAM files, they were ready for SNP calling using *freebayes* v1.1.0.46(Garrison & Marth, 2012). The variations from each chromosome were called separately, and then the obtained Variant Call Format (VCF) files were concatenated using *bcftools* v1.8 (Danecek et al., 2011).

#### 2.6.1.4.4. Filtering the variations

In order to exclude the variations with quality lower than 2000, depth lower than 20 and also to exclude the variations coming from Darmor-*bzh*, filtering had been applied using *bcftools-1.8*.

#### 2.6.1.4.5. Calculation of Bulk Frequency Ratios (BFRs)

The scoring was made by calculating the ratio between the frequency of each informative base at each variation position of the pools. For variations with an informative base derived from a responsive background, the BFRs were calculated by dividing the frequency in the responsive bulk by the frequency in the non-responsive bulk (Trick et al., 2012)

#### 2.6.1.4.6. *In silico* mapping

Histogram plots of the depths and the quality of the variations were created by using *R* v3.6.1 with *ggplot2* package (https://ggplot2.tidyverse.org/ , Wickham, 2016). The *ggplot2* package was also used to create the Manhattan plots with BFR values of each variation anchored to the chromosomes.

#### 2.6.1.4.7. Prediction of functional effects of variations

*SnpEff* (http://snpeff.sourceforge.net/), a functional effect prediction toolbox, was used for further evaluation of the variations obtained through the BSA pipeline. It annotates and predicts the effects of genetic variants on genes and proteins (Cingolani et al., 2012). Variations on each specific chromosome with peaks associated with the trait were obtained by using "grep" command then run in the analysis. Then the related information from VCF files obtained through *SnpSift* (http://snpeff.sourceforge.net/SnpSift.html). After that, VCF files converted to TXT file format by using *bcftools* v1.8 (Danecek et al., 2011) to prepare the input for running.

#### 2.6.1.4.8. Data Mining - BioMart

The output from *SnpEff* provided the information about annotated genes which might be affected most. Those genes are evaluated as candidate genes, and the web-based tool BioMart (Durinck et al., 2005, 2009) was used as Data-mining tool. The candidate gene list was sent as a query to identify any possible *A. thaliana* homologues and coded domain features of the *B. napus* genes.

#### 2.6.1.4.9. KASP primer design

KASP markers were developed by using PolyMarker (Ramirez-Gonzalez, Uauy, et al., 2015). A 200bp genomic sequence, including the SNP, was generated to start the pipeline. The SNP must be defined in the format [A/T] for a varietal SNP with alternative bases, A or T. Designed primers included standard FAM or HEX compatible tails (FAM tail: 5' GAAGGTGACCAAGTTCAT- GCT 3'; HEX tail: 5' GAAGGTCGGAGTCAACGGATT 3') for the KASP assay (Table 2.9) were ordered from Sigma.

#### 2.6.1.4.10. KASP assay

For the KASP assay, DNA was isolated from samples with known phenotypes from the $F_2$ population. The DNA plate contained 21 lines from: each bulked Pool (Pool1, Pool2, Pool3, and Pool4); 3 individual plant DNA samples from Ningyou1; 3 individual plant DNA samples from Ningyou7; and DNA samples of 6 different NLP-responsive *B. napus* lines (Swu8, Yudal, Chuanyou2, Tribune, Taisetsu, and ZS11) respectively. The primers were ordered from Sigma. DNA isolation and the validation of the SNPs was conducted by Richard Goram from Genotyping platform service, John Innes Centre.

#### 2.6.1.4.11. Genetic Map construction

Linkage analysis was made by using R version 3.6.1 with the *qtl* package version 1.46-2 (Broman, 2010). The output of the linkage analysis was first sorted automatically in excel according to each sample's genotype, then adjusted and re-submitted to linkage analysis. The output was then used to calculate the genetic distances of each marker to the phenotype based on recombination frequency.

**Table 2.9** KASP primer sequences and designed SNPs. The KASP markers used in the QTL mapping are stated as (Y) in Used section of the table.

| Name | Used | Reference | Alternative | Chromosome | SNP_type | A | B | Common | Primer Type | Orientation | Product Size |
|---|---|---|---|---|---|---|---|---|---|---|---|
| Nlp_1 | N | T | A | chrA04 | non-homoeologous | gagttggtagtaacttCgctactA | gagttggtagtaacttCgctactT | gctacccaagagaaacGgattT | chromosome_specific | reverse | 67 |
| Nlp_2 | N | T | A | chrA04 | non-homoeologous | ctacagaggcattatcacccttT | ctacagaggcattatcacccttA | aggcaagCgaggttaagtcG | chromosome_specific | forward | 84 |
| Nlp_3 | Y | C | A | chrA04 | non-homoeologous | ggaagatgaaggggagatggtC | ggaagatgaaggggagatggtA | tcttggaaacatctgcggca | chromosome_nonspecific | forward | 50 |
| Nlp_4 | N | A | G | chrA04 | non-homoeologous | tctaccccacccgaaatcT | tctaccccacccgaaatcC | tctgttgccgggtcgacC | chromosome_specific | reverse | 57 |
| Nlp_5 | Y | G | T | chrA04 | non-homoeologous | cttatcagtAtgccacaAaccagtC | cttatcagtAtgccacaAaccagtA | tgtcaaggttctAggacgggttT | chromosome_specific | reverse | 50 |
| Nlp_6 | Y | G | A | chrA04 | non-homoeologous | agcaatgagtttcagcctgtG | agcaatgagtttcagcctgtA | agcctgtattgcagctccag | chromosome_nonspecific | forward | 60 |
| Nlp_7 | Y | A | C | chrA04 | non-homoeologous | gcctttggctaagattaaaagcatA | gcctttggctaagattaaaagcatC | ccagCAggagtcaCgttcT | chromosome_specific | forward | 54 |
| Nlp_8 | Y | A | G | chrA04 | non-homoeologous | ccctcacctttcttagttttgattT | ccctcacctttcttagttttgattC | cgatgaatgtttagggtttcgt | chromosome_nonspecific | reverse | 52 |
| Nlp_9 | Y | G | T | chrA04 | non-homoeologous | gctagagaacggtttttggctC | gctagagaacggtttttggctA | acagaagaaaaagTtgaccaaaagA | chromosome_specific | reverse | 87 |
| Nlp_10 | N | C | T | chrA04 | non-homoeologous | tgaaggtgatagtgaagactgatC | tgaaggtgatagtgaagactgatT | tGgTaACTtactaGcgattGtGtaT | chromosome_specific | forward | 108 |
| Nlp_11 | Y | C | T | chrA04 | non-homoeologous | tgggagatacgagcttgcaG | tgggagatacgagcttgcaA | ccacgcttatagctgatgcA | chromosome_specific | reverse | 55 |
| Nlp_12 | Y | A | G | chrA04 | non-homoeologous | aatgagtttggaaggtgcgT | aatgagtttggaaggtgcgC | acaaacccaaattctccCcA | chromosome_specific | reverse | 59 |
| Nlp_13 | N | G | A | chrA04 | non-homoeologous | cactcacttttgtCggacctC | cactcacttttgtCggacctT | tcccttccttcTCaATTTtCAAttT | chromosome_specific | reverse | 110 |
| Nlp_14 | N | G | A | chrA04 | non-homoeologous | gtgtAaaagataagtggtttcgcC | gtgtAaaagataagtggtttcgcT | GtgtgtttCaCagctccatG | chromosome_specific | reverse | 52 |
| Nlp_15 | Y | T | C | chrA04 | non-homoeologous | ttgtctgtttccaaaagcaaaattT | ttgtctgtttccaaaagcaaaatC | agattgcgaaacaaaagtactgtC | chromosome_specific | forward | 139 |
| Nlp_16 | Y | T | G | chrA04 | non-homoeologous | ccttttttctcgtacgttttgggT | ccttttttctcgtacgttttgggG | acgaaattgagggtttagtggaga | chromosome_nonspecific | forward | 120 |
| Nlp_17 | Y | C | T | chrA04 | non-homoeologous | tcccaatttggtgaggaatgC | tcccaatttggtgaggaatgT | tctctccacaaacctccggt | chromosome_nonspecific | forward | 74 |
| Nlp_18 | Y | A | T | chrA04 | non-homoeologous | ttatttaggtacAggaaGgacttgT | ttatttaggtacAggaaGgacttgA | CgccccgattGgaaaagT | chromosome_specific | reverse | 81 |
| Nlp_19 | Y | T | A | chrA04 | non-homoeologous | acaaagacattttggcctctaaaaA | acaaagacattttggcctctaaaaT | gcttcatcattctgctgctaca | chromosome_nonspecific | reverse | 88 |
| Nlp_20 | N | G | A | chrA04 | non-homoeologous | agtttagtggtCGtagtcatgtaG | agtttagtggtCGtagtcatgtaA | gcgttggTtagataacaagaaaagT | chromosome_specific | forward | 71 |
| Nlp_21 | N | C | A | chrA04 | non-homoeologous | gcctcaagggtcacttcaagG | gcctcaagggtcacttcaagT | tggcggcttttgagaacaaa | chromosome_nonspecific | reverse | 102 |
| Nlp_22 | N | A | T | chrA04 | non-homoeologous | tCaaggCtataaggaatttaaggcA | tCaaggCtataaggaatttaaggcT | tcaaacaagtggaataacgttaaCA | chromosome_specific | forward | 56 |
| Nlp_23 | Y | A | C | chrA04 | non-homoeologous | gctcaatcacagatcggtttgtT | gctcaatcacagatcggtttgtG | tttcggtatcGtGcttatggaG | chromosome_specific | reverse | 50 |
| Nlp_24 | N | G | A | chrA04 | non-homoeologous | aggggtttagggctgtgG | aggggtttagggctgtgA | tgtccccatttttcgttttgtattT | chromosome_specific | forward | 74 |
| Nlp_25 | N | A | T | chrA04 | non-homoeologous | tcAgtatcaaatCcaagacaaggA | tcAgtatcaaatCcaagacaaggT | tggcatgtcaacataatagttaacG | chromosome_specific | forward | 108 |
| Nlp_26 | N | G | C | chrA04 | non-homoeologous | agagtaaaacgcAgaggagatC | agagtaaaacgcAgaggagatG | Ggttggtctcaccccgaat | chromosome_semispecific | reverse | 58 |
| Nlp_27 | Y | A | T | chrA04 | non-homoeologous | gccaaaAccaAtgaaGTttgCT | gccaaaAccaAtgaaGTttgCA | gagaaagaaccggagaCtgtT | chromosome_specific | reverse | 57 |
| Nlp_28 | Y | C | A | chrA04 | non-homoeologous | atgctgccgctgacAcCG | atgctgccgctgacAcCT | AGAaGgtaCCgatAGTtaGTtAGTG | chromosome_specific | reverse | 84 |
| Nlp_29 | Y | T | C | chrA04 | non-homoeologous | ggagttgatgtgGtcttgttgA | ggagttgatgtgGtcttgttgG | caaggcgtagttgaaacaagtaC | chromosome_specific | reverse | 96 |
| Nlp_30 | N | G | A | chrA04 | non-homoeologous | TgccaccgctgctagctC | TgccaccgctgctagctT | ctaaAtcagtTgctaaggtaACaCT | chromosome_specific | reverse | 111 |
| Nlp_31 | Y | G | T | chrA04 | non-homoeologous | tctgcTgtTgaatcTaatcaggttC | tctgcTgtTgaatcTaatcaggttA | cacAAgCTGAAacaaATtCTGaAC | chromosome_specific | reverse | 74 |
| Nlp_32 | Y | C | G | chrA04 | non-homoeologous | cactatcgacggtggttcC | cactatcgacggtggttcG | tcatTaacgccaaacaagtagaaG | chromosome_specific | forward | 57 |
| Nlp_33 | N | T | A | chrA04 | non-homoeologous | tcttAaTgagccaCtccggtttA | tcttAaTgagccaCtccggtttT | GACaatagcacaCCtCaTtgcA | chromosome_semispecific | reverse | 50 |
| Nlp_34 | Y | A | G | chrA04 | non-homoeologous | aacggtcagcgacatcaaA | aacggtcagcgacatcaaG | ccggtttgtCtggaTtgTtgA | chromosome_specific | forward | 60 |
| Nlp_35 | Y | A | C | chrA04 | non-homoeologous | tGtgtttgacaaggggctCtA | tGtgtttgacaaggggctCtC | aaccCaaagtctttactTctTccT | chromosome_specific | forward | 50 |
| Nlp_36 | N | A | G | chrA04 | non-homoeologous | tgaacggtccaaaacatgtcA | tgaacggtccaaaacatgtcG | CGaaagctggtgatgattctatT | chromosome_specific | forward | 52 |
| Nlp_37 | N | A | C | chrA04 | non-homoeologous | gcataccagcatctgcatttcA | gcataccagcatctgcatttcC | gggctccttgatgtagggaac | chromosome_nonspecific | forward | 57 |
| Nlp_38 | N | T | A | chrA04 | non-homoeologous | gagatggCtcatcatcatcatcT | gagatggCtcatcatcatcatcA | actccactcgtgatatgtacgA | chromosome_specific | forward | 71 |
| Nlp_39 | N | T | G | chrA04 | non-homoeologous | atggtttcttccagtatgctcA | atggtttcttccagtatgctcC | tgtgttgtagctggcgagtt | chromosome_nonspecific | reverse | 53 |
| Nlp_40 | N | C | T | chrA04 | non-homoeologous | gctagtgccaagtttaggaaaaC | gctagtgccaagtttaggaaaaT | atgcacaccttgtttacctct | chromosome_nonspecific | forward | 136 |
| Nlp_41 | N | G | T | chrA04 | non-homoeologous | gatcgtgttttcttggttcacG | gatcgtgttttcttggttcacT | cctgtagcctcgaacacaaga | chromosome_nonspecific | forward | 87 |

### 2.6.2. QTL mapping

The QTL mapping pipeline was created and completed by Dr. Peter Walley, University of Liverpool. The analyses were based on methods described in a previous study conducted for the creation of *B. oleracea* L. var. *italica* 'intra-crop' specific framework linkage map (Walley et al., 2012). Quantitative trait loci were estimated using MapQTL v6.0 (Ooijen, 2009) with first Interval Mapping (IM) followed by Multiple-QTL Mapping (MQM) analyses (Jansen, 1993). Genome-wide significance thresholds ($\alpha = 0.05$) were determined by permutation test (n.perm = 1, 000 iterations). Putative QTL intervals were delimited using a specific LOD approach, i.e., the 1.5-LOD support interval (cM) created as a reduction in peak LOD of +/- 1.5 LOD from the peak LOD score (Broman, 2001). QTL coordinates were illustrated relative to the framework linkage map using MapChart v2.2 (Voorrips, 2002). QTL were named according to the growth conditions, trait, and the linkage group number (with sequential numbering if more than one QTL for the same trait on a linkage). Growth condition abbreviations: C - Control, D - Drought, FC - Fold Change (in between the ROS response of drought treated plants and controls), $\Delta$ - Difference in lesion size (in between 2 different treatments). As, "Growth_condition/Difference_trait name_ QTL number" for example "D_50nM_flg22_7.0".

### 2.6.3. RNA Sequencing (RNA-seq)

#### 2.6.3.1. RNA isolation

For RNA sequencing, A12, GD, and AG5005 lines were used, grown under 2 different treatments - drought stress and control, as described in section 2.2.3. Three leaf samples each from individual plants were pooled to obtain one biological replicate, and 3 technical replicates were sent for sequencing from each sample. Samples were carefully ground into a fine powder using mortars and pestles. RNA was extracted with the RNeasy® plant mini kit (QIAGEN) according to the manufacturer's protocol. After isolation, each isolated RNA was treated with DNAse to remove the DNA. TURBO DNA-*free*™ kit (INVITROGEN) was used according to the manufacturer's protocol with minor changes.

#### 2.6.3.2. Quality control of the RNA material

Final RNA concentration was measured using a Nanodrop, and RNA samples were run on 1% Agarose gel to visualize any possible degradation.

#### 2.6.3.3. Sequencing

The prepared RNA samples were sent to Novogene (Cambridge, UK) following the company's recommendations. Sequencing was performed using the Illumina HiSeq platform with paired-end 150 bp (PE 150) with a sequencing plan of 20 Million pair reads (6 Gb) per each sample.

#### 2.6.3.4. Quality control of the RNA-Seq reads

The quality control of the reads and further alignment to reference genome TO1000 (https://www.ncbi.nlm.nih.gov/bioproject/217459, Parkin et al., 2014) was completed by Burkhard Steuernagel from John Innes Centre.

# CHAPTER 3

## Recognition of Necrosis- and Ethylene-Inducing Peptide 1 (Nep1)-Like Proteins (NLPs) Increases Resistance to *Botrytis cinerea* in *Brassica napus*

### 3.1. Background

Most studies on NLP recognition and its involvement in disease resistance have been conducted in *Arabidopsis*, but not extensively in crop species (Seidl & Van den Ackerveken, 2019). Mainly two methods have been used to investigate whether or not recognition of an NLP molecule has a significant effect on corresponding pathogen infection. One method has been pre-treatment of the plants with the purified NLP peptide before the disease assay. There are a number of studies indicating that pre-treatment of NLP-responsive plants can trigger the disease resistance against corresponded pathogens (Albert et al., 2015; Böhm et al., 2014). One of the key experiments was from the milestone study, demonstrating that NLP-triggered immunity is mediated by the *RLP23-SOBIR1-BAK1* complex in *Arabidopsis*. In that investigation, recognition of NLP was shown to reduce disease susceptibility to *Hyalonospora arabidopsidis.* The conidiophore numbers of nlp24 (HaNLP3) pre-

treated Col-0 showed increased disease resistance to *H. arabidopsidis* when compared with nlp24 pre-treated *rlp23* and *sobir1* mutant genotypes. The other method is transgenic expression of the receptor gene in one of the non-responsive species. As Solanum species are non-responsive to NLP, *S. tuberosum* was used to create RLP23-GFP transgenic line to test against two aggressive potato pathogens – *Phytophthora infestans* and *Sclerotinia sclerotiorum*, which have 1 and 2 cytotoxic NLPs respectively. When the lesion sizes compared with the wild-type, the responsive transgenic line showed significantly decreased disease susceptibility (Albert et al., 2015).

Although there have been many advances in our understanding of PAMP recognition, the regulatory processes controlling this are still a matter of debate for scientists (H. Shi, Yan, et al., 2013; Tang & Zhou, 2015). In previous studies, it was proposed that the signalling cascade is quite similar following recognition of NLP and flg22. In a study aiming to compare the signalling pathways of RLKs and RLPs, nlp20 and flg22 were used as representative PAMP molecules. It was found that the immune responses induced by nlp20-recognition overlap partially with the ones that are induced by the flg22-recognition. It has been shown that nlp20-upregulated genes only comprising a fraction of the flg22-upregulated genes. However, some major differences were noted, especially with flg22-recognition resulting in earlier MAPK activation and ROS burst when compared with nlp20-recognition. This was interpreted with having RLK rather than requiring to be physically associated with another co-receptor to initiate the downstream signalling cascade as with RLPs. Another investigation revealed that BIK1 is a common regulator for flg22 and nlp20 signalling cascades, but with positive and negative regulation role respectively (Wan et al., 2019).

Whilst studies with *A. thaliana* may reveal underlying mechanisms of NLP recognition, it is important to translate these findings into crop species. However, this presents challenges since crop species have more complex and larger genomes which could influence the significance of NLP responsiveness and the downstream recognition pathway. As previously explained in section 1.1.2.2, there are some

studies conducted with crop species such as cultivated lettuce *L.sativa* cv. Olof (Raaymakers, 2018) and *Cucurbitaceae* cultivars (Azmi et al., 2018; Irieda et al., 2014). The contribution of NLP-recognition to disease resistance in *B. napus* however, has not been demonstrated. The study presented in this chapter is aiming to investigate the effect of NLP-recognition on *B. cinerea* disease resistance in *B. napus*. With this aim, a disease assay experiment was designed with a cross between responding (Ningyou1) and non-responding (Ningyou7) parent lines. The phenotypic data of responsiveness obtained through a high throughput ROS Assay method. This approach also enabled me to compare flg22- induced ROS burst in each NLP-responsive and non-responsive individual plant. An intriguing outcome from this comparison suggested there may be competition between PRRs responsible for BcNEP2 and flg22 perception for the shared components of the signalling pathway.

## 3.2. Results

### 3.2.1. Resistance of *Brassica napus* to *Botrytis cinerea* infection is strongly correlated with recognition of NLP

The production of reactive oxygen species (ROS) in response to 50nM BcNEP2 and 20nM flg22 of 160 individuals from Ning7xNing1 $F_2$ population was measured, and they were also assayed for resistance to *B. cinerea* (Figure 3.1).

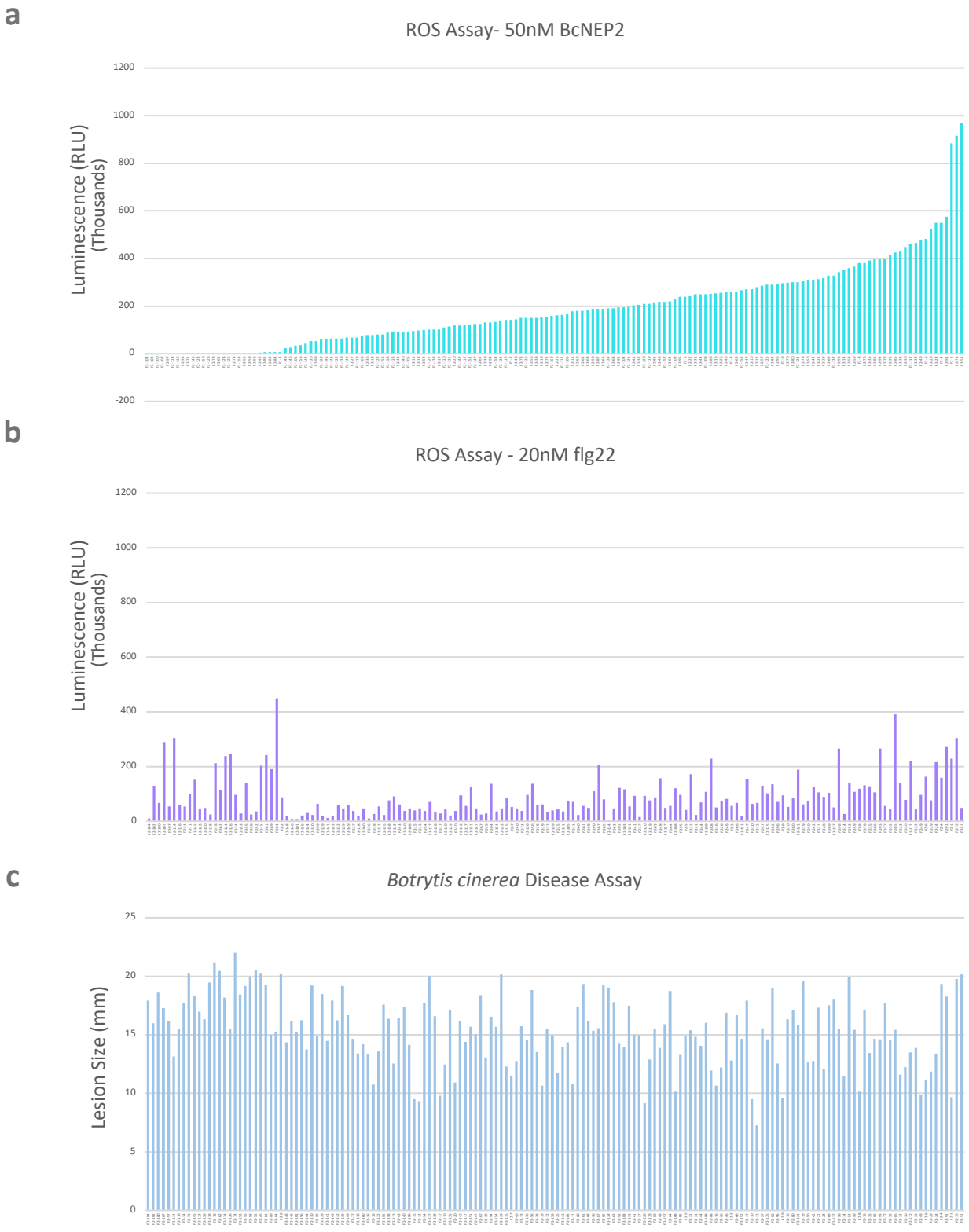


**Figure 3.1** Phenotype data of each of 160 individuals from Ning7xNing1 $F_2$ population. The order of the individual lines from the population is arranged according to the increasing magnitude of the BcNEP2 ROS response, as shown in (a) and is the same for all graphs. (a) ROS response to 50nM of BcNEP2 (b) ROS response to 20nM of flg22. Data represent total RLU read over 40 minutes. (c) Lesion sizes of *B. cinerea* infection. Data represented as lesions size of *B. cinerea* infection on *B. napus* plant leaves 3 dpi.

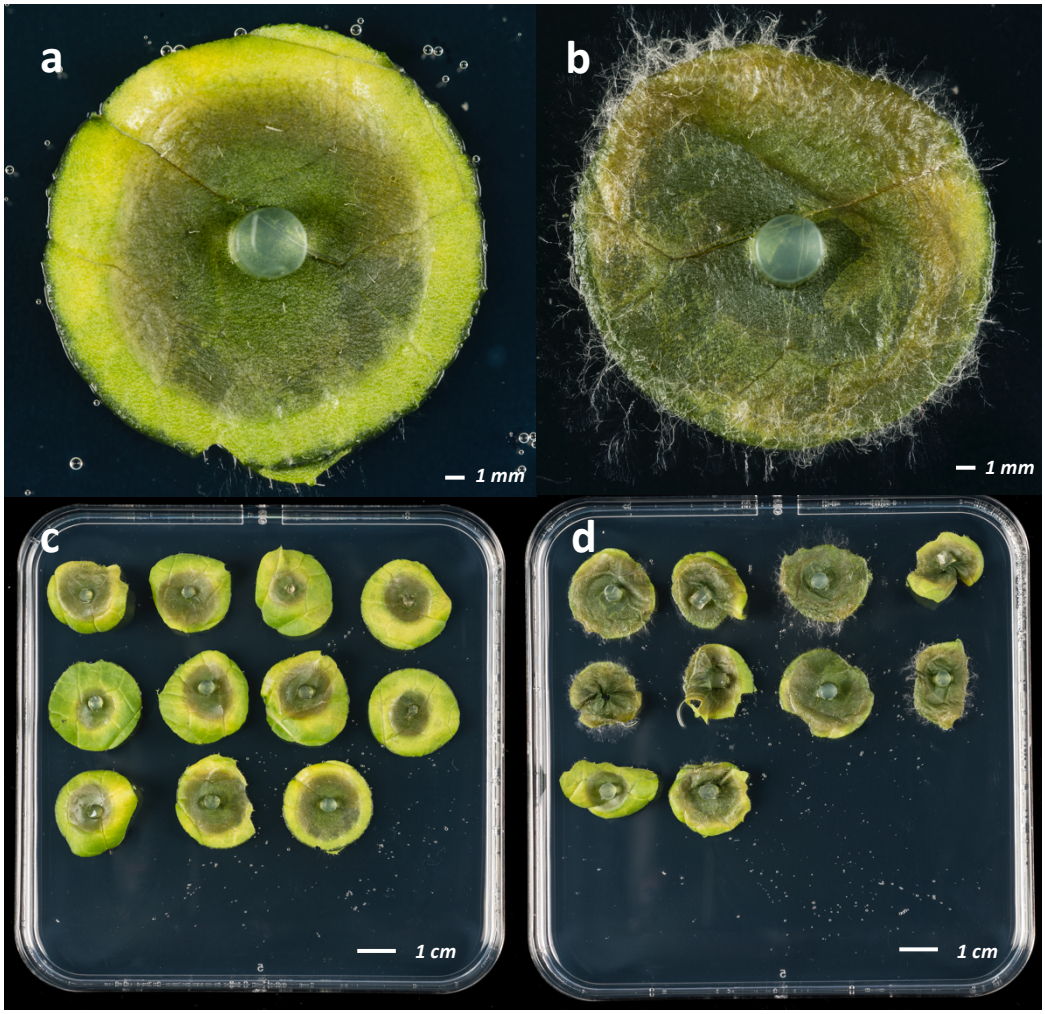


**Figure 3.2** Five-week-old *B. napus* leaf discs were infected with *B. cinerea* plugs. Leaves were photographed at 3 DPI. (a) *B. cinerea* infected leaf disc taken from a "Responder" $F_2$ plant. (b) *B. cinerea* infected leaf disc taken from Ningyou7 (Non-responder to NLP) which is the parental line of the $F_2$ population. (c) A plate overview containing leaf disc samples from the "Responder" $F_2$ plant. (d) A plate overview containing leaf disc samples from the "Non-responder" $F_2$ plant.

The difference of the lesion sizes can be seen between the "Responder" and the "Non-responder" *B. napus* individual plants (Figure 3.2 a,b). Whilst there is variation between the leaf samples taken from the same plant (Figure 3.2 c,d), the statistical differences of lesion sizes between Responder and Non-responder were highly significant. The results demonstrate that the $F_2$ *B. napus* individuals that respond to BcNEP2 have smaller lesion sizes.


**Figure 3.3** The difference between the Responder & Non-responder groups based on their corresponding lesion size. Violin plot illustrating the distributions of lesion sizes belongs to 2 different groups of 133 Responder (Rose) and 27 Non-responder (Blue) $F_2$ individuals, showing the significant differences between the groups (p-value = 4.262e-07***).

To further investigate the effect of the NLP-recognition, the phenotypic data coming from each individual $F_2$ plant was classified into two groups according to their NLP response as "Responder" & "Non-responder". The difference between the Responder & Non-responder groups based on their corresponding lesion sizes are illustrated with a violin plot (Figure 3.3). The statistical analysis with ANOVA showed there is a highly significant difference between *B. cinerea* lesion sizes for the Responsive and Non-responsive plants (p-value is $4.262e^{-07}$***). The mean ± SD values of the Lesion size for the *B. cinerea* infection of Responder and Non-responder groups are 14.9 ± 2.8 mm and 18.3 ± 2.2 mm, respectively. This analysis showed that the NLP-recognition of *B. napus* significantly increases resistance to *B. cinerea* infection.

### 3.2.2. The magnitude of NLP-response does not have a significant effect on *Botrytis cinerea* disease resistance

The data obtained from the flg22-induced ROS response showed that the ROS-producing mechanism of all individual plants from the Ning1xNing7 $F_2$ population was operational. To investigate whether the magnitude of PAMP-induced ROS response has an effect on disease resistance as BcNEP2-recognition, the flg22 and BcNEP2-induced ROS bursts of 60 individual plants were statistically tested with ANOVA. There was no significant difference between 'low' and 'high' responders of BcNEP2 and flg22 for *B. cinerea* disease resistance. ($p\text{-value}_{flg22} = 0.597$, $p\text{-value}_{BcNEP2} = 0.439$). For flg22, the shape of the plots was highly similar for both Responders and Non-responders. The $F_2$ individuals with a higher magnitude of ROS induced after NLP-recognition have significantly smaller *B. cinerea* lesion size when compared to those individual with a high ROS production after flg22-recognition (Figure 3.4 a,b). The low NLP-responders tended to have more plants with bigger lesion sizes with a median value of 15.34; however, the differences were not significant. ($Median_{High\ NLP\text{-}responder} = 14.74$). Overall, the resistance of *B. napus* to *B. cinerea* infection is significantly affected by the ability to respond to NLP, but not by the magnitude of either NLP or flg22-induced ROS response.

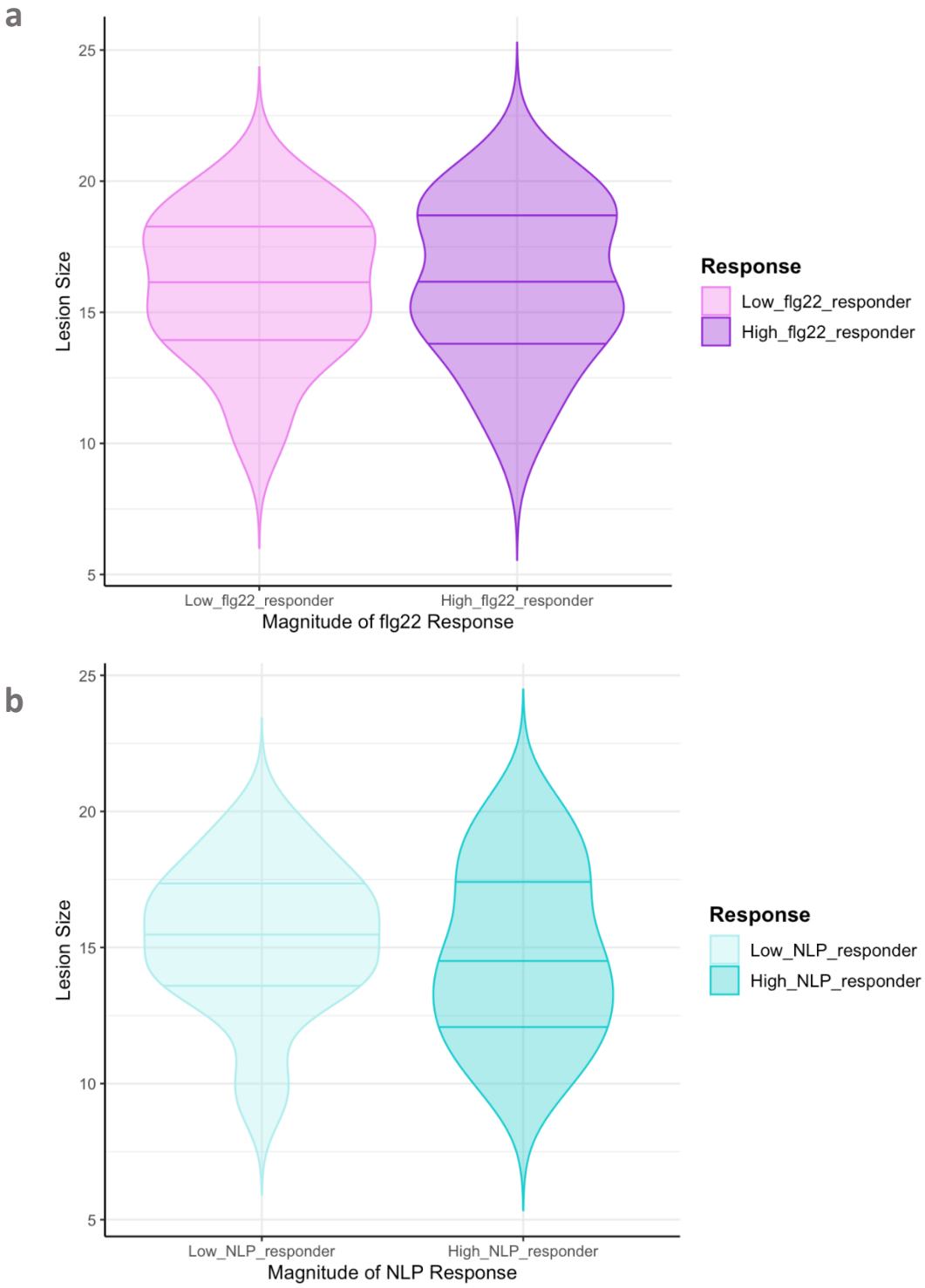


**Figure 3.4** (a) Violin plot illustrating the distributions of lesion sizes belongs to 2 different groups of 30 Low flg22 Responder (Pink) and 30 High flg22 Responder (Purple) $F_2$ individuals. (b) Violin plot illustrating the distributions of lesion sizes belongs to 2 different groups of 30 Low NLP Responder (light blue) and 30 High NLP Responder (Blue) $F_2$ individuals.

### 3.2.3. The $F_2$ individuals blind to NLP molecule have significantly higher flg22-induced ROS response

Interestingly, the ability of the plant to respond to NLP affects the magnitude of the response to flg22. The "Responder" & "Non-responder" groups described above were used to test the relation between recognition of NLP with flg22 response. The difference between the Non-responder and Responders' group can be seen in the violin plot (Figure 3.5). Although the Responders and Non-responders' 1st quartile value was similar to each other (40,455 RLU and 51,123 RLU respectively), the median values were found quite distinct from each other ($Median_{Responder}$ = 61,438 RLU, $Median_{Non\text{-}responder}$ = 100,187 RLU). As illustrated in the plot, the number of plants with high flg22 ROS response is higher in the Non-responder group than in Responder group. The statistical analysis with ANOVA showed there is a highly significant difference between them (p-value=0.00247 **).


**Figure 3.5** Violin plot illustrating the distributions of flg22-induced ROS responses belongs to 2 different groups of 133 Responder (Rose) and 27 Non-responder (Blue) $F_2$ plants, showing the significant differences between the groups (p-value = 0.00247 **).

There was a significant difference between the NLP-responsive and blind $F_2$ plants in their flg22-induced ROS response phenotype. When only the NLP-responsive $F_2$ plants used in the correlation analysis, the results showed that there is a strong positive correlation between the magnitude of ROS production in response to BcNEP2 and flg22 with a correlation coefficient value equal to 0.58 (Figure 3.6).

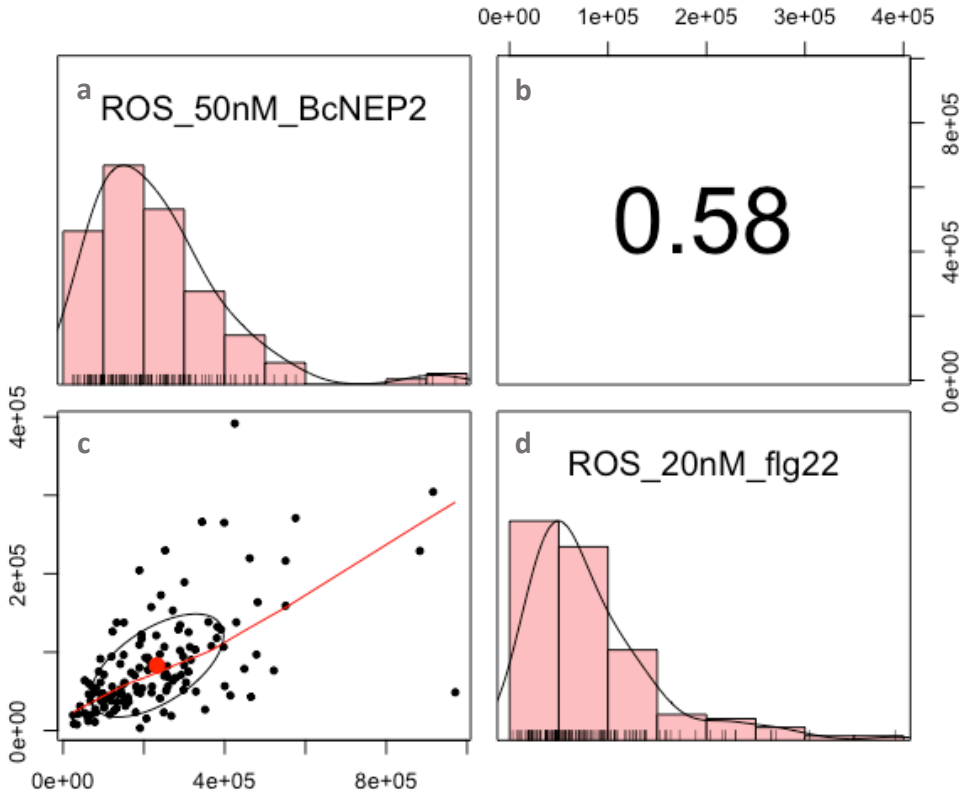


**Figure 3.6** Correlation analysis between the 50nM BcNEP2-induced ROS response results of $F_2$ individuals from Ning7xNing1 population and corresponding 20nM flg22-induced ROS response results. The histogram plots integrated with rug plots of total RLU in response to 50nM BcNEP2 (a) and 20nM flg22 (d). The scatter plot (c) drawn with loess smooth and shows the positive correlation between the results. The panel upper right (d) is showing the correlation coefficient value.

### 3.3. Discussion

In this chapter, the effect of NLP-recognition to gray mold (*B. cinerea*) disease resistance in *B. napus* was investigated within a specific $F_2$ population created with a cross between responsive (Ningyou1) and nonresponsive (Ningyou7) parental lines. Individual $F_2$ plants able to recognize BcNEP2 showed decreased lesion size when compared to Non-responsive plants. However, compared to low NLP-responders, high NLP-responders showed no significant difference in lesion size (p-value is 0,439). In conclusion, disease resistance is significantly affected NLP recognition, but not by the magnitude of the ROS response in responding lines.

The study is the first demonstration that NLP recognition affects disease resistance in *B. napus*. The *B. napus* $F_2$ segregating population in this study was created specifically to investigate the effect of NLP recognition on disease resistance. One of the parental lines, Ningyou1 is direct parental line of Ningyou7 (J. Zou et al., 2019), therefore, there is considerable amount if genetic similarity between 2 parental lines (X. Wang et al., 2017). This unique feature of the population, gave me advantage of eliminating the noises that might occur in the genetic background which might interfere with the disease assay results. By eliminating noises in the genetic background, together with the high throughput ROS quantification and disease assay method which allowed me to simultaneously assess NLP and flg22-induced ROS burst and resistance to *B. cinerea* for each plant, I could reveal the positive effect of NLP-recognition on *B. cinerea* disease resistance.

The study in this chapter supports the hypothesis that PTI is contributing to quantitative disease resistance, which is corroborating with the previous studies. Most of the studies are carried out in *Arabidopsis,* however, further investigations on various crop species such as tomato (Fradin et al., 2011; Lacombe et al., 2010), rice (Schwessinger, Bahar, et al., 2015), potato (Albert et al., 2015) and wheat (H.-J. Schoonbeek et al., 2015) were carried out via ectopic expression of PRRs. it has been showed that recombinant protein expression of the corresponded *Arabidopsis* receptor genes on crop species, enhances the immunity to the fungal and bacterial

infections. Those PRRs genetically transferred to crop species are RLP23 and EFR, recognizing nlp20 and elf18 respectively. Transfer of RLP23 in potato resulted in significantly decreased disease susceptibility against *P. infestans* and *S. sclerotiorum* (Albert et al., 2015). In the same paper, It has been also suggested that RLP23-mediated pathogen resistance is much broader spectrum as recognized motif could be found on taxonomically unrelated plant pathogens . In this chapter, this suggestion is verified by adding fungus *B. cinerea* to the list of the pathogens that NLP-recognition of the host is contributing the QDR against it.

An interesting result is that, when compared to the NLP-responsive group of plants, the NLP-non-responsive group had a significant increase in the amount of flg22-induced ROS response (Fig. 3.5). It has been previously reported in a study with *A. thaliana* that the downstream immunity-related genes upregulated by cytotoxic NLPs strongly overlapped with the genes that are induced by flg22 (Oome et al., 2014; Oome & Van den Ackerveken, 2014; Wan et al., 2019). It is already known that most of the downstream components of the cascades are also shared between the different PRRs (Albert et al., 2015). Also, as investigated in this PhD project (Chapter 5), co-receptor *AtBSK1* was found to physically associate with the flg22 receptor of FLS2, has a role in flg22-induced ROS burst(H. Shi, Shen, et al., 2013). Furthermore, in this PhD study, it has been proved that *AtBSK1* is also involved in NLP-induced ROS burst in *A. thaliana*. Thus, this significant difference of flg22-induced ROS response between Non-responsive and Responsive plants could be because many proteins having a role in the NLP-induced signalling cascade are also shared with flg22-induced ROS burst signalling cascade. This hypothesis is supported by the significant positive correlation between the magnitude of ROS production in response to BcNEP2 compared to flg22 within individual $F_2$ plants (Figure 3.6). This hypothesis also indicates the capacity for ROS production in each line is similar regardless of the PAMP motives, or receptor type (RLK for flg22 or RLP for BcNEP2). Thus, the superfluity of the shared common co-receptors that different PRRs may operate during signal transduction would explain the increased capacity to respond to the flg22 molecule in the absence of the NLP receptor.

# CHAPTER 4

## Mapping of NLP-recognition and NLP-induced ROS response in *Brassica napus* by Bulk-Segregant Analysis

### 4.1. Background

This chapter is based on preliminary work in the group initiated in the research project 'MAQBAT, Mechanistic Analysis of Quantitative disease resistance in Brassicas by Associative Transcriptomics'. That project aimed to map PAMP responses and resistance to several Brassica pathogens to identify candidate genes for crop improvement. Part of the MAQBAT included surveying NLP responsiveness in diverse Brassica species and accessions selected from the Triangle of U (Cheng et al., 2015). Within *B. napus*, only 12 out of 192 lines respond to NLPs, and no *B. oleracea* accessions (C genome) were responsive (Henk-jan Schoonbeek, personal communication). However, there were enough *B. napus* lines responding to NLP to enable preliminary mapping of the trait by Association transcriptomics, a type of Genome-wide association study (GWAS). The result from this GWAS study suggested that the region associated with that NLP recognition may be located on ChrA04 in *B. napus* genome (Rachel Wells, personal communication). However, the results of the

GWAS did not identify a candidate receptor for NLPs. An important reason for this could be the reference genome used in that analysis was Darmor-*bzh* (Chalhoub et al., 2014) which is non-responsive to NLP. Additionally, GWAS would work more effectively if there were an even match of phenotype scoring, so the proportion of 12 responsive out of 192 lines was not ideal for the analysis. A different approach was needed to map the region with higher resolution to define the gene responsible for NLP recognition. The method selected in this study was Bulk Segregant Analysis (BSA), a powerful technique to identify candidate genes by sequencing pools of DNA selected from lines with contrasting phenotypes (C. Zou et al., 2016). BSA is more effective when the phenotype is very easy to discriminate, and ideally if the contrasting lines are genetically similar to each other; both of these features apply in this study.

To identify the genetic loci responsible for recognition of the NLP motif via BSA, a biparental mapping population segregating for NLP-recognition created by using Ningyou1 (NLP-responsive) and Ningyou7 (NLP-nonresponsive) parental lines. Ningyou1 and Ningyou7 are spesifically used in this study. The known *B. napus* ancestors of Ningyou7 are NLP-responsive unlike their offspring. Most interestingly, the ancestors are including Shengliyoucai (*B. napus*- AACC), Chengduai (*B.rapa* - AA), Chuanyou (*B. napus*- AACC) and Ningyou1 (*B. napus*- AACC) (J. Zou et al., 2019). Additionally, in a recent study, it has been showed that, the genetic contribution to Ningyou7 genome is mostly form direct parental lines; Ningoyu1 and Chuanyou, which are both NLP-responsive, as 40% and 46% respectively. The rest of the inheritance pattern of the genome were identified as ~6% from Chengduai and ~8% from Shengliyoucai (X. Wang et al., 2017). I took the advantage of this 40% inheritance of the Ningyou7 genome from Ningyou1 in this study.

In Chapter 3, I demonstrated that NLP recognition significantly increases resistance to *B. cinerea* in *B. napus*. In this Chapter, I develop the PhD study further to genetically map the loci involved in NLP recognition in *B. napus* genome. For this purpose, I used an $F_2$ population derived from two lines differing in their ability to recognise and respond to NLPs. This segregating population was specifically created

for Bulk Segregant Analysis. The data obtained from high throughput ROS Assay was then used to create the DNA bulks followed by sequencing. A specific BSA pipeline, using the most recent and powerful bioinformatical tools was designed specifically for this study and used to reveal the loci highly associated with NLP-recognition on *B. napus* genome. In order to pin down to the gene level, several other data-mining tools were used and finally KASP markers were designed to map the region containing the hypothetical receptor gene on *B. napus* genome.

## 4.2. Results

### 4.2.1. $F_1$ Plants derived from NLP-responsive and non-responsive parents are all NLP-responsive

In order to create DNA pools for Bulk-Segregant Analysis, two NLP-responsive and two NLP-nonresponsive lines were used to create the crosses. The responsive lines are N02D-1952, and Ningyou 1, the non-responsive lines that are used in this study as parents are, Tapidor DH and Ningyou 7. Details about the crosses generated in this study can be found in section 2.1.3.1 and Table 2.3. Five seedlings from each reciprocal cross were grown to form $F_1$ plants.

**Table 4.1** *Brassica napus* varieties with their details regarding their NLP-responsiveness, used in this study to create the BSA population.

| Accession name | Crop type | Origin | Source | NLP-responsiveness |
|---|---|---|---|---|
| Ningyou1 | Semi-winter OSR | China | OCRI, Wuhan | Responsive |
| Tapidor | Winter OSR | France | UKVGB, Warwick | Non-responsive |
| N02D-1952 | Spring OSR | Australia | UKVGB, Warwick | Responsive |
| Ningyou7 | Semi-winter OSR | China | OCRI, Wuhan | Non-responsive |

After obtaining the $F_1$ plants to achieve segregation of the responsible regions, $F_1$ plants were selfed and $F_2$ seeds obtained from them. During this step, each $F_1$ plant was phenotyped by investigating the ROS responses to NLP molecules and genotyped by using SSR markers to prevent the usage of seeds from selfed plants. In the $F_1$ plants that are offspring of at least one responsive parent, no non-responsive phenotypes were observed (Figure 4.1). However, the genotyping studies revealed that 6 out of 60 of the $F_1$ plants were not heterozygous (Figure 4.3).

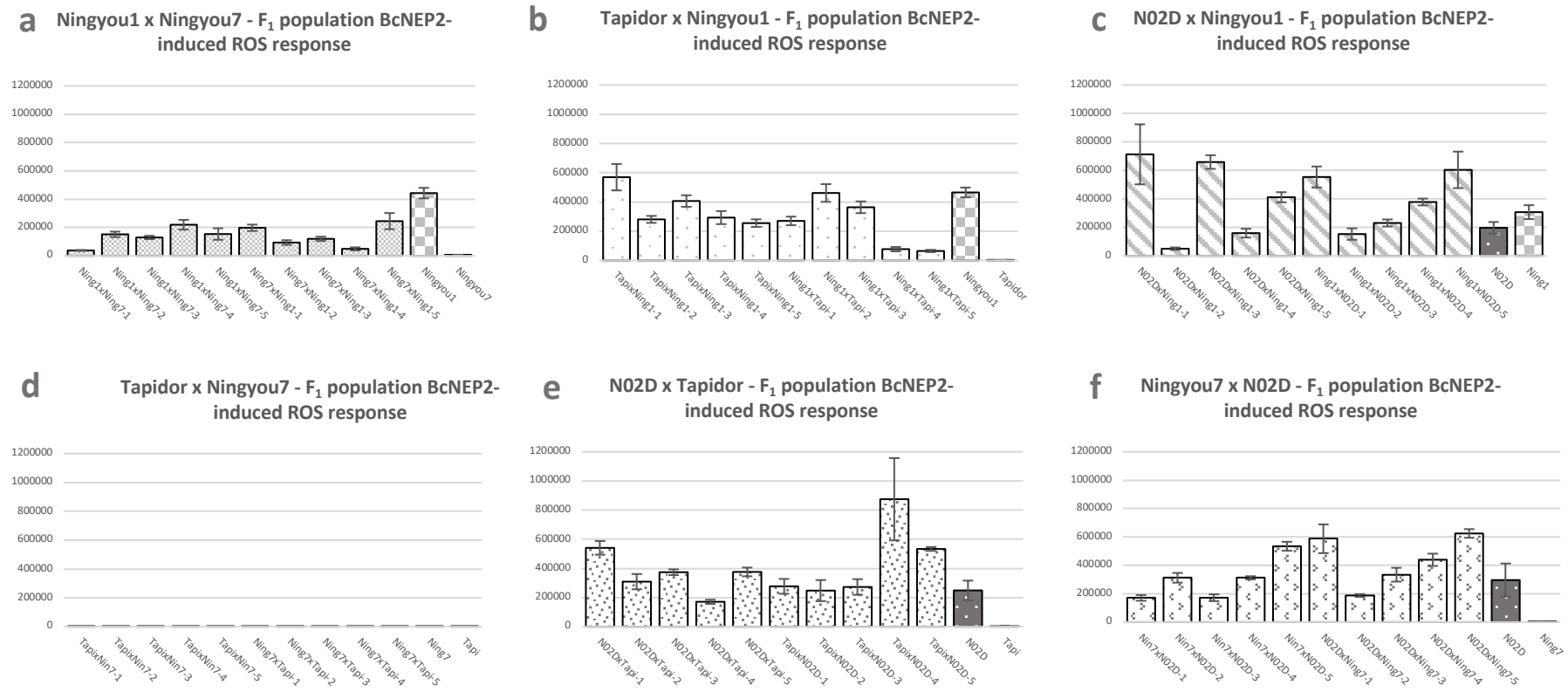


**Figure 4.1:** 50nM BcNEP2-induced ROS response results from 10 $F_1$ plants derived from 6 different reciprocal crosses. (a) Ningyou1 x Ningyou7, (b) Tapidor x Ningyou1, (c) N02D x Ningyou1, (d) Tapidor x Ningyou7, (e) N02D x Tapidor, (f) Ningyou7 x N02D. Bars represent total RLU read over 40 minutes. Error bars are the standard error of 8 biological replicates.

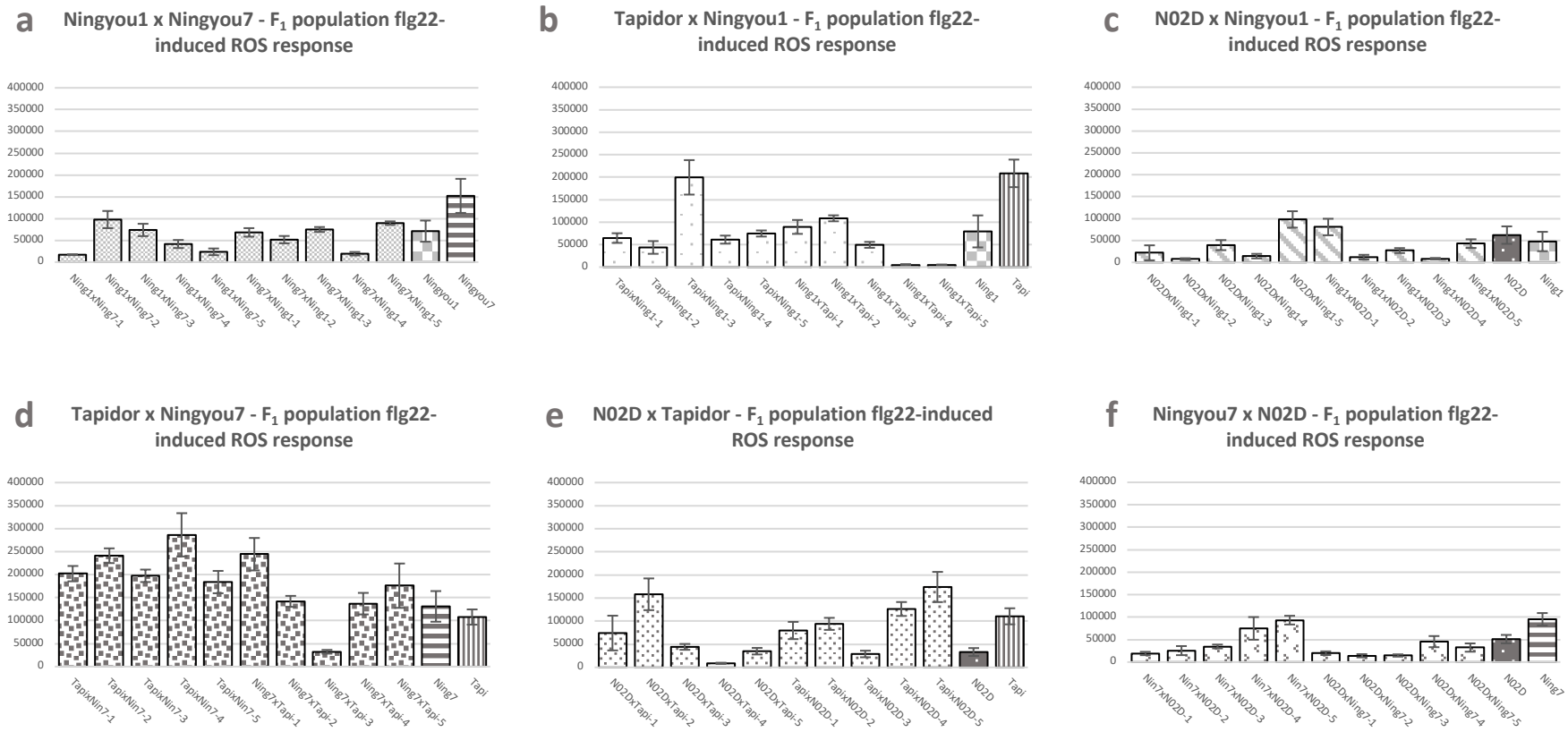


**Figure 4.2:** 20 nM flg22-induced ROS response results from 10 $F_1$ plants derived from 6 different reciprocal crosses. (a) Ningyou1 x Ningyou7, (b) Tapidor x Ningyou1, (c) N02D x Ningyou1, (d) Tapidor x Ningyou7, (e) N02D x Tapidor, (f) Ningyou7 x N02D. Bars represent total RLU read over 40 minutes. Error bars are the standard error of 8 biological replicates.

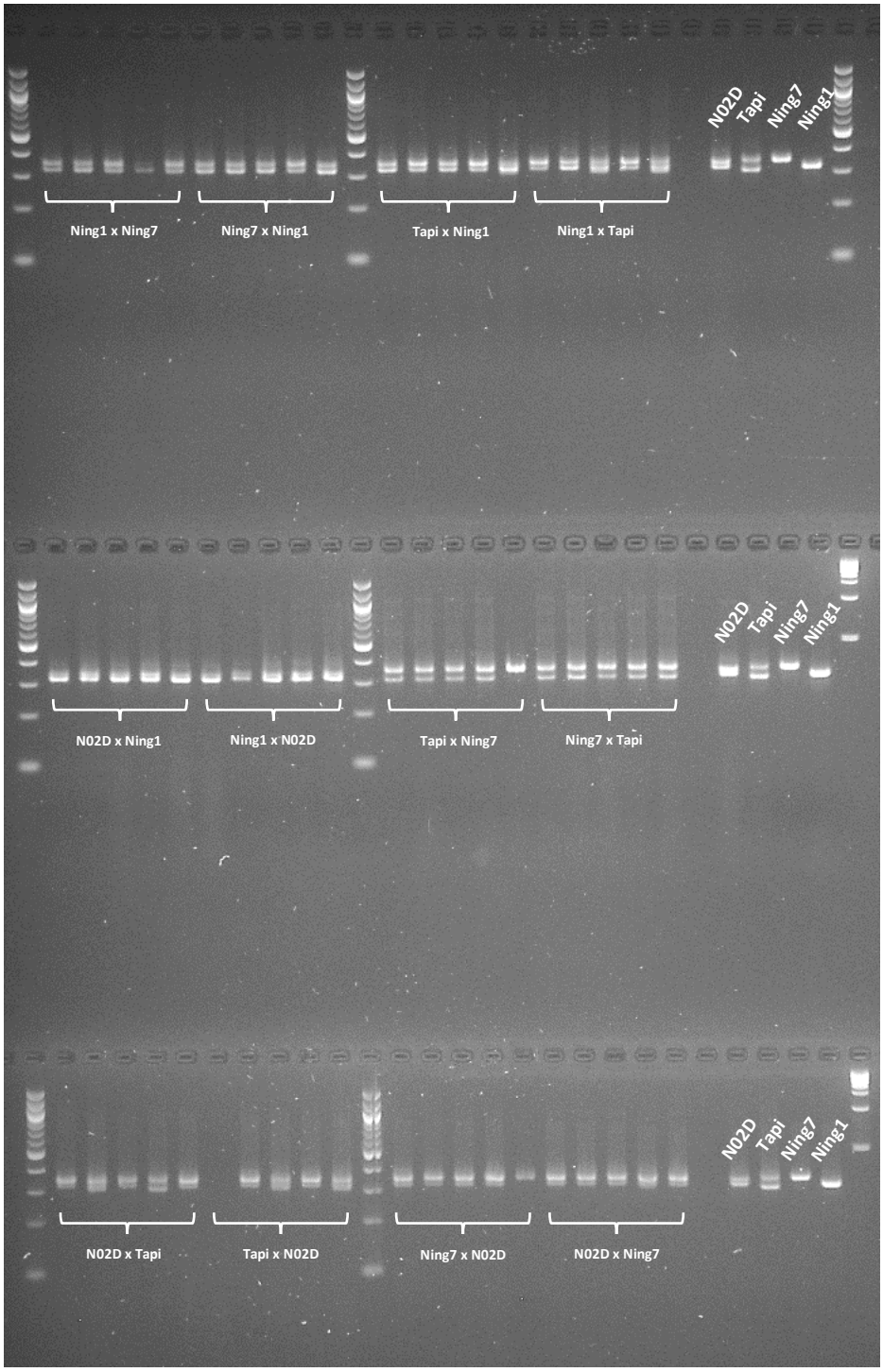


**Figure 4.3:** Amplification of microsatellite marker sR12095-Saskatoon in reciprocal crosses and parental lines. The fragments were separated in a 3.0% denatured Agarose gel. The 1st and 12th lane of all rows are 100bp DNA Ladder (NEB #B7025), the last lane of 2nd and 3rd row are 1kb DNA Ladder (NEB #B7025). The rest of the lanes and their corresponding sample names are represented in the figure. Polymorphism of microsatellites among the Ningyou1 (Ning1), N02D (N02D), Ningyou7 (Ning7), and Tapidor (Tapi) parents seen on the last four lanes on the right side of the gel.

After microsatellite marker screening of the $F_1$ individual crosses, the non-heterozygous lines were discarded as they are likely to be self-pollinated. Ningyou1 and Ningyou7 are genetically similar lines making them ideally suited to BSA, as their genomes improve the signal of contrasting markers, which could not be achieved with more complex genomes. Therefore, a population derived from Ningyou1 and Ningyou7 was chosen to carry out the further experimental processes (X. Wang et al., 2017).

In total 960 $F_2$ plants were sown in Controlled Environment Rooms (CERs). Of those, only 925 $F_2$ plants could be used further for phenotyping as 45 plants were lost due to the germination problems and selection during the transplanting process. The amount of flg22-induced and NLP-induced ROS burst of each individual was measured. Each 96-well plate run in the ROS assay also included parental lines as a control for normalisation purposes. The normalisation calculations were done to make each result independent from specific experimental factors, such as PAMP concentration variations due to the pipetting problems or using different Varioscan machines to detect the ROS burst. Therefore, all of the results belonging to individual samples were normalised according to their own control leaf discs in the same plate.

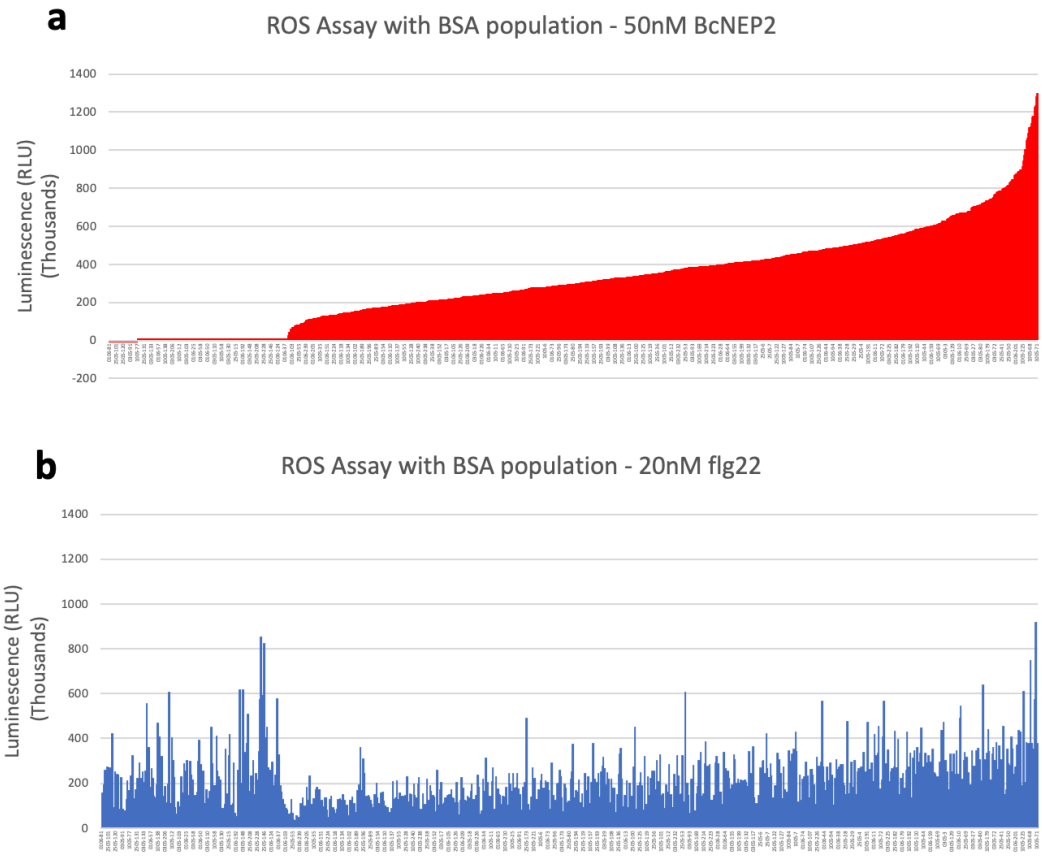


**Figure 4.4** Phenotype data of each of 925 individuals from the $F_2$ BSA population. The order of the individual lines from the population is arranged according to the increasing magnitude of the BcNEP2 ROS response, as shown in (a) and is the same for both graphs. (a) ROS response to 50nM of BcNEP2 (b) ROS response to 20nM of flg22. Data represent total RLU read over 40 minutes.

In accordance with the ROS response of the $F_2$ plants to the 50 nM BcNEP2, it was observed that there is a segregating variation in ROS response to BcNEP2 ranging from ~ $2.6x10^3$ to $1.3x10^6$ RLU for the responding $F_2$ individuals (Figure 4.4a). For the ROS response to 20 nM flg22,there is segregating variation, demonstrating that the ROS machinery of all the plants is functional (Figure 4.4b). However, 178 out of 925 $F_2$ individuals gave no ROS response to BcNEP2, representing ~19% of the population. This ratio was expected to be ~25% (3:1, responsive: non-responsive) if a single dominant gene model ($X^2$-test; $P$<0.001) is predicted. Although the ratio obtained is still close to that model for a single dominant gene, the slight difference is probably a result of the seedling selection during the transplanting process. Specifically, during the phenotyping process, it was observed that many of the non-responding individuals had chlorosis, and plants were relatively smaller than the responding

individuals. It is possible that they might have been selected against during transplantation in order to increase the number of vigorous and healthy plants. The hypothesis that a single dominant gene is responsible for NLP-recognition is supported by results that show: 1) All the heterozygote $F_1$ individuals derived from at least one responsive parent recognised the BcNEP2 and 2) All $F_1$ plants derived from both non-responsive parent (Ningyou7 and Tapidor) were completely unable to recognise BcNEP2.

### 4.2.2. Experimental design and creation of a pipeline for Bulk Segregant Analysis

The frequency of NLP-induced ROS response of the responding individuals has a normal distribution (Figure 4.5). The recognition of the NLP molecule in this segregating population is binary (yes/no phenotype), a great advantage for selecting individuals for creating Responsive and Non-responsive pools. Also, there is huge difference of around 1.0E6 RLU between the magnitude of ROS produced within the NLP-responding individuals. (Figure 4.4a). This huge difference also enabled the creation of pools from strongly and weakly responding individuals for BSA analysis, potentially enabling the identification of genes modulating the NLP response.

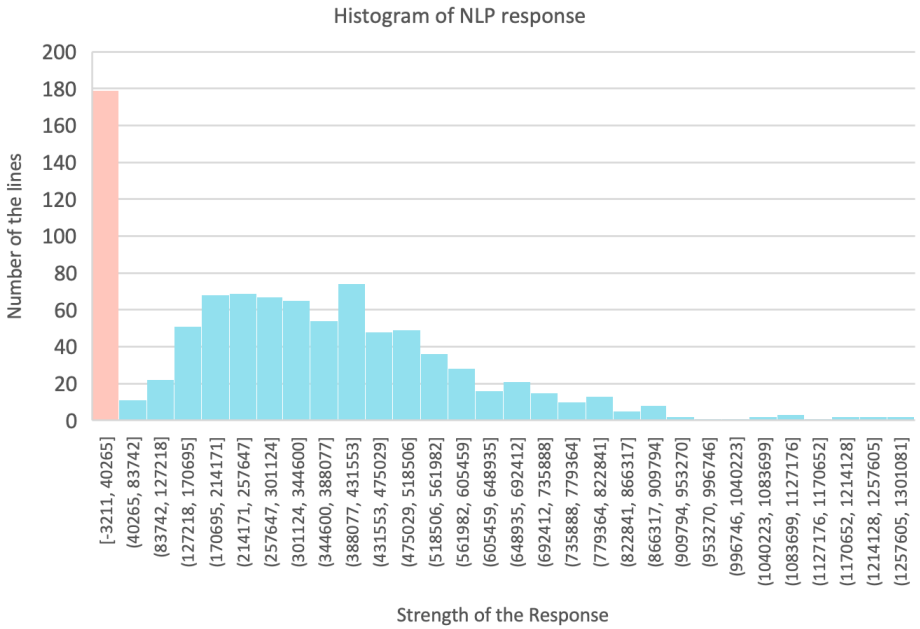


**Figure 4.5** Histogram created with 50nM BcNEP2-triggered ROS burst data of 925 Ning7xNing1 $F_2$ individuals (Number of the bins = 30).

A similar trend of responses was observed when the NLP data was compared with that for flg22(Figure 4.4b). This result suggests that, when creating the pools based on their NLP-responsiveness, the $F_2$ individual plants would also be selected as strong and weak responders to flg22. Thus, it was possible to define pools to characterise: 1) binomial response to NLP (on/off), 2) the magnitude of NLP response and 3) the magnitude of flg22 response. Each pool consist of 37 plants, for each low and high response extreme, was obtained based on the calculation of 5% of the 747 NLP-Responsive $F_2$ plants. Therefore, 30 individual $F_2$ plants were sampled per each pool. The details of the selected $F_2$ individual with their corresponded 50nM BcNEP2 & 20nM flg22 ROS phenotype can be seen in Figure 4.6. (C. Zou et al., 2016).

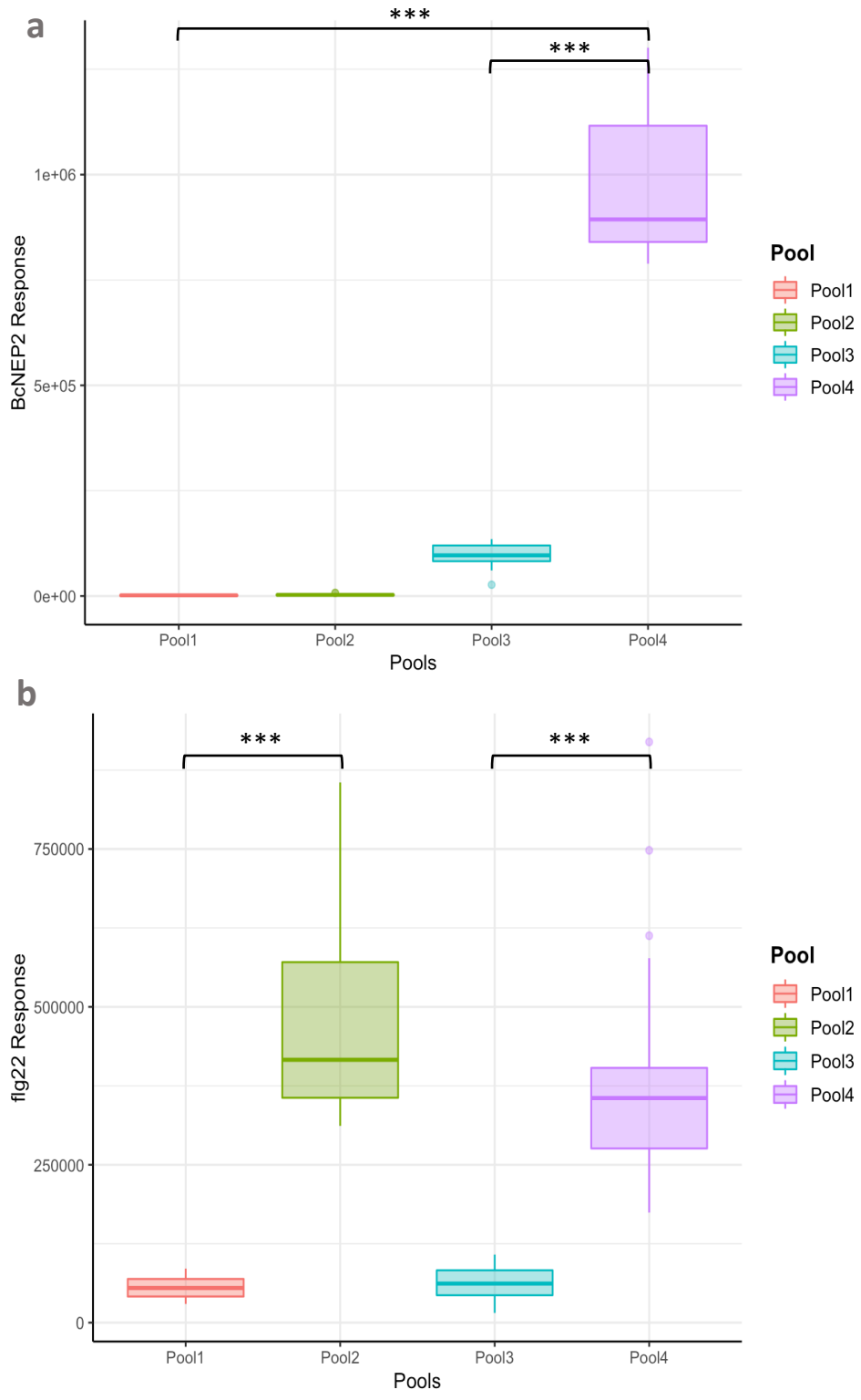


**Figure 4.6** The difference between the Pools based on their corresponding (a)50 nM BcNEP2-induced ROS response (b) 20 nM flg22-induced ROS response. Box plot illustrating the distributions of ROS responses belonging to 4 different Pools of 30 Pool1 (Rose), 30 Pool2 (Green), 30 Pool3 (Blue), and 30 Pool4 (Purple) $F_2$ individuals from BSA population showing maximum phenotypic differences between the pools.

(***p-values are lower than $5.3e^{-14}$)

To ensure the DNA obtained after the isolation had a high yield with no RNA or protein contamination and no degradation, in brief, to prepare a suitable sample for Illumina sequencing, a special CTAB-based method described in section 2.6.1.2, was used. The quality check steps showed that the isolated DNA was not degraded (Figure 4.7), and the concentration of the samples was enough to send to sequencing (Table 4.2).

**Table 4.2** Nanodrop results of the DNA libraries created for sequencing.

| Name | Species | Tissue | Total Amount (ng) | Conc. (ng/µL) | Volume (µL) |
|---|---|---|---|---|---|
| Pool_1 | *B. napus* | Leaf | 1692.32 | 60.44 | 28 |
| Pool_2 | *B. napus* | Leaf | 3466.96 | 123.82 | 28 |
| Pool_3 | *B. napus* | Leaf | 1584.8 | 56.6 | 28 |
| Pool_4 | *B. napus* | Leaf | 1449.28 | 51.76 | 28 |
| Ning_1 | *B. napus* | Leaf | 1746.08 | 62.36 | 28 |
| Ning_7 | *B. napus* | Leaf | 1311.24 | 46.83 | 28 |

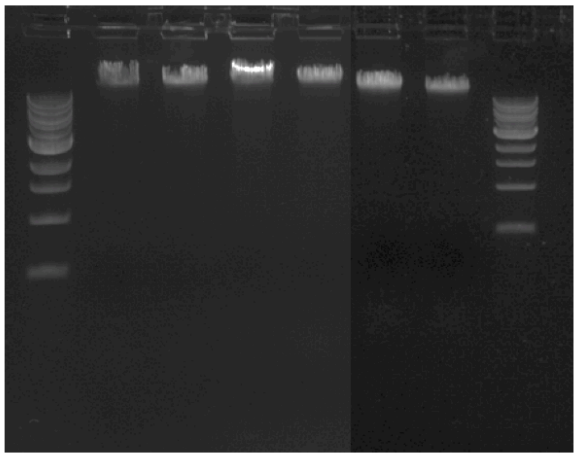

**Figure 4.7** Agarose gel (1%) electrophoresis result of DNA libraries respectively, Pool1, Pool2, Pool3, Pool4, Ningyou 1 & Ningyou 7.

The data QC report showed in around ~1.8billion raw sequence reads were obtained from each sample with a GC content of around ~38% in all samples. Summary of the sequencing data information can be seen in Appendix A. This result is similar to that previously found with a GC content result of *B. napus* ZS11 genome with ~40% GC content, with higher GC content in telomeric regions(Song et al., 2020).

The SNP calling pipeline was created based on methods described in a previous study conducted for mapping of *Yr15* gene in wheat (Ramirez-Gonzalez, Segovia, et al., 2015). After the quality control, the reads were aligned to the *Brassica napus* cv Darmor-*bzh* reference genome (Chalhoub et al., 2014, https://wwwdev.genoscope.cns.fr/brassicanapus/data/) using *bwa* v0.7.1(H. Li & Durbin, 2010). The alignments were sorted to remove the duplications and subsequently merged with *samtools* v1.9 (H. Li et al., 2009). *freebayes* v1.1.0. 46(Garrison & Marth, 2012) was used for INDELs and SNP calling. The INDELs and SNPs from each chromosome were called in parallel across the HPC cluster (https://github.com/hicretyalcin/BSA_Brassica_napus). This method (section 2.6.1.4.3), when compared to call all the variations in a single job, saved time and also gives the opportunity to investigate each chromosome INDELs and SNPs separately. Figure 4.8 shows the details of the INDELs and SNP calling pipeline.

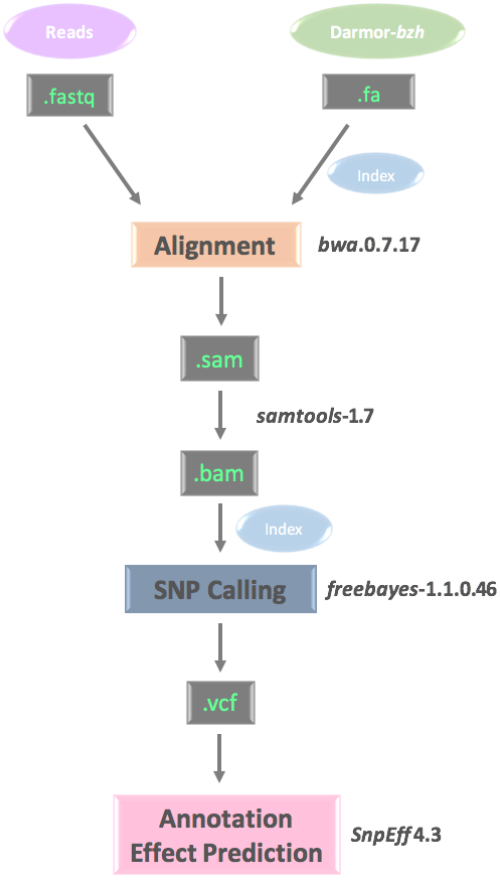


**Figure 4.8** The schematic representation of the created INDELs and SNP calling pipeline.

### 4.2.3. Bulk Segregant Analysis identifies variations highly associated with NLP-recognition located on ChrA04

In total 4,916,296 variations (SNPs and Indels) were found, of those 3,801,929 could be anchored to chromosomal positions on the *B. napus* genome. However, the *vcf* file also included variations that are the same for both parents but different from the reference line Darmor-*bzh*. *bcftools-1.8* was used to filter out the SNPs contained in both parent Ningyou1 and parent Ningyou7 (section 2.6.1.4.4).

After filtering the variations arising from differences between the parents and Darmor-*bzh*, the total number of variations anchored to chromosomes decreased to 823,799. These variations were then filtered based on their quality and depth. To define the filtering thresholds, histogram plots were created with the quality and the depth of the data belonging to each sample and chromosome. The quality of most of the variations in ChrC02 and ChrC09 was lower than the other chromosomes (Figure 4.9g). It was important to include most of the real variations while reducing the false positives to maintain the quality of further steps of the analysis. The limits were set at 2000 for quality and 20 for depth. With the quality filtering, the number of the variations anchored to chromosomes left with more than 2000 QUAL and 20 DP was decreased to 555,016.

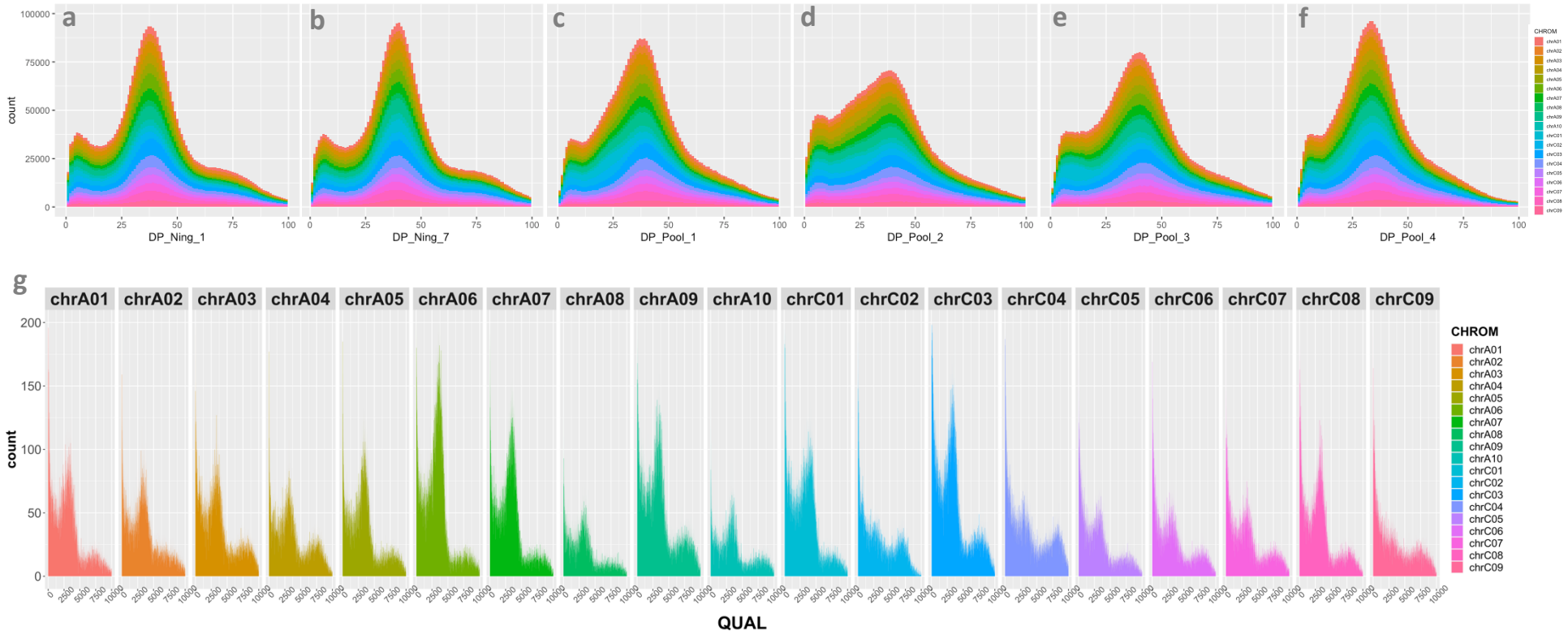


**Figure 4.9** Histogram plot of depth (DP) and quality (QUAL) values for 3,801,929 variations colour coded based on their locations on the *B. napus* chromosomes. (bin width= 1).

(a) DP – Ningyou1 (b) DP – Ningyou7 (c) DP – Pool 1 (d) DP – Pool 2 (e) DP – Pool 3 (f) DP – Pool 4 (g) Quality values of all variations in each corresponded chromosome (bin width= 1).

Each variation was scored with their corresponding Bulk Frequency Ratio (BFR). An explanation for this calculation can be found in Chapter 1 (Figure 1.2), which originated from Martin Trick and his colleagues' paper (Trick et al., 2012).

The ratio between the frequency of each informative base at each variation position of the responsive (Pool4) and non-responsive (Pool1) bulk was calculated. For variations with an informative base derived from an NLP-responsive background, the BFRs were calculated by dividing the frequency in the responsive bulk by the frequency in the non-responsive bulk. In the *vcf* files, the extracted variations have two values named "AO" and "RO"; these values state the count of variations derived from the Alternative allele and Reference allele, respectively. The BFR AO values take into consideration the fact that the reference genome is non-responsive in this analysis. The Manhattan plots, based on BFR AO values of the variations after filtering, demonstrate that the noise in the background has been eliminated. Also, the variations with the highest BFR, which are mostly associated with the NLP-response trait, are still there (Figure 4.10c).

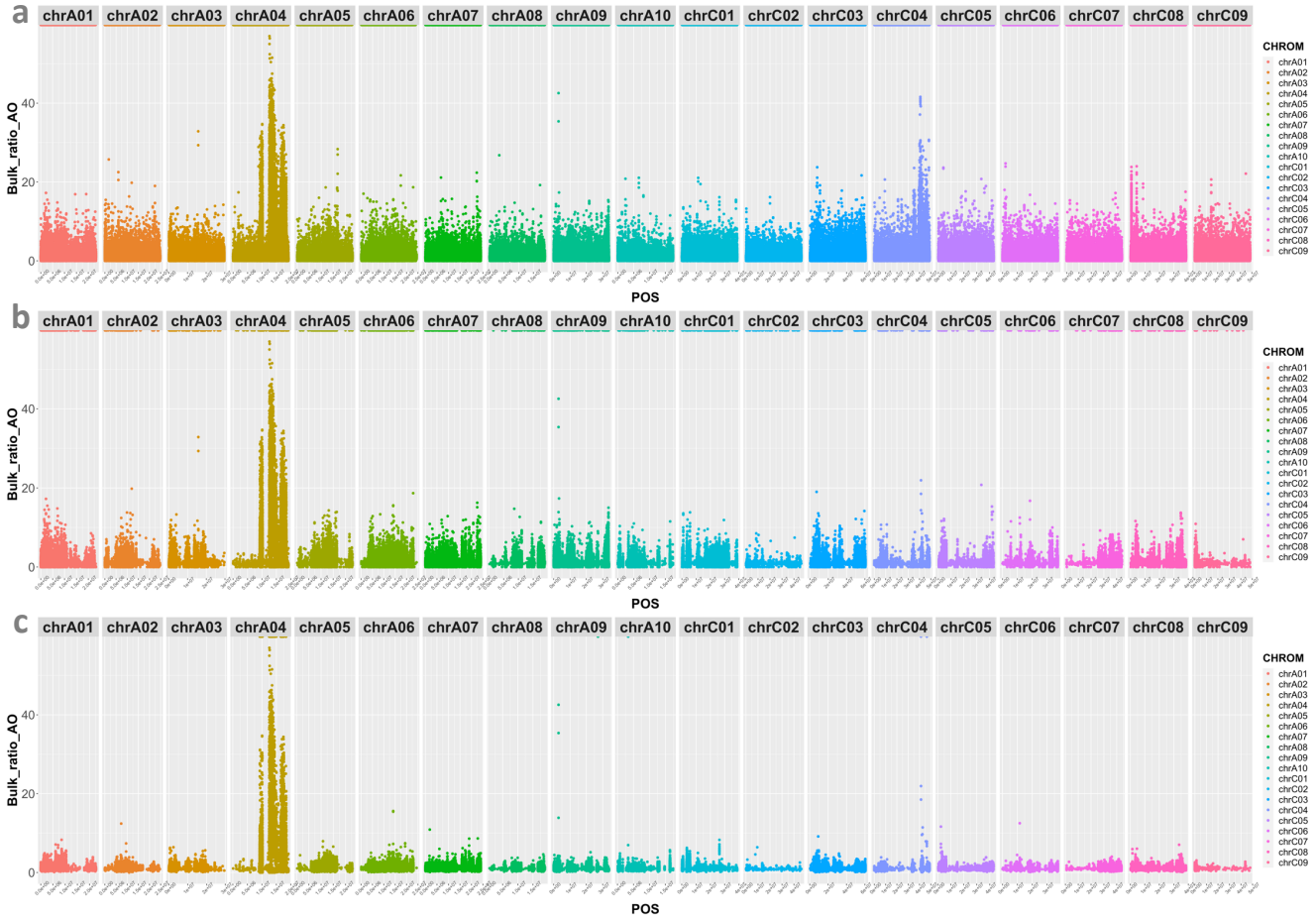


**Figure 4.10** Manhattan plots created with corresponding calculations of the Bulk Frequency Ratios of the variations. These plots show the highest associated peaks for the NLP-recognition; BFR ratios are calculated between Pool4 and Pool1. (a) The positions of the 3,801,929 variations are plotted along the X-axis on the full genome. (b) After parental filter - positions of the 823,799 variations are plotted along the X-axis on the full genome. (c) Additional quality and depth filter - positions of the 555,016 variations are plotted along the X-axis on the full genome.

In the GWAS study described earlier, a peak with highly associated SNPs was found on ChrA04. In this Bulk-Segregant Analysis, the variations with highest BFR are found on the ChrA04 which is supported by the results from the previous GWAS study. After applying the filters described above, the number of variations in ChrA04 was detected as 24,636 (Figure 4.11).

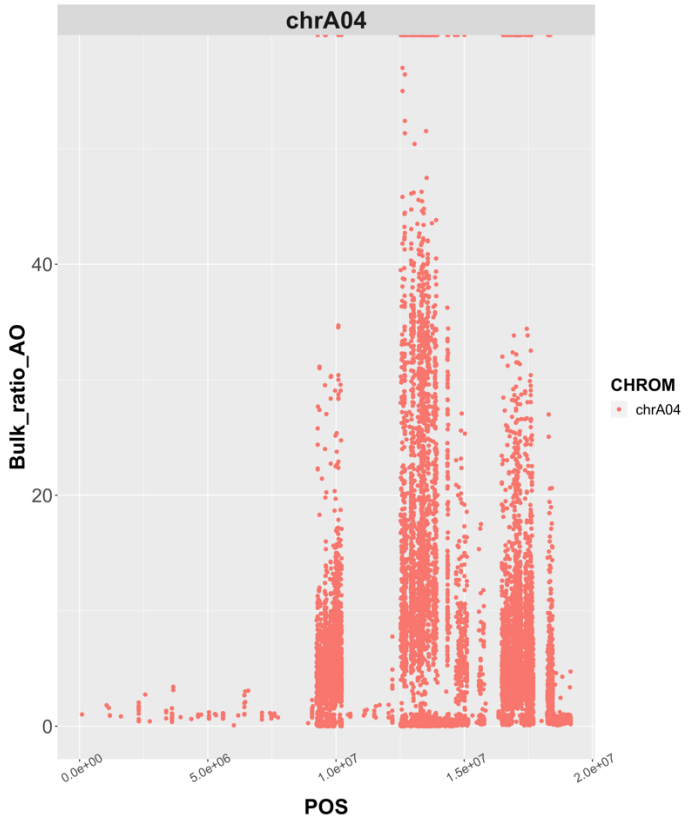


**Figure 4.11** Manhattan plots created with corresponding calculations of the Bulk Frequency Ratios of the variations between Pool4 and Pool1. The positions of the 24,636 variations are plotted along the X-axis on BnaChrA04.

By calculating the BFR values between Pool4 (Responsive) and Pool1 (Non-responsive), 3 main peaks, which cover almost half of the chromosome, were obtained (Figure 4.11). To obtain more defined peaks, pools were merged *in silico* to increase the coverage of the variations most highly associated with the responsiveness to NLP. Rather than having 30 individuals in each DNA pool, with the new merged pools, there were 60 "Responsive" and 60 "Non-responsive" individuals. This *in silico* merging was expected to increase the depth/coverage of the variations highly associated with NLP-responsiveness.

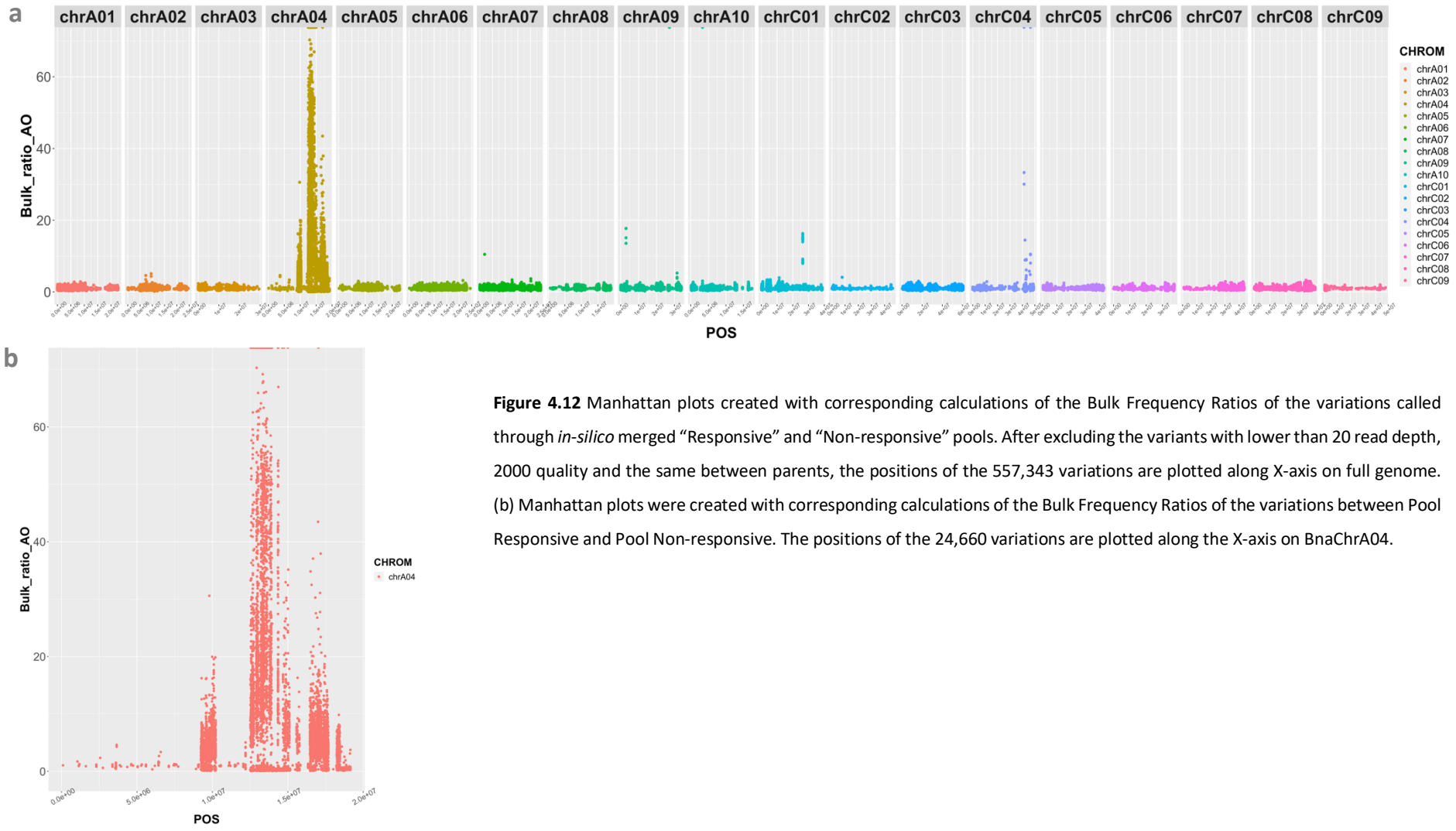


**Figure 4.12** Manhattan plots created with corresponding calculations of the Bulk Frequency Ratios of the variations called through *in-silico* merged "Responsive" and "Non-responsive" pools. After excluding the variants with lower than 20 read depth, 2000 quality and the same between parents, the positions of the 557,343 variations are plotted along X-axis on full genome. (b) Manhattan plots were created with corresponding calculations of the Bulk Frequency Ratios of the variations between Pool Responsive and Pool Non-responsive. The positions of the 24,660 variations are plotted along the X-axis on BnaChrA04.

After merging the data *in silico*, the same pipeline was applied to Non-responsive and Responsive pools. In total 4,788,639 variations were obtained, of which 3,713,757 could be anchored to chromosomal positions on the reference genome. After excluding the alleles identical between the parental lines, the variations with depth under 20, and quality under 2,000, the total number of the variations remaining was 557,343. As expected, the total number of variations were similar to that obtained previously with 4 pools. Additionally, the merging increased the BFR AO values to give a much clearer and more defined peak on BnaChrA04 (Figure 4.12). As can be seen from the figure, 3 main peaks were obtained again as a result of this pipeline. The genomic length of the 1$^{st}$ and the 3$^{rd}$ peak was ~1 Mbp, and the genomic area covered by the highest peak (2$^{nd}$) was spread on ~ 2.5Mbp.

### 4.2.4. High-throughput functional effect prediction and annotation of the variations

A variation can have more than one predicted effect on several different genes depending on its position relative to the affected genes. *SnpEff* tool predicts and categorizes the effects of each variation, and, as the *B. napus* reference genome is already well-annotated, it is possible to use this toolbox to predict the effect & its impact for each variation. The latest version of the Darmor-*bzh* annotation file (*v5* - https://wwwdev.genoscope.cns.fr/brassicanapus/data/) and the SNP-calling output - 557,343 variations with higher than 20 depth, 2000 quality and each anchored to chromosomes, were used to run through *SnpEff* tool. The examples of the effects and how they are classified as HIGH, MODERATE, LOW, or MODIFIER are shown in Table 4.3.

**Table 4.3** The classification of the SNP effect impacts and their corresponded meanings regarding examples (http://snpeff.sourceforge.net/SnpEff_manual.html#input).

| Impact | Meaning | Example |
|---|---|---|
| **HIGH** | The variant is assumed to have a high (disruptive) impact in the protein, probably causing protein truncation, loss of function, or triggering nonsense-mediated decay. | stop_gained, frameshift_variant |
| **MODERATE** | A non-disruptive variant that might change protein effectiveness. | missense_variant, inframe_deletion |
| **LOW** | Assumed to be mostly harmless or unlikely to change protein behaviour. | synonymous_variant |
| **MODIFIER** | Usually non-coding variants or variants affecting non-coding genes, where predictions are difficult or there is no evidence of impact. | exon_variant, downstream_gene_variant |

Variations on each specific chromosome with peaks associated with NLP responsiveness trait (Figure 4.12) were obtained, and particularly variations on A09, C01, and C04 were investigated further (section 2.6.1.4.7). The list of genes obtained from SnpEff was then used as input for Ensembl *BioMart* data mining tool. *BioMart* was used to summarise the role of the genes associated with NLP-recognition.

On chromosome A09, 3 variations with high BFR values are shown on Figure 4.12. Further evaluation of those variations showed that all have a predicted effect on BnaA09g06090D gene (Table 4.4), a homologue of *A. thaliana myb96* (Table 4.5). MYB96 is a transcription factor involved in the activation of the genes that have a role against drought stress through abscisic acid (ABA) signalling (Seo & Park, 2010).

Ensembl BioMart did not contain any *A. thaliana* homologue or any defined InterPro ID for the gene BnaC01g28470D, which is the only predicted gene associated with NLP response on C01. In order to reveal any possible data about this gene which might have a role in NLP-recognition, I retrieved the sequences from Darmor-*bzh* and ZS11 reference genomes. Both sequences were then blasted against the *A. thaliana* genome. However, the analysis failed to find any hit with query coverage of more than 13%. Then, I compared the sequences from reference genomes as they are distinct from each other based on their NLP-responsiveness. However, they were found 99.72% identical to each other, therefore the valid data suggests that there is no predicted effect of this gene on the loss of NLP-recognition. A probable explanation is that this region is not well annotated on Darmor-*bzh* genome. The annotated gene is 1803 bp long with 2 exons 247 bp and 39 bp long. Also, there is no particular protein domain or aligned sequence that can be assigned to this gene. Further BSA analysis with ZS11 reference genome might reveal the possible gene/genes that might have a role in NLP-recognition on C01.

The C genome was evaluated further for effect predictions and functional annotations and even gave a peak on a possible RLP homologue gene (BnaC04g42570D). However, it has been already shown that from 6 species from the Brassica clade only the species containing A or B genome are capable of recognising NLPs derived from Brassica pathogens (Schoonbeek et al, in preparation). Therefore, the focus for further work was to define the candidate receptor gene located on chromosome A04. For the most significant peak, there were 24,660 variations left after all filtering stages. All those variations were also run through *SnpEff*. The output was then aligned based on BFR AO values. There were 1170 different variations with computable BFR values between 70 and 20, affecting 245 annotated genes in total.

So, the number of candidate genes obtained through the BSA analysis was too many to identify a single candidate gene. Additionally, 22 homologues of *Atrlp23* were detected on Darmor-*bzh* genome, 4 of them on A04 chromosome clustering together did not help determine the candidates (Table 4.7). Additional analysis was therefore required to reduce the list of candidate genes. Most attention-grabbing genes highly associated with the trait were the *A. thaliana* RLP homologues and with LRR type domains on that peak (Table 4.6).

**Table 4.4** Annotation and Effect prediction of the variations highly associated with the NLP-recognition with corresponding locations on the Darmor-*bzh* genome and computed bulk frequency ratio (BFR AO) values (AO: counts of Alternative (Alternative) variation).

| Chromosome | Position | Reference | Alternative | Quality | Depth | Predicted Effect | Effect Impact | Annotated Gene | BFR AO |
|---|---|---|---|---|---|---|---|---|---|
| chrA09 | 2955726 | G | A | 2948.86 | 227 | upstream_gene_variant | MODIFIER | BnaA09g06090D | 17.72 |
| chrA09 | 2956215 | ATTTTTTTTA | ATTTTTTTA | 2506.3 | 184 | upstream_gene_variant | MODIFIER | BnaA09g06090D | 15.11 |
| chrA09 | 2955381 | G | A | 2867.03 | 242 | upstream_gene_variant | MODIFIER | BnaA09g06090D | 13.57 |
| chrC01 | 26285584 | G | A | 3654.88 | 260 | intron_variant | MODIFIER | BnaC01g28470D | 16.31 |
| chrC01 | 26285696 | C | T | 3448.39 | 245 | intron_variant | MODIFIER | BnaC01g28470D | 15.97 |
| chrC01 | 26285702 | CCTCGAG | TCTCAAA | 3325.87 | 230 | intron_variant | MODIFIER | BnaC01g28470D | 15.36 |
| chrC01 | 26285633 | A | C | 3437.49 | 259 | intron_variant | MODIFIER | BnaC01g28470D | 15.08 |
| chrC01 | 26285667 | A | G | 3092.58 | 234 | intron_variant | MODIFIER | BnaC01g28470D | 14.69 |
| chrC01 | 26285673 | T | C | 3091.19 | 229 | intron_variant | MODIFIER | BnaC01g28470D | 14.52 |
| chrC01 | 26285597 | ATG | TTA | 3414.02 | 256 | intron_variant | MODIFIER | BnaC01g28470D | 13.98 |
| chrC01 | 26285776 | GC | AT | 2523.94 | 200 | intron_variant | MODIFIER | BnaC01g28470D | 9.15 |
| chrC01 | 26285797 | CACGA | TACGG | 2013.29 | 194 | intron_variant | MODIFIER | BnaC01g28470D | 8.87 |
| chrC01 | 26285722 | A | C | 3446.91 | 243 | intron_variant | MODIFIER | BnaC01g28470D | 8.31 |
| chrC01 | 26285727 | C | T | 3532.82 | 248 | intron_variant | MODIFIER | BnaC01g28470D | 8.26 |
| chrC01 | 26285570 | A | T | 3705.5 | 270 | intron_variant | MODIFIER | BnaC01g28470D | 8.10 |
| chrC01 | 26285732 | T | C | 3567.59 | 246 | intron_variant | MODIFIER | BnaC01g28470D | 7.98 |
| chrC04 | 41344408 | C | T | 2558.98 | 209 | intron_variant | MODIFIER | BnaC04g40340D | 33.31 |
| chrC04 | 41344448 | G | T | 2146.92 | 214 | intron_variant | MODIFIER | BnaC04g40340D | 30.06 |
| chrC04 | 43102497 | G | C | 3706.89 | 257 | upstream_gene_variant | MODIFIER | BnaC04g42570D | 9.08 |
| chrC04 | 43102488 | C | A | 3683.64 | 261 | upstream_gene_variant | MODIFIER | BnaC04g42570D | 8.92 |
| chrC04 | 43102397 | A | C | 2813.86 | 196 | upstream_gene_variant | MODIFIER | BnaC04g42570D | 6.15 |
| chrC04 | 43105763 | C | A | 3085.79 | 205 | missense_variant | MODERATE | BnaC04g42570D | 4.56 |
| chrC04 | 43105578 | A | G | 3192.99 | 235 | missense_variant | MODERATE | BnaC04g42570D | 4.12 |

**Table 4.5** Functional annotation *and A.thaliana* homologues *of* the genes associated with NLP-recognition on chromosome A9, C4, and C1.

| **Gene name** | **InterPro Short Description** | ***A. thaliana* gene name** | ***A. thaliana* gene stable ID** |
|---|---|---|---|
| BnaA09g06090D | SANT/Myb<br>Homeobox-like_sf<br>Myb-like_TF<br>Myb_dom | MYB96 | AT5G62470 |
| BnaC04g42570D | Leu-rich_rpt<br>Leu-rich_rpt_typical-subty<br>LRR_dom_sf | AtRLP39<br>AtRLP40<br>AtRLP41<br>AtRLP42 | AT3G25010<br>AT3G24900<br>AT3G25020<br>AT3G24982 |
| BnaC04g40340D | SDR_fam<br>NAD(P)-bd_dom_sf | - | AT2G29340<br>AT2G29320<br>AT2G29300 |
| BnaC01g28470D | - | - | - |

**Table 4.6** Functional annotation *and A. thaliana* homologues *of* the genes associated with NLP-recognition on chromosome A4.

| Gene Name | Interpro Short Description | *A. thaliana* gene stable ID | *A. thaliana* gene name | Highest Computed BFR_AO value |
|---|---|---|---|---|
| *BnaA04g16450D* | Prot_kinase_dom, Leu-rich_rpt, Leu-rich_rpt_typical-subtyp, Ser/Thr_kinase_AS, Kinase-like_dom_sf, LRR_N_plant-typ, Protein_kinase_ATP_BS, LRR_dom_sf | | | 60.35 |
| *BnaA04g16400D* | Leu-rich_rpt, Leu-rich_rpt_4, LRR_dom_sf | | | 53.53 |
| *BnaA04g16790D* | Prot_kinase_dom, Ser-Thr/Tyr_kinase_cat_dom, Ser/Thr_kinase_AS, Kinase-like_dom_sf, Protein_kinase_ATP_BS, Malectin-like_Carb-bd_dom, LRR_dom_sf | AT2G28990, AT2G28970 | | 52.32 |
| *BnaA04g18930D* | Leu-rich_rpt, Leu-rich_rpt_typical-subtyp, LRR_dom_sf | AT2G32660 | *AtRLP22* | 35.14 |
| *BnaA04g18920D* | Leu-rich_rpt, Leu-rich_rpt_typical-subtyp, LRR_dom_sf | AT2G32660 | *AtRLP22* | 35.14 |
| *BnaA04g18870D* | Leu-rich_rpt, Leu-rich_rpt_typical-subtyp, LRR_dom_sf | AT2G25440 | *AtRLP20* | 32.44 |
| *BnaA04g18480D* | LRR_dom_sf | AT3G25010, AT3G24900, AT3G25020, AT3G24982 | *AtRLP41, AtRLP39, AtRLP42, ATRLP40* | 29.43 |
| *BnaA04g18600D* | Prot_kinase_dom, Leu-rich_rpt, Ser/Thr_kinase_AS, Kinase-like_dom_sf, LRR_dom_sf | AT2G31880 | *SOBIR1* | 26.14 |
| *BnaA04g18490D* | Leu-rich_rpt, Leu-rich_rpt_typical-subtyp, LRR_dom_sf | AT3G25010, AT3G24900, AT3G25020, AT3G24982 | *AtRLP41, AtRLP39, AtRLP42, ATRLP40* | 20.27 |
| *BnaA04g18520D* | Leu-rich_rpt, Leu-rich_rpt_typical-subtyp, LRR_dom_sf | AT3G25010, AT3G24900, AT3G25020, AT3G24982 | *AtRLP41, AtRLP39, AtRLP42, ATRLP40* | 20.27 |

**Table 4.7** Homologues of *AtRLP23* orthologs on the Darmor-*bzh* genome.

| | ID | Chromosome | Position - Start | Position - End | Homologue | Gene Length |
|---|---|---|---|---|---|---|
| **1** | *D_Bna.RLP23.A04-1* | chrA04 | 14750113 | 14752425 | *AtRLP23* | 2312 |
| **2** | *D_Bna.RLP23.A04-2* | chrA04 | 14758020 | 14760741 | *AtRLP23* | 2721 |
| **3** | *D_Bna.RLP23.A04-3* | chrA04 | 15000817 | 15003390 | *AtRLP23* | 2573 |
| **4** | *D_Bna.RLP23.A04-4* | chrA04 | 15093473 | 15096191 | *AtRLP23* | 2718 |
| **5** | *D_Bna.RLP23.A04.random-1* | chrA04_random | 1094074 | 1096245 | *AtRLP23* | 2171 |
| **6** | *D_Bna.RLP23.A04.random-2* | chrA04_random | 1099015 | 1101653 | *AtRLP23* | 2638 |
| **7** | *D_Bna.RLP23.A05* | chrA05 | 5608302 | 5610983 | *AtRLP23* | 2681 |
| **8** | *D_Bna.RLP23.Ann-1* | chrAnn_random | 17234233 | 17236722 | *AtRLP23* | 2489 |
| **9** | *D_Bna.RLP23.Ann-2* | chrAnn_random | 32941086 | 32943786 | *AtRLP23* | 2700 |
| **10** | *D_Bna.RLP23.C04-1* | chrC04 | 8706420 | 8709110 | *AtRLP23* | 2690 |
| **11** | *D_Bna.RLP23.C04-2* | chrC04 | 9441572 | 9444033 | *AtRLP23* | 2461 |
| **12** | *D_Bna.RLP23.C04-3* | chrC04 | 43105519 | 43108236 | *AtRLP23* | 2717 |
| **13** | *D_Bna.RLP23.C04-4* | chrC04 | 43112725 | 43115445 | *AtRLP23* | 2720 |
| **14** | *D_Bna.RLP23.C04-5* | chrC04 | 43124412 | 43127114 | *AtRLP23* | 2702 |
| **15** | *D_Bna.RLP23.C04-6* | chrC04 | 43493535 | 43496131 | *AtRLP23* | 2596 |
| **16** | *D_Bna.RLP23.C04-7* | chrC04 | 43563720 | 43566372 | *AtRLP23* | 2652 |
| **17** | *D_Bna.RLP23.C04-8* | chrC04 | 43599943 | 43602361 | *AtRLP23* | 2418 |
| **18** | *D_Bna.RLP23.C04-9* | chrC04 | 43611101 | 43613799 | *AtRLP23* | 2698 |
| **19** | *D_Bna.RLP23.C04-10* | chrC04 | 43871784 | 43874348 | *AtRLP23* | 2564 |
| **20** | *D_Bna.RLP23.C04-11* | chrC04 | 44110290 | 44112984 | *AtRLP23* | 2694 |
| **21** | *D_Bna.RLP23.C04.random* | chrC04_random | 4059729 | 4062356 | *AtRLP23* | 2627 |
| **22** | *D_Bna.RLP23.C05* | chrC05 | 12780751 | 12783200 | *AtRLP23* | 2449 |

**Note:** Loci with over 60% homology to the *Arabidopsis* genes were identified by BLASTN against the respective genomes and the coding sequence of the corresponding gene-model retrieved for phylogenetic analysis. Gene-IDs were composed for each CDS based on sourcing genome, gene-family, and position on the chromosome. If genes were detected on contigs not assembled into chromosomes they were indicated with Ann or Cnn for contigs mapped to unplaced scaffolds of the A or C genome.

### 4.2.5. Genetic Mapping of NLP-recognition loci using KASP markers

To narrow down the region associated with the NLP responsiveness, 41 (Appendix A) Kompetitive allele specific PCR (KASP) markers were designed from those highly associated SNPs identified in the BSA analysis The KASP assay was conducted to validate the SNPs that are highly associated with the trait and also for the construction of the genetic map of the trait. PolyMarker, an automated bioinformatics pipeline for SNP assay development, was used to design the KASP primers (Ramirez-Gonzalez, Uauy, et al., 2015).

Two key features of the SNPs were used as criteria for deciding the candidate SNPs to design KASP markers. The computed BFR AO value was the first feature as the values, selected to be between 40 & 72. Second, the functional predicted effects on the annotated genes of the SNPs were evaluated using the output from the SnpEff tool. The list of the SNPs used in KASP marker design, along with their corresponding features, is shown in Table 4.8.

A DNA test panel with samples from 77 $F_2$ plants and parental lines was used to validate the 41 markers with specific FAM tail and HEX tail. The primers used in the assay are shown in Table 2.7 in Chapter 2. The test panel included 6 lines that are responsive to NLPs in order to confirm the marker is diagnostic on lines external to the mapping population. 21 out of 41 markers were suitable for genetic map construction with their p-value over 1E-10. Also, 9 out of 21 KASP markers were able to validate the responsiveness in the other 6 lines out of the $F_2$ BSA population. The full genotyping results of the $F_2$ individuals in the plate are shown in Appendix B. The loci carrying the hypothetical receptor gene could be mapped on the ChrA04, and the SNPs highly associated with the NLP response phenotype was reduced to 3.25 cM (Figure 4.13). The flanking markers NLP_31 and NLP_12 are away from the markers that are linked to the interested locus as 2.6 cM and 0.65 cM respectively. There are four markers (NLP_23, 17, 18, and 19) that are perfectly linked in this population. To reduce the mapping interval, a larger population or an $F_3$ population with the critical recombinants can be used in future experiments.

a

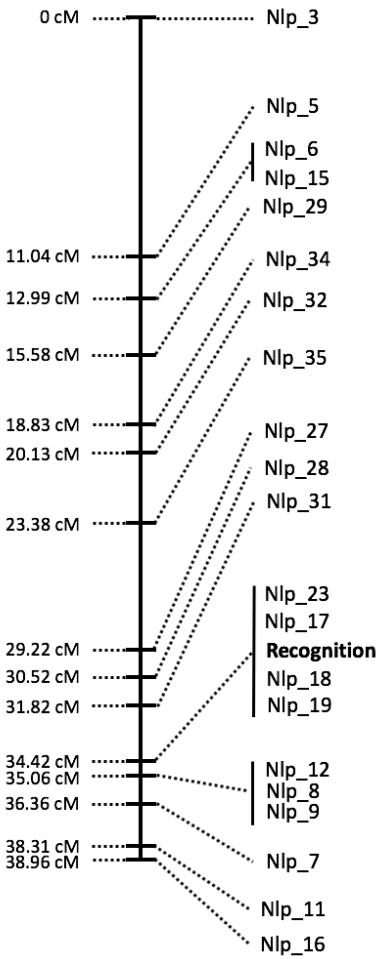


b

| Nlp_28 | Nlp_31 | Nlp_23 | Nlp_17 | Recognition | Nlp_18 | Nlp_19 | Nlp_12 | Nlp_8 | # of Individuals |
|---|---|---|---|---|---|---|---|---|---|
| A | A | A | A | NR | A | A | A | A | 31 |
| H | H | A | A | NR | A | A | A | A | 1 |
| H | A | A | A | NR | A | A | A | A | 2 |
| A | A | A | A | NR | A | A | H | H | 1 |
| A | A | H | H | R | H | H | H | H | 1 |
| H | H | H | H | R | H | H | H | H | 20 |
| H | H | B | B | R | B | B | B | B | 2 |
| B | B | B | B | R | B | B | B | B | 19 |

c

| | Nlp_28 | Nlp_31 | Nlp_23 | Nlp_17 | Recognition | Nlp_18 | Nlp_19 | Nlp_12 | Nlp_8 |
|---|---|---|---|---|---|---|---|---|---|
| **Recombination** | | 2 | 4 | 0 | 0 | 0 | 0 | 1 | 0 |
| **Distance (cM)** | | 1.30 | 2.60 | 0 | 0 | 0 | 0 | 0.65 | 0 |
| **Location (cM)** | 30.52 | 31.82 | 34.42 | 34.42 | 34.42 | 34.42 | 34.42 | 35.06 | 35.06 |

**Figure 4.13** Genetic map of "NLP-recognition" region on *B. napus* genome ChrA04. (a) QTL map of "NLP-recognition" region of 77 plants from $F_2$ plants with 21 KASP markers. (b) Genotypic features of each individual in the testing panel (in total 77 plants) for 8 markers that are closely linked to the trait (NR; Non-responsive (Red), R; Responsive (Green), H; Heterozygous (Yellow)). (c) Details of each marker; number of recombination occur in between the markers next to each other and their corresponding locations on the generated genetic map.

**Table 4.8** Annotation and Effect prediction of SNPs used in the KASP assay to design the markers, with corresponding locations on Darmor-*bzh* genome and computed bulk frequency ratio (BFR) values. (AO: counts of Alternative (ALT) SNP, RO; counts of Reference (REF) SNP)

| Marker | Chromosome | Position | REF | ALT | Quality | RO | AO | DP | Predicted Effect | Impact | Annotated Gene | BFR_AO_Res_Nonres | BFR_RO_Res_Nonres |
|---|---|---|---|---|---|---|---|---|---|---|---|---|---|
| Nlp_3 | chrA04 | 9,869,554 | C | A | 3207.83 | 124 | 107 | 232 | stop_gained | HIGH | BnaA04g11350D | 4.18 | 0.35 |
| Nlp_5 | chrA04 | 12,590,399 | G | T | 2935.91 | 142 | 91 | 233 | intergenic_region | MODIFIER | BnaA04g15080D | 57.65 | 0.26 |
| Nlp_6 | chrA04 | 12,920,723 | G | A | 3257.27 | 116 | 103 | 219 | stop_gained | HIGH | BnaA04g15640D | #DIV/0! | 0.23 |
| Nlp_7 | chrA04 | 12,920,864 | A | C | 3494.2 | 86 | 105 | 191 | stop_lost | HIGH | BnaA04g15640D | 0.18 | #DIV/0! |
| Nlp_8 | chrA04 | 12,935,023 | A | G | 3587.58 | 129 | 110 | 239 | upstream_gene_variant | MODIFIER | BnaA04g15670D | 70.30 | 0.12 |
| Nlp_9 | chrA04 | 12,998,985 | G | T | 2730.3 | 122 | 87 | 209 | synonymous_variant | LOW | BnaA04g15740D | 50.58 | 0.29 |
| Nlp_11 | chrA04 | 13,248,612 | C | T | 2737.32 | 104 | 91 | 195 | synonymous_variant | LOW | BnaA04g16190D | 52.81 | 0.14 |
| Nlp_12 | chrA04 | 13,262,249 | A | G | 2489.86 | 131 | 79 | 211 | synonymous_variant | LOW | BnaA04g16230D | 44.11 | 0.36 |
| Nlp_15 | chrA04 | 13,373,588 | T | C | 3326.32 | 116 | 103 | 219 | upstream_gene_variant | MODIFIER | BnaA04g16380D | 67.94 | 0.12 |
| Nlp_16 | chrA04 | 13,376,311 | T | G | 3861.2 | 87 | 122 | 209 | splice_donor_variant&intron_variant | HIGH | BnaA04g16390D | 0.30 | 13.65 |
| Nlp_17 | chrA04 | 13,454,192 | T | C | 5363.25 | 117 | 166 | 283 | synonymous_variant | LOW | BnaA04g16450D | #DIV/0! | 0.14 |
| Nlp_18 | chrA04 | 13,550,948 | A | T | 4344.13 | 122 | 138 | 261 | stop_gained | HIGH | BnaA04g16580D | 22.51 | 0.25 |
| Nlp_19 | chrA04 | 13,555,045 | T | A | 2869.37 | 155 | 92 | 247 | upstream_gene_variant | MODIFIER | BnaA04g16580D | 66.11 | 0.22 |
| Nlp_23 | chrA04 | 13,740,102 | A | C | 2535.33 | 85 | 81 | 166 | stop_lost | HIGH | BnaA04g16790D | 0.10 | 43.10 |
| Nlp_27 | chrA04 | 14,208,010 | A | T | 4003.66 | 94 | 122 | 216 | stop_lost | HIGH | BnaA04g17480D | 0.29 | 41.23 |
| Nlp_28 | chrA04 | 14,242,994 | C | A | 3361.48 | 68 | 106 | 174 | stop_gained | HIGH | BnaA04g17540D | 0.35 | 33.71 |
| Nlp_29 | chrA04 | 14,349,111 | T | C | 2148.08 | 114 | 71 | 186 | missense_variant | MODERATE | BnaA04g17800D | 42.14 | 0.29 |
| Nlp_31 | chrA04 | 14,372,201 | G | T | 3285.25 | 139 | 106 | 245 | splice_region_variant&intron_variant | LOW | BnaA04g17830D | 66.96 | 0.18 |
| Nlp_32 | chrA04 | 14,715,600 | C | G | 3585.34 | 63 | 112 | 175 | stop_lost | HIGH | BnaA04g18380D | 0.40 | 16.81 |
| Nlp_34 | chrA04 | 14,773,177 | A | G | 3697.65 | 103 | 117 | 220 | synonymous_variant | LOW | BnaA04g18530D | 0.15 | 20.05 |
| Nlp_35 | chrA04 | 15,010,155 | A | C | 3426.09 | 151 | 114 | 265 | stop_lost | HIGH | BnaA04g18890D | 6.78 | 0.34 |

### 4.2.6. Variations highly associated with the magnitude of NLP-induced and flg22-induced ROS response found distinct on *B. napus* genome

It was assumed that the ROS response created due to flg22 or BcNEP2 PAMP motives would have some specific differences based on their associated regions on the genome. In order to identify genes modulating the NLP response, Pool4 (High NLP-responsive) and Pool3 (low NLP-responsive) (Figure 4.6) were included additionally in BSA analysis. For this analysis, only quality and depth filtering were applied. In total, 3,801,929 SNPs and Indels were found as anchored to chromosomal positions on the *B. napus* genome, after filtering, 2,676,098 variations remained with more than 2000 QUAL and 20 DP. To identify variations most associated with the high NLP-responsiveness, the BFRs were calculated by dividing the frequency of the high NLP-responsive bulk (Pool4) by the frequency in the low NLP-responsive bulk (Pool3). Results clearly demonstrate that the regions associated with the NLP-recognition and the magnitude of NLP-response are different (Figure 4.14).

To detect the variations associated with high flg22-responsive background, the BFRs were calculated by dividing the frequency in the high flg22-responsive bulk (Pool2) by the frequency in the low flg22-responsive bulk (Pool1) As it can be seen in the Figure 4.14b, some variations on ChrA04 having the highest BFR value, but also there is a clear peak appearing at the beginning of the ChrA02. Variations Highly Associated with High NLP-induced ROS response and High flg22-induced ROS response are not far more distinct from each other. However, unlike the peak on the ChrA04 associated with High NLP-induced ROS response, it is much more defined and clearer for High flg22-induced ROS response at the end of ChrA04. Another apparent distinctive peak was on ChrA01; a higher association was observed for High NLP-induced ROS response when compared with flg22-induced ROS response.

Interestingly, on ChrA01, some specific variations associated with the high NLP-induced ROS response phenotype found to have effect on the *BnaA01g02190D* gene. This gene is homologue of *Atbsk1* (*At4g35230*), which is *BR-SIGNALLING KINASE1* physiologically associating with *FLS2* (H. Shi, Shen, et al., 2013).

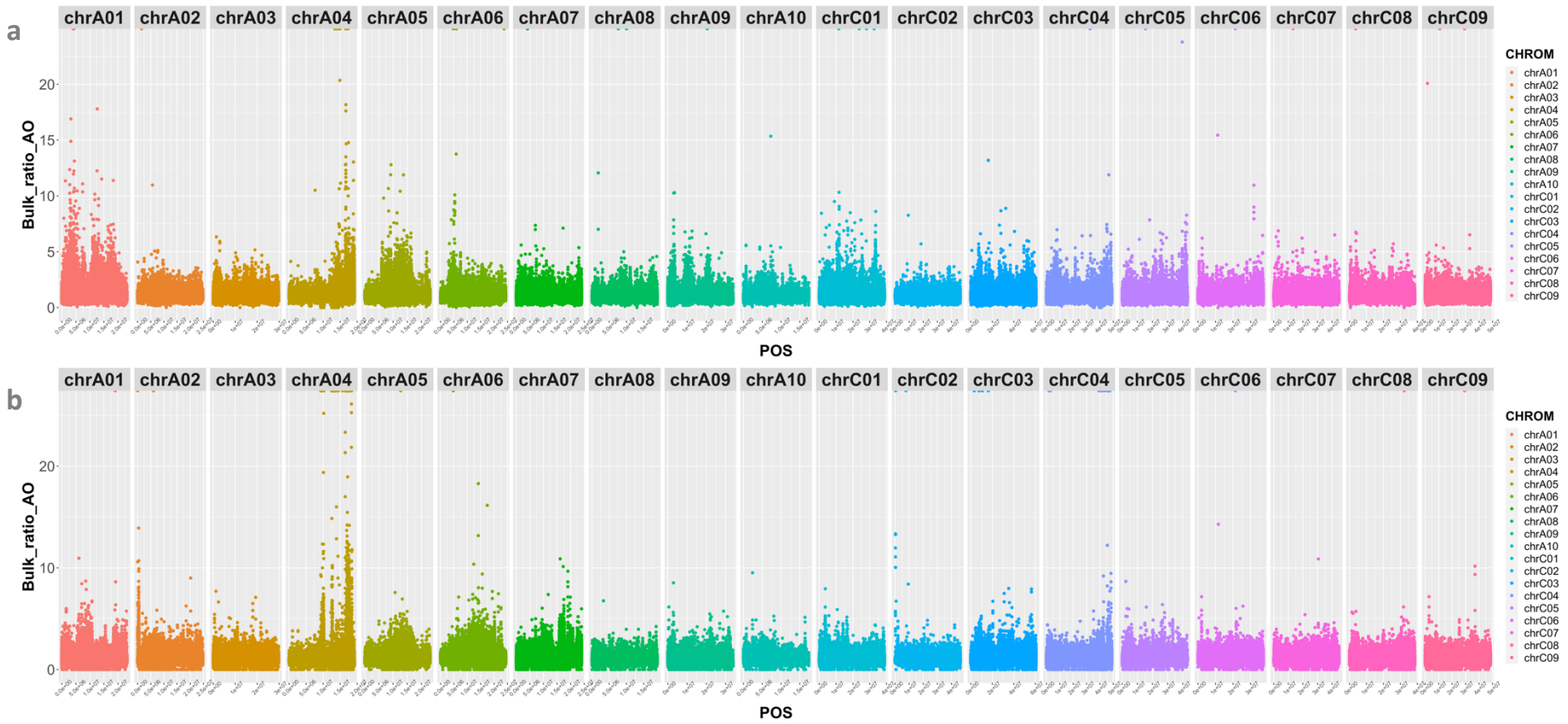


**Figure 4.14** Manhattan plots created with corresponded calculations of the Bulk Frequency Ratios of the variations. (a) The highest associated peaks for the High NLP-responsiveness, BFR ratios are calculated between Pool4 and Pool3. INDELs and SNPs are plotted along the X-axis on the full genome. (b) The highest associated peaks for the High flg22-responsiveness, BFR ratios are calculated between Pool2 and Pool1. INDELs and SNPs are plotted along the X-axis on the full genome.

### 4.3. Discussion

The slight deviation from the expected 3:1 segregation does not impact on the BSA analysis in the Chapter, as pools were selected from individual plants phenotyped for NLP responsiveness. Whilst the slight deviation may result from subconscious selection during the transplantation process, it is also possible that a genetic effect may be influencing segregation. As *B. napus* has an allotetraploid genome (AACC, 2n=4x=38), the inheritance mode is expected to be different from diploid genomes. Although allotetraploids are expected to have fixed heterozygosity due to preferential pairing of homologues chromosomes (Warnke et al., 1998), it has been proved that recombination events might take place between homeologus chromosomes and can interfere with the inheritance (Nguepjop et al., 2016). Moreover, complex recombination patterns between A and C genome in *B. napus* can result in different modes of inheritance from other allotetraploid species (Cai et al., 2014).

The BSA analysis Identified a peak associated with NLP response on Chromosome A04, and identified a list of candidates for the NLP-responsive gene. The result obtained was consistent with the locus identified from the previous GWAS study. Although the resolution was improved, further work was needed before a convincing candidate could be identified. KASP also narrowed the region and created a genetic map. To narrow the region further, it will be necessary to increase the number of plants in the KASP assay. In order to test the KASP markers and create an initial genetic map, 77 $F_2$ plants were used in the initial assay. 4 designed markers Nlp_23, Nlp_17, Nlp_18 & Nlp_19 were shown to closely map to the region for NLP response. However, in total, there are 925 $F_2$ plants available from BSA population derived from Ningyou1 x Ningyou7 crosses; this number will be enough to identify new recombination points on the mapped NLP-recognition locus. In future work, increasing the number of individuals in the KASP assay will improve resolution and potentially narrow down the region associated with the trait.

The candidates identified so far could reasonably be involved in the NLP response. One of them was BnaA04g18600D, found highly associated with the NLP-recognition with BFR AO value of 26 (Table 4.6). Additionally, it is found with the annotation analysis that, this gene is the homologue of SOBIR1 which has a key role in NLP-recognition in *A. thaliana*. SOBIR1 forms a complex with RLP23 and this functional complex then recruits BAK1 to start the signalling cascade(Albert et al., 2015). Another strong association was found with BnaA09g06090D on A09 which is homologue of MYB96 from *A. thaliana*. Interestingly, a gain of function mutant of this MYB transcription factor showed enhanced resistance to *P. syringae* infection due to the accumulation of pathogenesis-related (PR) genes (Seo & Park, 2010). Even though some of the genes strongly associated to the NLP-recognition found high homology to the *A. thaliana* genes having role NLP-triggered immunity, the most likely candidates for NLP-recognition are RLP-like proteins since these are associated with the perception of the NLPs and inititating the signalling mechanism (Table 4.6).

Significant difference between the flg22-induced ROS response of NLP-Responders and Non-responders could be observed from Figure 4.4. That is consistent with the earlier result in section 3.2.3. Additionally, when we look closely at flg22 and NLP-induced ROS burst of the NLP-responder individuals, the capacity of the individual $F_2$ plant s to each PAMP motif (flg22 or NLP) was similar. The observed relation between NLP-recognition and the increase in the magnitude of flg22-induced ROS response was already discussed in the previous Chapter 3. In addition, results from this chapter show that, although they have common regions associated with the magnitude of the induced ROS response for both flg22 and NLP, they also have distinct regions associated with response to each PAMP. *BnaA01g02190D* was found to be associated with a high NLP-induced ROS response phenotype in section 4.2.6. This gene is homologue of *Atbsk1* (*At4g35230*), which is *BR-SIGNALLING KINASE1* physiologically associating with *FLS2* (H. Shi, Shen, et al., 2013). Therefore, this association was further investigated in this PhD with model organism *A. thaliana* and will be presented in Chapter 5.

# CHAPTER 5

# *BnaBSK1.A01* is associated with High NLP-induced ROS response in *Brassica napus* - the role in ROS response and Quantitative Disease Resistance to *Botrytis cinerea* verified in *Arabidopsis thaliana*

## 5.1. Background

### 5.1.1. *BnaBSK1.A01* is associated with high NLP-induced ROS response by Genome Wide Association Studies in *Brassica napus*

As previously described in Chapter 4, earlier screening of the *B. napus* diversity set within the group demonstrated that 12 out of the 192 *B. napus* lines respond to BcNEP2. Results from subsequent GWAS analysis indicated that Bna*BSK1.A01* might be associated with NLP-induced ROS (Figure 5.1). However, the results from those GWAS studies were only just significant in one repeat, and not significant in a second repeat. The association of the SNP derived from the GWAS study was just below the threshold of 6.64, with a value of 6.44. One potential reason for the low level of significance was that there were only 12 NLP-responding cultivars out of 192 accessions which can reduce the resolution of GWAS (Rachel Wells, personal communication).

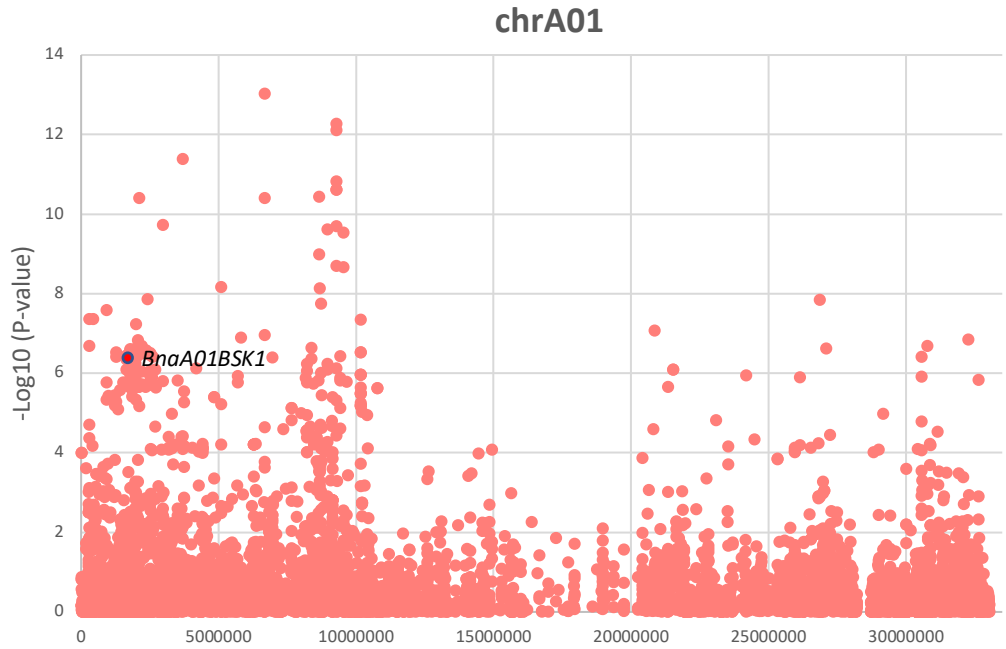


**Figure 5.1** Distribution of mapped markers on A04 associating with the NLP-induced ROS production (GWAS figure is generated by Dr. Rachel Wells with data generated from *B. napus* diversity set).

As members of receptor-like cytoplasmic kinases (RLCK) subfamily XII, BRASSINOSTEROID SIGNALLING KINASES (BSKs) have an important role in immunity as well as in BR signalling (Lozano-Durán & Zipfel, 2015). Several RLCKs are required by PRRs to enable downstream signalling following perception of the cognate PAMP molecule during infection (Liang & Zhou, 2018). In *Arabidopsis*, BSK5 has an active role in immunity and membrane localisation, phosphorylation by PRRs, and kinase activity are required for its function (Majhi et al., 2019).

In previous studies in *Arabidopsis*, it has been also indicated that BSK1 has a dual role in immunity and BR-mediated growth. In plant immunity, BSK1 physically associates with FLS2 receptor. Also, the *bsk1-1* single mutant displayed enhanced susceptibility to *Golovinomyces cichoracearum*, *Pseudomonas syringae* pv *tomato (Pto)* DC3000, and *Hyaloperonospora arabidopsidis* (H. Shi, Shen, et al., 2013). However, the role of BSK1 in NLP recognition and defence activation is not known.

In chapter 4, genomic loci associated with the magnitude of the NLP-induced ROS response were identified by computing the BFR values of the variations derived from pools of 'high' and 'low' NLP responding $F_2$ individuals. In this chapter, I show how

*BnaBSK1.A01* was found to be associated with high NLP response using this approach and test this finding in model plant *Arabidopsis thaliana*. For this purpose, *Arabidopsis bsk1-1* mutant lines obtained from Prof. Tang (H. Shi, Shen, et al., 2013; H. Shi, Yan, et al., 2013) were used to investigate whether this gene has a role in NLP-triggered immune responses, such as, ROS burst, induction of the defence gene expressions or increased disease resistance against an NLP-bearing pathogen *B. cinerea*. Considering the increase in disease resistance of *bsk1-1* mutant lines against *B. cinerea* might be due to other type of early immune responses, such as camalexin synthesis, camalexin sensitive mutant *ΔBcatrB4* (Stefanato et al., 2009) was also used. The effect of the mutation on NLP-triggered immunity were further investigated by measuring gene expression. The induction patterns of the genes having key role in JA pathway such as *JAR1* (Suza & Staswick, 2008) and a transcription factor involved in plant defence *WRKY33* (Birkenbihl et al., 2012; Zheng et al., 2006) were examined after NLP treatment at certain time points.

## 5.2. Results

### 5.2.1. *BnaBSK1.A01* is associated with high NLP-induced ROS response by Bulk Segregant Analysis in *Brassica napus*

Some specific variations associated with the high NLP-induced ROS response phenotype were found to have an effect on *BnaA01g02190D* gene on ChrA01 (Figure 5.2). This gene is homologue of *Atbsk1* (*At4g35230*), which is *BR-SIGNALLING KINASE1* physiologically associating with *FLS2* (H. Shi, Shen, et al., 2013) and has a major role in flg22 recognition. The results showed that variations had an effect on this gene, with higher BFR values for high NLP-induced ROS response when compared to the BFR values derived from the association to high flg22-induced ROS response phenotype (Appendix C).


**Figure 5.1** Manhattan plot created with corresponding calculations of the Bulk Frequency Ratios of the variations between Pool4 (High responder) and Pool3 (Low responder). The positions of the variations are plotted along the X-axis on BnaChrA01 (The variation with 4.59 BFR AO value with predicted effect on BnaA01BSK1 labelled just above the position of the variation).

### 5.2.2. *Atbsk1-1* mutants have significantly lower NLP-induced ROS burst compared to wild type *Arabidopsis thaliana* Col-0 line

To functionally test the effect of *BSK1 (BR-SIGNALING KINASE1)* in BcNEP2-induced ROS response, *A. thaliana bsk1-1* mutants (H. Shi, Shen, et al., 2013) were obtained from Prof. Dingzhong Tang`s group. Before screening with the ROS assay, the *A. thaliana* mutant *bsk1-1* and the Col-0 were genotyped for their mutations. A CAPS marker designed to detect the *bsk1-1* mutation was used to amplify the region of interest. The PCR fragments were obtained and digested with BsuRI (HaeIII) enzyme. As expected, it was observed from the image of agarose gel electrophoresis (Figure 5.1), the Col-0 doesn't have a *bsk1-1* mutation in its genome, so it migrates at 82 and 77 base pairs instead of 159 base pairs. The *bsk1-1* mutation is confirmed by the fragment, which remains undigested by the enzyme and so migrates at 159 bp.

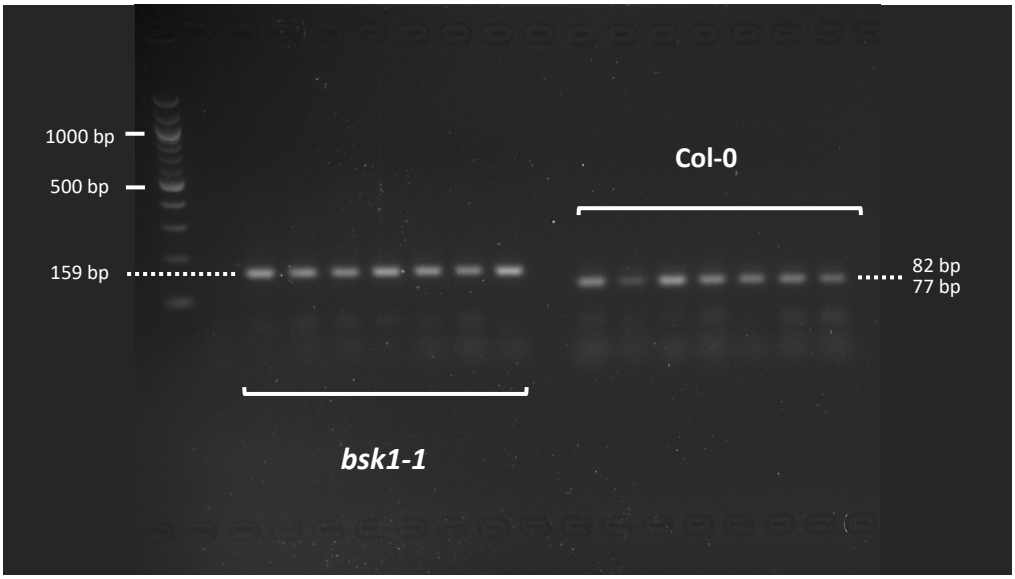


**Figure 5.1** The image of cloned and digested fragments from the mutation region of 8 Col-0 and 8 *bsk1-1* plants in 2.4% Agarose gel containing ethidium bromide.

To test the possible effect of a mutation on *BSK1* on NLP-induced ROS, bsk*1-1* mutant seeds and the Col-0 were compared in the ROS assay using different concentrations of BcNEP2 and flg22 There was a gradual decrease in ROS production corresponding to decreasing concentration of both PAMPs. Similar results were observed in Col-0 by both BcNEP2 and flg22 PAMP motives. In contrast, the previous work done by Shi

et al., no significant difference could be found between the wild type and *bsk1-1* mutant line for any concentration (H. Shi, Shen, et al., 2013). However, unlike the flg22 response, a significant difference was found between the *bsk1-1* mutant and the Col-0 in response to 50 nM BcNEP2. Also, there was a clear trend of the response of *bsk1*-1, measured by RLU, being reduced compared to Col-0 at all concentrations. This significant difference and trend support the hypothesis that BSK1 is involved in NLP-triggered ROS response (Figure 5.2).

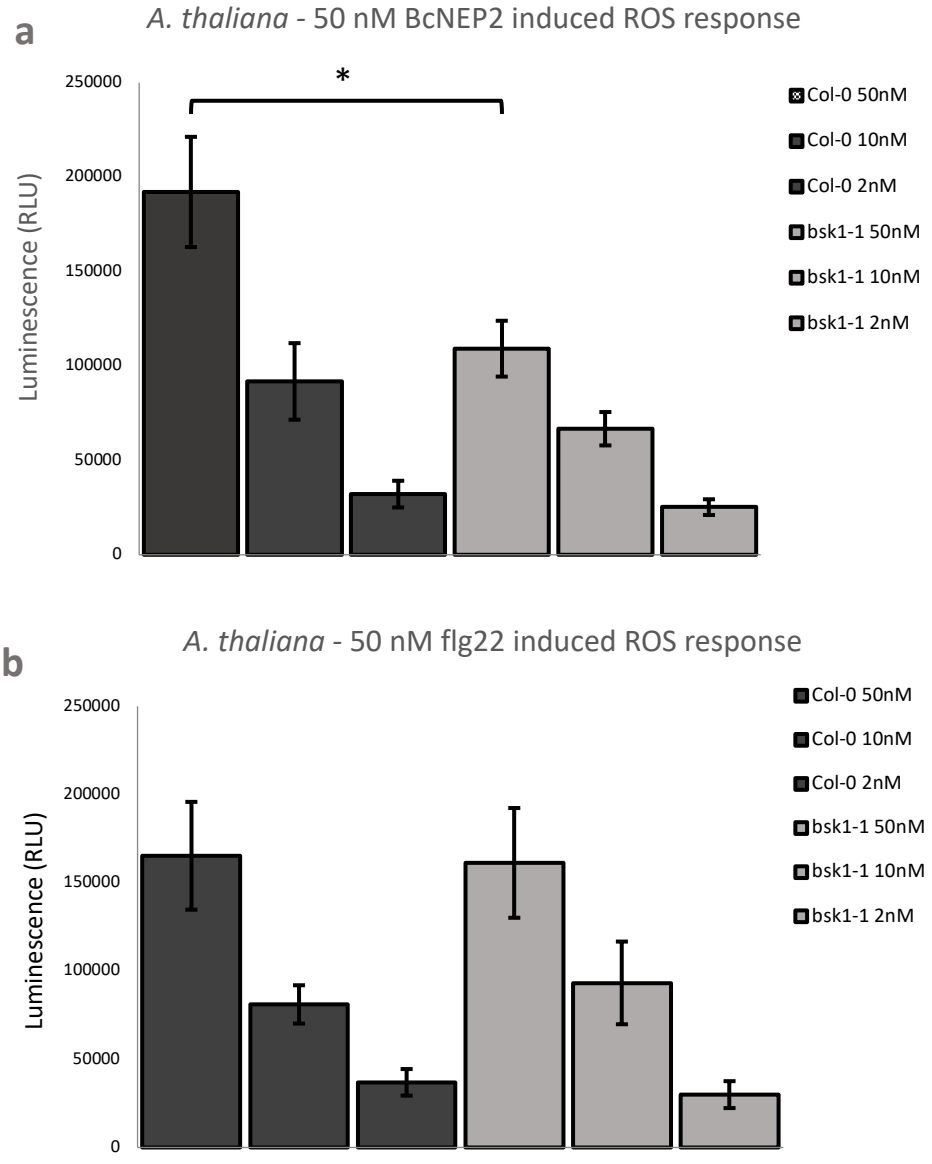


**Figure 5.2** Leaves of the Col0 (wild type), *bsk1-1* mutant lines were treated with (a) 50nM, 10nM, 2nM BcNEP2 and (b) 50nM, 10nM, 2nM flg22 incubated with luminol and horseradish peroxidase to detect ROS. Data represent total RLU read over 40 minutes. Error bars are the standard error of 8 biological replicates. (p-value=0.0287*)

### 5.2.3. *Atbsk1-1* has significantly decreased Quantitative Disease Resistance to *Botrytis cinerea* infection

The involvement of co-receptor *BSK1* to disease resistance against the necrotrophic pathogen *B. cinerea* was tested by using Col-0 and *bsk1-1* mutant lines. In the disease assay, both the B05.10 (wild type) strain and a camalexin sensitive mutant ΔBcatrB4 strain were used. Figure 5.3 shows the result of the disease assay of the *bsk1-1* mutant line and Col-0, inoculated with the 2 strains of *B. cinerea.* Camalexin sensitive mutant ΔBcatrB4 was not more infectious to either of the lines. However, the *bsk1-1* mutant line showed significantly higher susceptibility to *B. cinerea* wild type strain with larger lesions compared to Col-0.

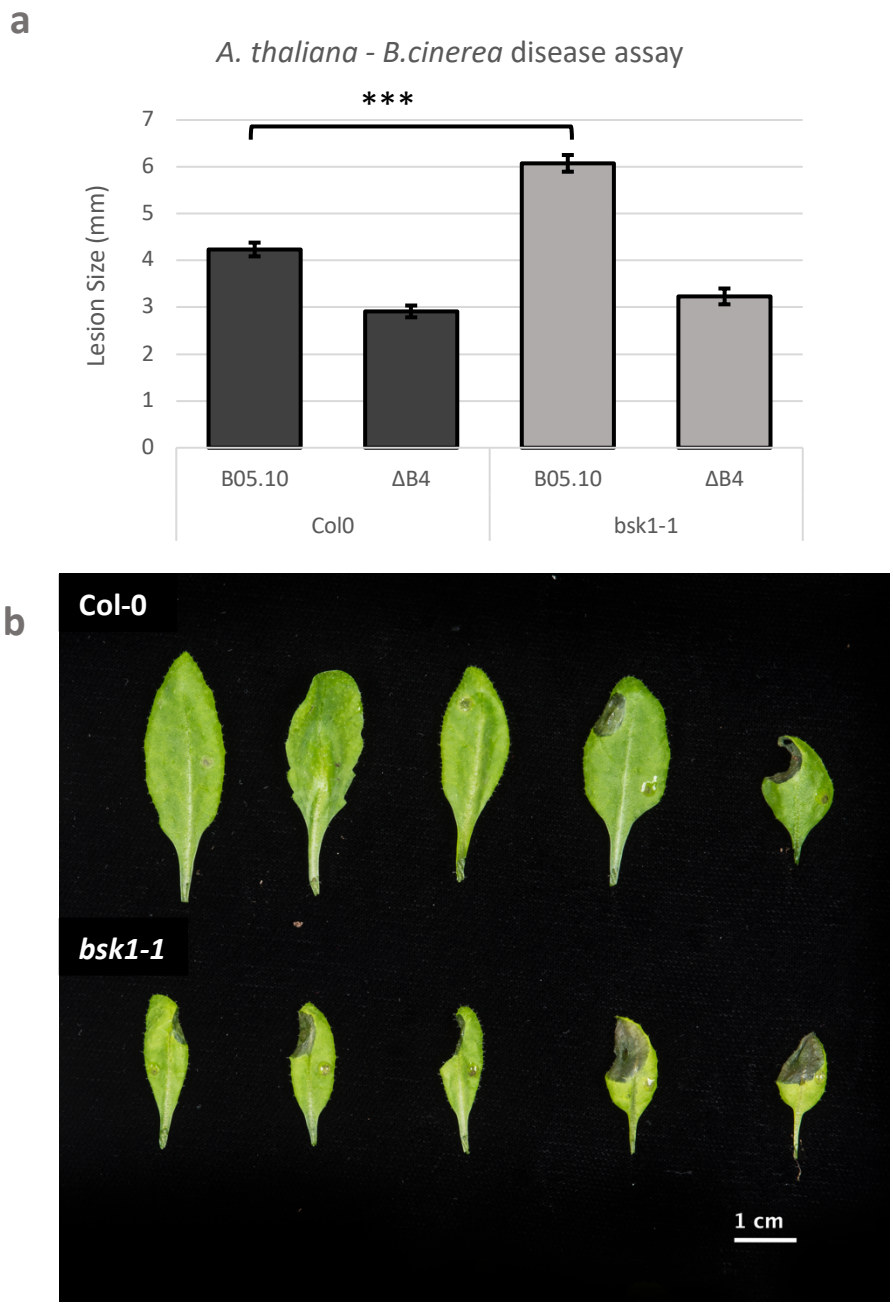


**Figure 5.3** *B. cinerea* disease screening of leaves from *A. thaliana* plants. (a) Data represented as lesion size of *B. cinerea* infection on *A. thaliana* plant leaves 3 DPI. Error bars represent standard error of 12 biological replicates (***p-value=1.12E-14). (b) Five-week-old *Arabidopsis* plants were infected with *B. cinerea*. 5 µl drops from B05.10 strain placed on the upper part of the leaf, and 5 µl drops of ΔBcatrB4 mutant strain placed on the lower part of the leaf. The plants were photographed at 3 DPI.

### 5.2.4. Defence related genes are differentially induced in Col-0 and *bsk1-1* mutant line with BcNEP2 treatment

To visualize the expression of the *BSK1* and *RLP23* gene either in the mutant or wild type background, qRT-PCR was carried out. It was observed that the *bsk1-1* mutation neither negatively nor positively affects the expression levels of the *BSK1* and *RLP23* genes. Additionally, there was no significant induction due to BcNEP2 treatment for these 2 genes when compared with the mock-treated samples.

There was significant induction in WRKY33 expression of the wild type BcNEP2 treated plants when compared with wild type mock-treated plants within 12 and 24 hours after PAMP treatment. In contrast, the *bsk1-1* mutant line did not show any significant induction of *WRKY33* at the same time points when compared with its mock-treated plants. There was a trend of increased induction at 12hpi (hours post-injection) in the mutant line, returning to its basal level at 24hpi (Figure 5.4).

A similar result was observed for *JAR1* gene induction. At 12hpi, there was significant induction in *JAR1* expression in both wild type and mutant lines, whereas, at 24 hpi, the significant induction was only detected in wildtype BcNEP2 treated plants when compared with the mock-treated ones (Figure 5.4).

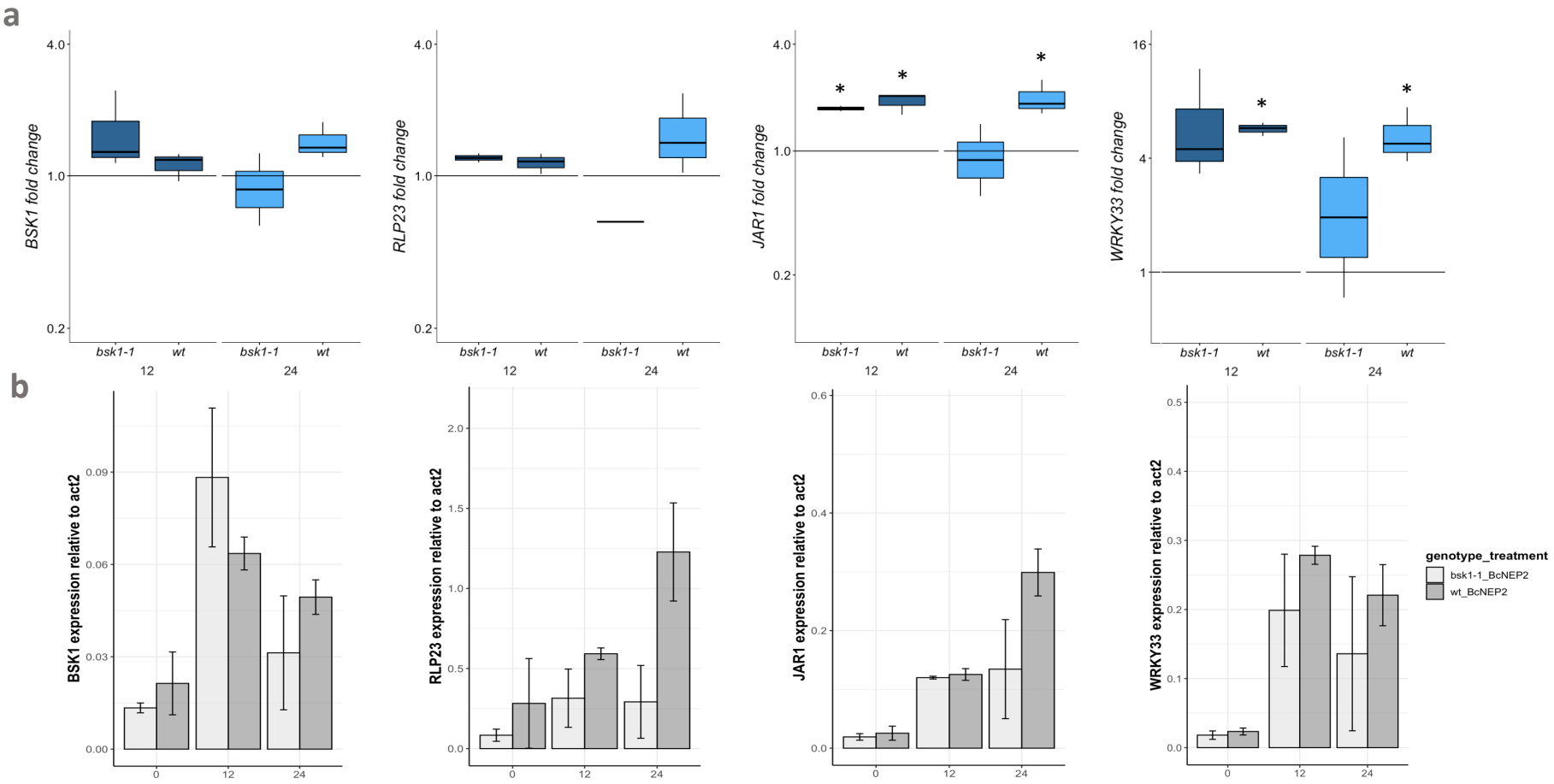


**Figure 5.4** Quantification of (a)induction and (b)expression of *BSK1, RLP23, JAR1,* and *WRKY33* genes after 100 nM BcNEP2 treatment. mRNA levels of the genes were measured by qRT-PCR in BcNEP2-treated and mock-treated plants. ACTIN2 was used as a normaliser. Bars represent means of three biological replicates ± SEM. Asterisks indicate significant differences between expression levels in mock and treated leaves (Student's t-test *, P < 0.05).

### 5.3. Discussion

The results demonstrate that BcNEP2-induced ROS response is reduced in *bsk1-1 Arabidopsis* mutants compared to wild type Col-0 and is the first demonstration of an association between BSK1 and NLP recognition. The results suggest that BSK1 could modulate NLP-induced ROS burst, possibly through its involvement in a complex similar to that reported for BAK1/SOBIR1 (Albert et al., 2015).

Although the NLP-induced ROS burst result was significantly reduced in *bsk1-1* mutant lines, I was not able to repeat the previously reported reduced flg22-induced ROS burst (H. Shi, Shen, et al., 2013). One possible reason for this could be the environmental conditions used in my experiments were different from those used by Shi et al. Since BSK1 is involved with BR signalling, it is reasonable to suggest that the environment could affect the result. BR sensing is involved in both the regulation of immunity and also of growth (Lozano-Durán & Zipfel, 2015), and it is also well-known that different results are obtained for *Arabidopsis* between labs (Massonnet et al., 2010). My results suggest, however, that NLP-induced ROS is affected to a greater extent in *bsk1-1* mutants than flg22-induced ROS.

The results obtained from the *B. cinerea* disease assay proved that *BSK1* positively contributes to resistance against *B. cinerea*. Lack of significant difference between the Col-0 and *bsk1-1* mutant line in corresponding disease resistance against camalexin sensitive mutant ΔBcatrB4 (Stefanato et al., 2009) shows that the mutation in *BSK1* does not have a significant effect on the camalexin-derived defence pathway of the *A. thaliana* against *B. cinerea.* However, the growth of the camalexin sensitive mutant was less than the wild type, and so this might have affected the level of significance in the comparison.

A previous report indicated that *WRKY33* expression is induced at 24 and 48 hours after *B. cinerea* infection (Zheng et al., 2006). In this study, significant induction of *WRKY33* gene mRNA levels at 12hpi and 24 hpi was observed in wild type PAMP treated plants. The results could indicate the involvement of PTI during the infection

process of *B. cinerea*. It has already been showed that ET- and JA-mediated defences have a key role through immunity against *B. cinerea* in *A. thaliana*. In addition to that, WRKY33 function is required for *B. cinerea* resistance via its feature to suppress SA-mediated responses (Birkenbihl et al., 2012). Therefore, it is proved that this feature of the transcription factor WRKY33 is preventing the antagonistic effect of SA-mediated pathways on JA-mediated responses. As a consequence, the loss of JAR1 induction at 24hpi of the *bsk1-1* mutant line might be due to lack of induction in *WRKY33* gene expression.

In this chapter, the results demonstrated that BSK1 can have a modulating effect on NLP-induced PTI responses and also contribute to QDR against necrotrophic pathogen *B. cinerea.* Furthermore, the results also suggest that an underlying mechanism could be related to the JA-mediated pathway, although this would require further investigation. Previous work has shown that BSKs could have a dual function in immunity or growth, although how this balance is achieved, regulated, and influenced by the environment is still a matter of debate for the scientists (Lozano-Durán & Zipfel, 2015). In the next Chapter 6, I further investigate the effect of the environment on PAMP-triggered immunity, taking advantage of a well-characterised mapping population of *Brassica oleracea*.

# CHAPTER 6

## Effects of Environmental stress on PTI-induced ROS response and Quantitative disease resistance (QDR) of *Brassica oleracea* to *Botrytis cinerea*

### 6.1. Background

The previous chapters focussed on characterisation of the NLP responses in *B. napus* and described subsequent progress towards the identification of candidate genes involved. The work identified potential genes and genetic loci involved in the recognition and modulation of the NLP-induced ROS response. Chapter 5 described how BSK1 was identified in modulating the NLP response and, since BR signalling pathway components are involved, highlighted the link between growth and defence and how the environment can influence these.

Environmental stress is a general term covering many factors which can be either abiotic or biotic. Abiotic and biotic stresses can influence the balance between growth and the immune response of the plants. This crosstalk between abiotic and biotic stress is increasingly being studied, and the mechanisms behind this are being revealed. Recent studies have highlighted the overlap between signalling

mechanisms for abiotic and biotic stresses, and some stress-inducible genes were identified and associated with the defence responses (Nejat & Mantri, 2017).

In this chapter, I investigate the effect of the environment on PTI. This work was initiated at the beginning of my research project but was later discontinued as I focussed on the NLP-related investigations. However, with the identification of BSK1 as a modulator of PTI, this research has become much more relevant to the other studies in my thesis. This work was undertaken with *Brassica oleracea*, a model C genome species, using a previously-studied double haploid population for which genomic sequence was available. The population *Brassica oleracea* ssp *alboglabra* (A12DHd) and *B. oleracea* ssp *italica* (Green Duke GDDH33) (hereafter known as A12xGD population) was previously generated (Sparrow et al., 2004). I also used the well-studied PAMPs elf18 and flg22. Mapping of flg22 and elf18 induced ROS response, and disease resistance was previously carried out using this population (Simon Rhys Lloyd, 2014). Using this population, preliminary investigations uncovered a novel phenotype whereby ROS production in the line AG1012 could be induced by an undefined stress response. This observation could potentially provide a mechanism to investigate both abiotic and biotic stresses and the potential links between them. Moreover, since a mapping population was available, this could provide the basis for identifying the underlying genes.

Fungal pathogen-derived PAMP molecules such as chitin and BcNEP2 are also considered to use in this study; however, 2 main issues arose from a problem in *B. oleracea* plants; increased chitinase enzyme activity in the leaves and being non-responsive to NLP respectively.

In this chapter, I demonstrate that drought stress is the condition that causes the induction of the ROS response. The main hypothesis for this chapter is that drought induces changes in gene expression that affect PTI and disease resistance. Also, I made progress in defining the genetic loci and potential genes that might be involved. Firstly, I define the experimental conditions that cause the induction of ROS production induced by PAMPs in AG1012 *B. oleracea* line under controlled

conditions. I then performed the same experiment with the whole population to make progress in identifying the underlying genes via two main methods; QTL mapping and RNA-seq. In total 77 lines were grown in defined drought stress and control conditions and screened with ROS assay in response flg22 and elf18 and also resistance to *Botrytis cinerea*.

## 6.2. Results

### 6.2.1. Quantitative disease resistance to *B. cinerea* in *B. oleracea* is correlated with ROS production during PTI

While double haploid lines from the A12xGD cross population were being phenotyped, progeny line AG1012 was identified as having a low ROS phenotype, shown in Figure 6.1 with the red coloured bar. Additionally, it was observed that a similar trend of results was obtained for both flg22- and elf18- induced ROS production. The result indicates that generally, there is a similar capacity of each line for the ROS burst generated by both PAMPs, although there are a few exceptions to this.

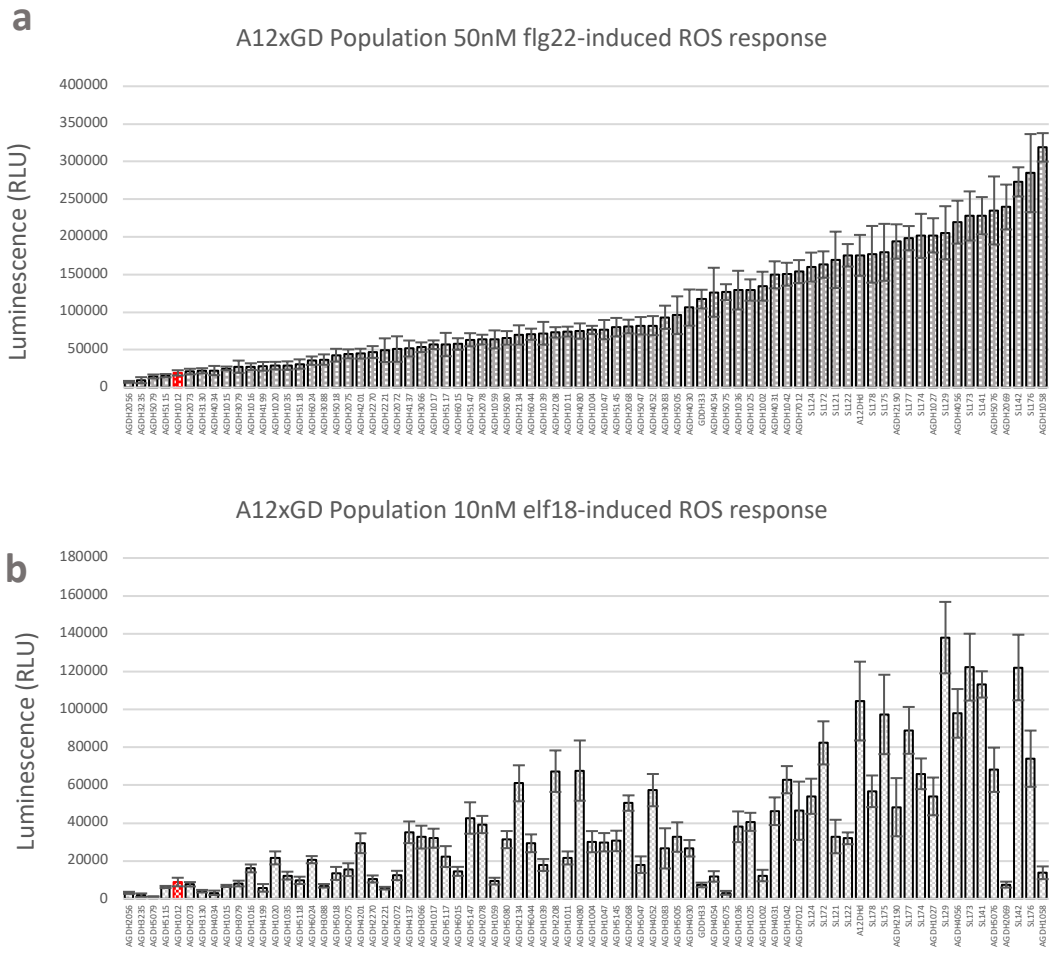


**Figure 6.1** Total ROS response of 77 lines from A12xGD population under control conditions treated with 50nM flg22 for 40 min and RLU measured every 30s. Bars represent the mean of 16 leaf discs from 8 biological replicates for each line. Total RLU from AG1012 is represented in red. Error bars are the standard error of 8 biological replicates.

Another interesting result was obtained with the *B. cinerea* disease assay with A12xGD population; correlation analysis showed that there is a significant negative correlation between the QDR to *B. cinerea* and ROS burst with 0.48 absolute correlation value (Figure 6.2).

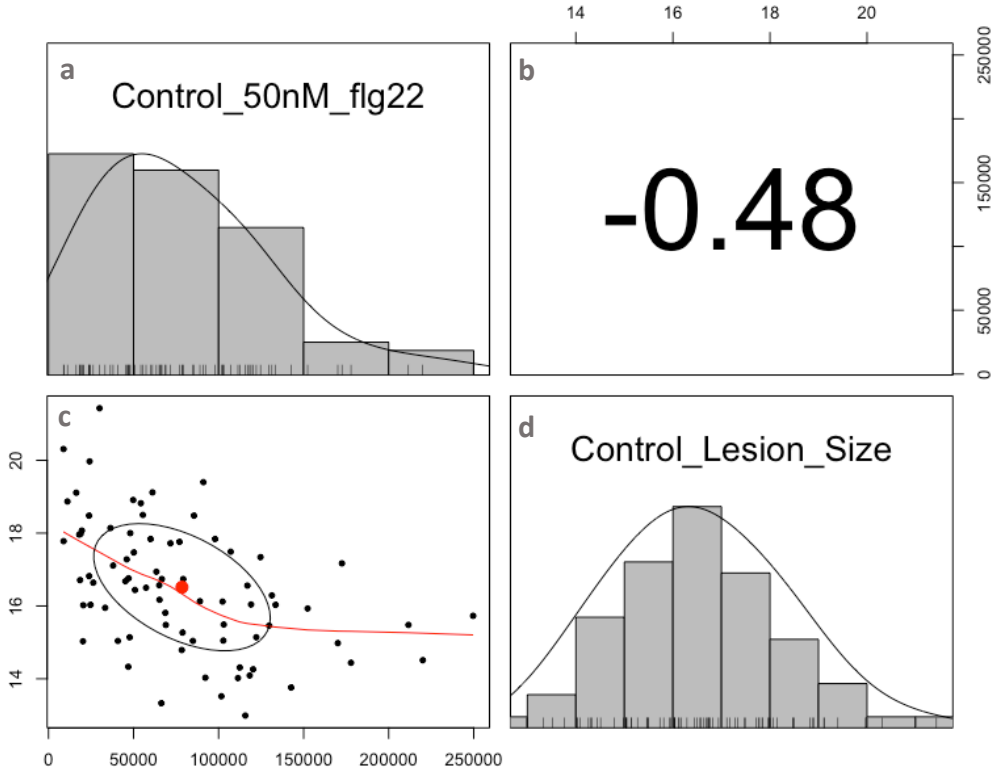


**Figure 6.2** Correlation analysis between *B. cinerea* disease assay results of individual lines from A12xGD population and corresponding ROS burst results of each line. The histogram plots integrated with rug plots of total RLU in response to 50nM flg22 (a) and Lesion size (mm) of *B. cinerea* infection at 3dpi (d). The scatter plot (c) drawn with loess smooth (A smooth curve – synonym of lowess (Locally Weighted Scatterplot Smoothing)), showing the negative correlation between the results. The panel (b) is showing the correlation coefficient value.

### 6.2.2. Experimental design to define unknown abiotic stress conditions

In previous studies in the group, it was shown that the ROS response of AG1012 line could be induced, although the conditions for this were not defined. Therefore, I performed experiments to determine the abiotic stress conditions and to define the stress limit of the *B. oleracea* plants using different temperatures and watering regimes. These experiments performed with A12, Green Duke, and AG1012.

After treatment with different stress conditions (Table 2.6), significant induction in ROS response to 50nM flg22 was observed in AG1012 samples, especially those grown at 21 °C and 6 °C. Drought stress conditions when compared with the control (21 °C / Normal watering). Induction in ROS response to 50nM flg22 was also observed for A12 samples grown with drought stress conditions at all temperatures although to a lesser extent. Another interesting result gained from this experiment was the suppression of the ROS response by increased humidity level (Figure 6.3).

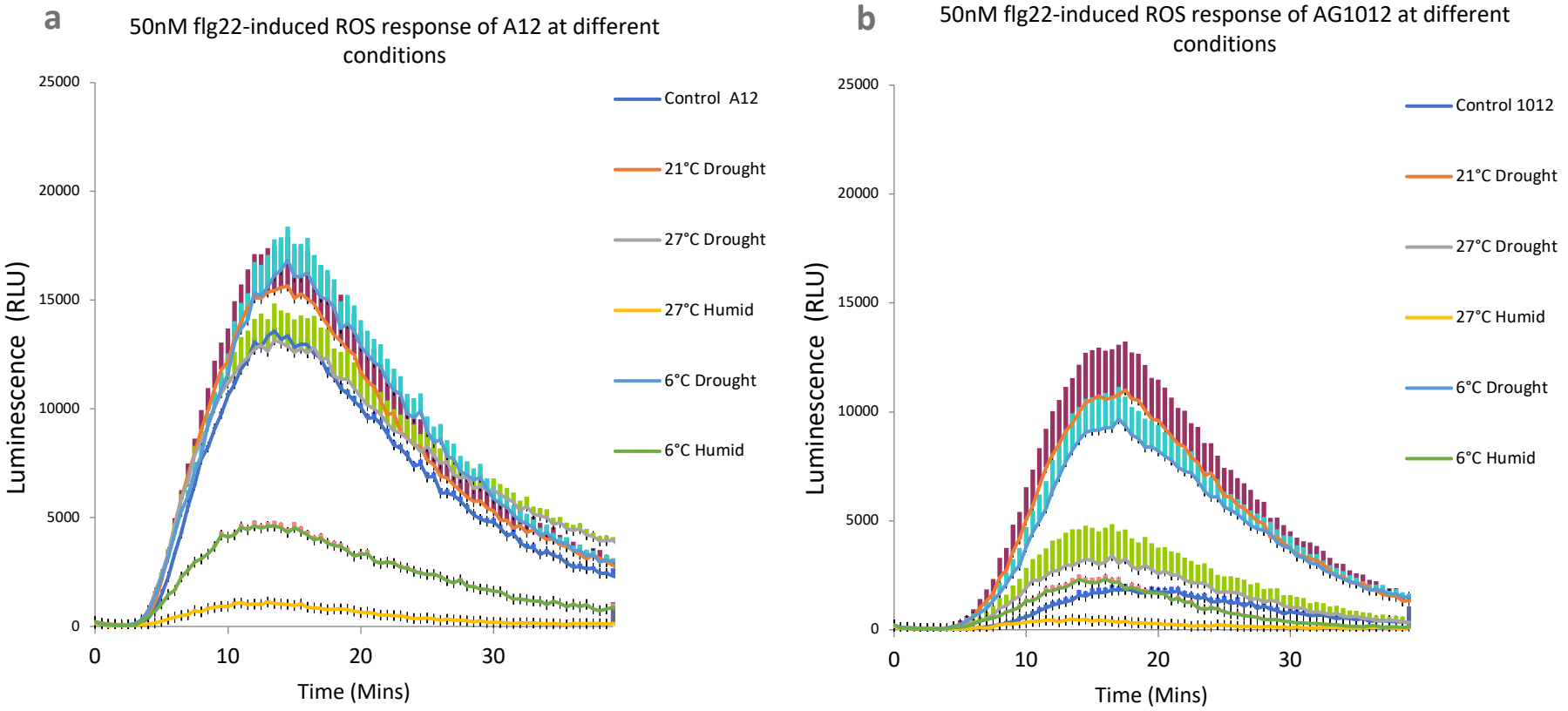


**Figure 6.3** Effect of 3 different temperatures and different watering regimes on the oxidative burst of A12(a) and AG1012(b) in response to 50nM flg22. Data represent Luminescence RLU read over 40 minutes. Error bars are the standard error of 8 biological replicates.

Since the drought stress treatment gave the most significant differences of the phenotypes for fine-mapping studies, these conditions were also used for the whole population. Therefore, the abiotic stress conditions were defined as; 21 °C / Normal Watering and 21 °C / Drought Stress.

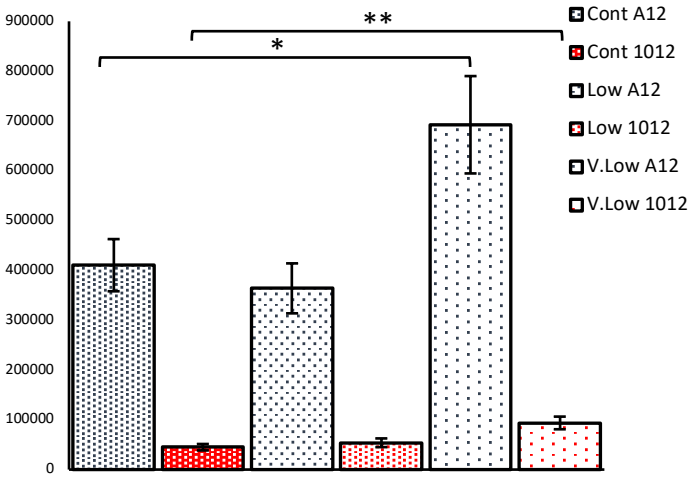


**Figure 6.4** ROS response to 50nM of flg22 of A12 (Gray) and AG1012 (Red) at different watering regime; Control (30ml/day), Low (20ml every workday +15ml Monday/Friday), Very Low (10 ml Monday/Wednesday/Friday) in CER. Data represent total RLU read over a period of 40 minutes. Error bars are the standard error of 8 biological replicates ($p\text{-value}_{A12} = 0.0278$*, $p\text{-value}_{AG1012} = 0.0062$**)

Preliminary trials for drought stress conditions at B18 controlled environment rooms (CERs) were performed so that the optimal conditions for the experiment could be defined before progressing to the entire mapping population. A12 and AG1012 and were used for defining the watering regimes (which will determine the stress level) and to understand the effect of environmental conditions of the CERs to stress treated plants. In the control conditions, AG1012 showed a low ROS response phenotype again but, when the drought was increased, the induction level of the ROS response significantly increased. (Figure 6.4). So, the watering regime was defined as 5ml water on Monday, Wednesday, and Friday for 2 weeks.

### 6.2.3. The A12xGD population is segregating for induced ROS burst under drought stress conditions

After defining the optimal abiotic stress conditions for inducing flg22-induced ROS burst AG1012, the A12xGD cross population was grown under the same conditions. ROS production after application of various PAMP molecules was measured for individual lines of the A12xGD population following drought stress and compared to non-stressed control plants. Lines in the population showing the most highly-induced ROS were AG2056, AG5079, and AG5005, with their over 1700% increase compared to the control response. Parental lines A12 and Green Duke showed distinct phenotypes after drought stress treatment. A12 had a low increase in ROS response when compared to the general population, with a 226% increase. However, Green Duke was completely different from the rest of the population, with only 11% increase in ROS response under drought conditions. Those specific lines of the mapping population with the greatest change in ROS phenotype after drought stress treatment could be particularly informative for further experiments. (Figure 6.5).

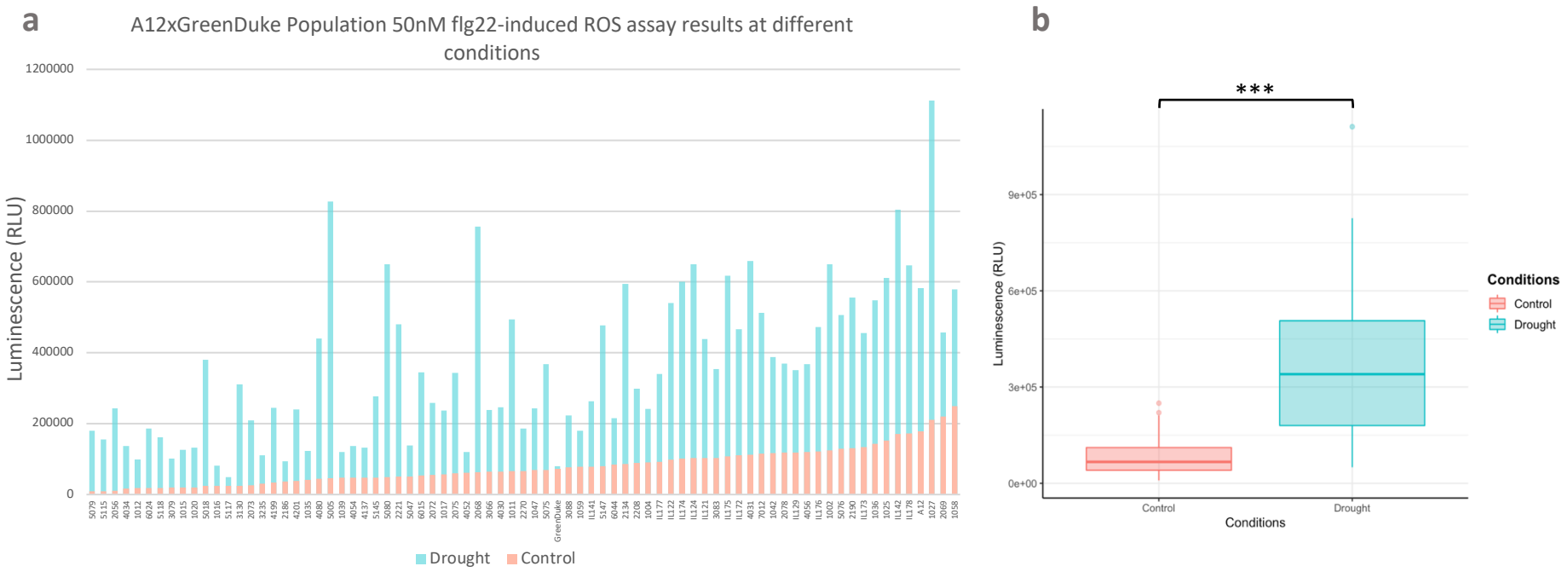


**Figure 6.5.** Effect of drought stress conditions on the oxidative burst of A12xGD mapping population. (a) Total ROS response of 77 A12xGD lines under drought and control conditions were treated with 50nM flg22 for 40 min, and RLU measured every 30s. Bars represent the mean of 16 leaf discs from 16 biological replicates for each line. (b) Box plot representation of A12xGD Population 50nM flg22-induced ROS assay results grown under drought (green box) and control (orange) conditions (p-value < 2.2e-16 ***)

### 6.2.4. Drought stress induces resistance to *B. cinerea* in the A12xGD biparental population

To further investigate the crosstalk between abiotic stress and biotic stress, *B. cinerea* disease resistance of the control and the drought stress treated AG lines were tested. For the parental lines, A12 gave smaller lesions to *B cinerea* than Green Duke in both conditions. There was clear variability across the AG population, and drought stress enhanced the resistance to *B. cinerea* for almost all lines significantly except for AG1011(Figure 6.6). The level of increased resistance also showed variability across the population. A demonstration of increased resistance to *B. cinerea* is shown in the plate figure with infected Green Duke leaf disks (Figure 6.7). There was a negative correlation between the magnitude of ROS response produced and the disease resistance against *B. cinerea* of the A12xGD population treated with drought stress (correlation coefficient = -0.35, Figure 6.8). However, the correlation was greater under control conditions (correlation coefficient = -0.48, Figure 6.2).

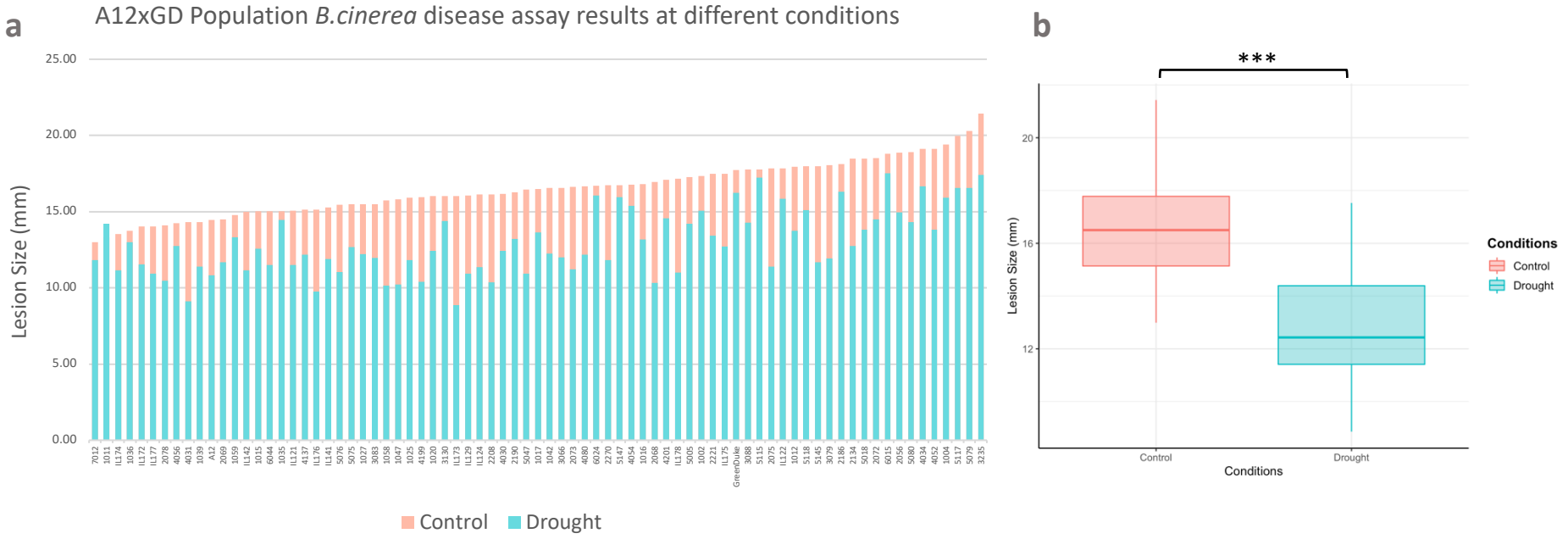


**Figure 6.6** *B. cinerea* disease screening of A12xGD mapping population grown under drought stress and control conditions. (a) Bars represent mean lesion size (diameter) of 32 leaf discs from each line of *B. cinerea* infection on A12xGD mapping population. Leaf discs of *B. oleracea* lines that grow under drought stress conditions (green bars) or control conditions (Orange bars) inoculated with agar plugs of *B. cinerea* strain B05.10 and measured 3 days post-infection (dpi). (b) Box plot representation of *B. cinerea* disease assay Lesion Sizes (mm) from A12xGD population, grown under drought (green box) and control (orange) conditions (p-value < 2.2e-16 ***)

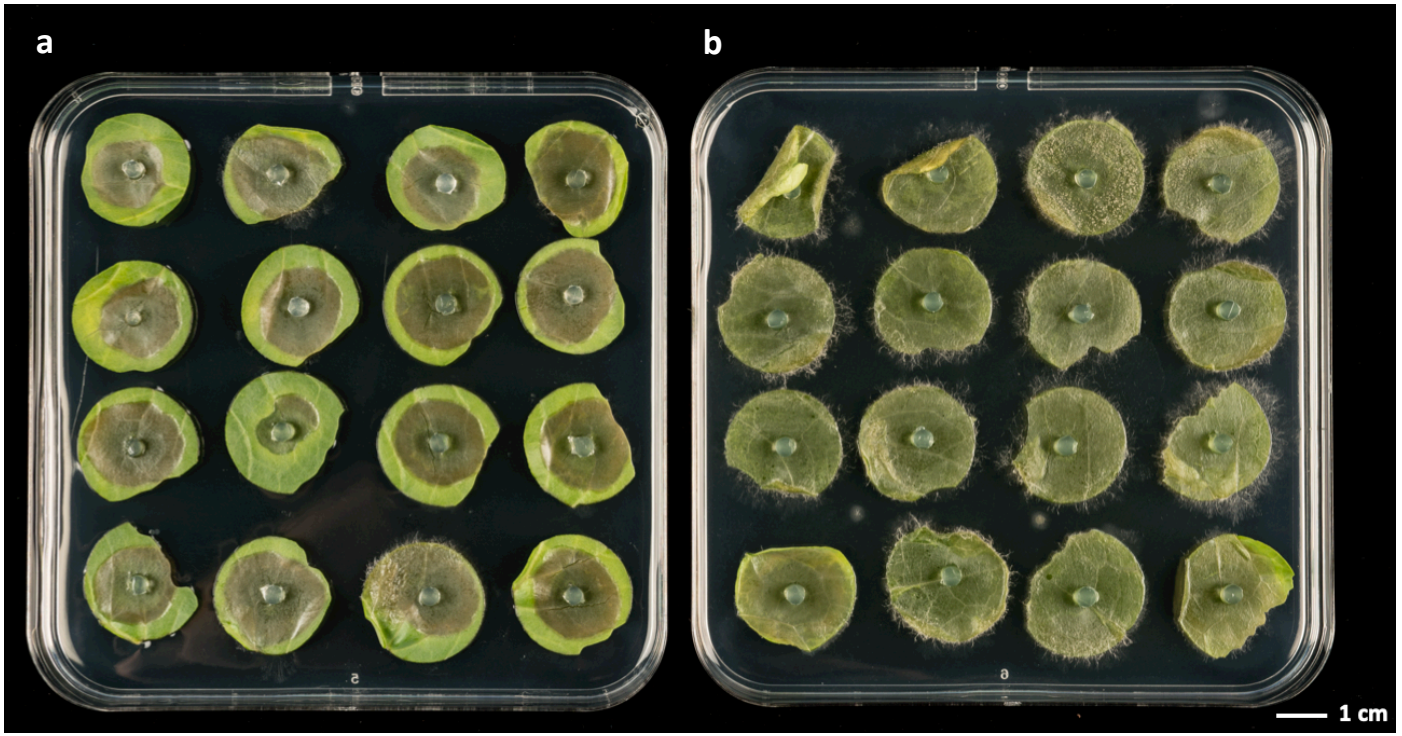


**Figure 6.7** Six-week-old *B. oleracea* leaf discs were infected with *B. cinerea* plugs. Leaves were photographed at 3 DPI. (a) A plate overview containing *B. cinerea* infected leaf discs taken from drought stress treated Green Duke line. (b) A plate overview containing B. *cinerea* infected leaf discs taken from Green Duke line grown in Control watering conditions.

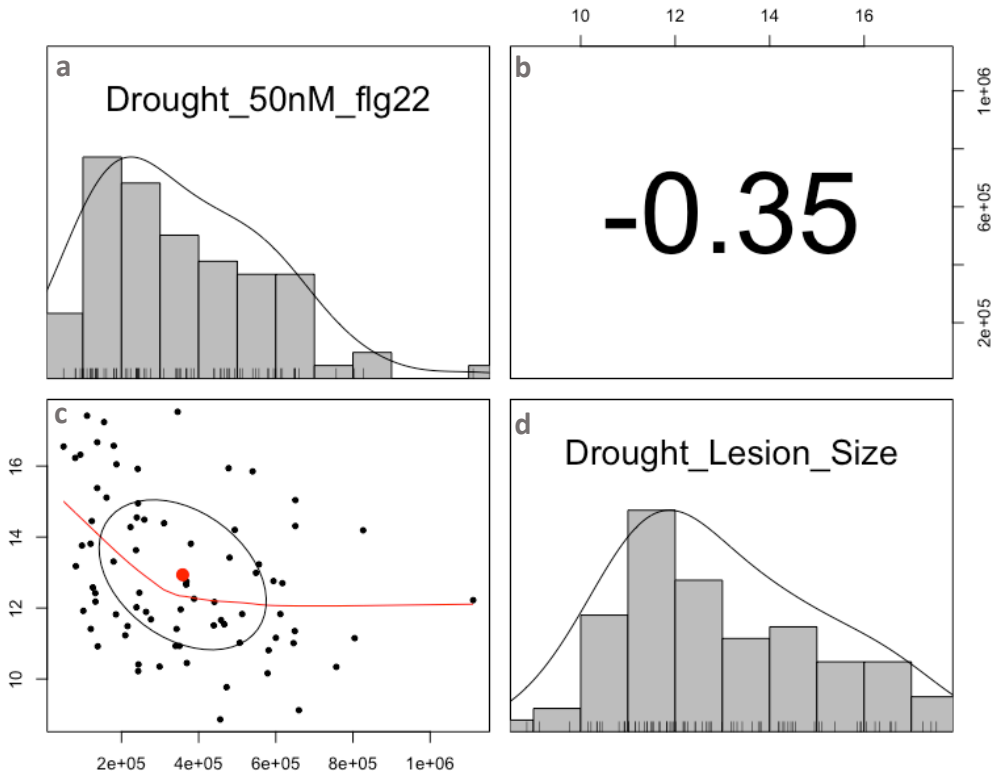


**Figure 6.8** Correlation analysis between *B. cinerea* disease assay results of individual lines from A12xGD population and corresponding ROS burst results of each line treated with drought stress for 2 weeks. The histogram plots integrated with the actual position of each value at the bottom, as rug plots, of total RLU in response to 50nM flg22 (a) and Lesion size (mm) of *B. cinerea* infection at 3dpi (d). The scatter plot drawn with loess smooth (c) showing the negative correlation between the results. The panel (b) is showing the absolute correlation value.

### 6.2.5. QTL Mapping of the regions associated with ROS induction and increase in QDR

In previous studies within the group (Simon Rhys Lloyd, 2014), a significant QTL on C9 was found for the flg22-triggered ROS response. In my study, to increase the resolution of the fine mapping, in addition to the number of the lines from A12xGD population used for previous QTL mapping studies of PAMP-induced ROS response I included 9 new lines from the A12xGD population and 13 substitution lines (SLs) to the screening (Ramsay et al., 1996). Screening of the whole population was performed by measuring ROS response to 2 nM, 10nM, and 50nM of flg22 and elf18. Also a *B. cinerea* disease assay was completed. The phenotypic results were provided to Dr. Peter Walley at Liverpool University, who has access to unpublished marker data specific for this population, and he performed QTL mapping as part of a collaborative project with the group.

In the QTL analysis, data representing the ROS burst against 2nM, 10nM, and 50nM flg22 and 2nM and 10nM elf18 in both growing conditions were used. A genetic map of A12xGD population was run in MAPQTL first for Interval Mapping then for Multiple-QTL Mapping (MQM) analysis by Dr. Peter Walley. Each QTL associated with Control ROS response, Drought ROS response and induced traits in response due to drought stress are represented by a specific LOD approach. The location of each QTL depicted by a reduction in LOD of >1.5 from the peak LOD score is shown in Appendix Table D.

The results for the mapping revealed 'Global QTL' which I define as a region on the genome significantly associated with almost all traits regardless of the type of the PAMP or the growing conditions. A Global QTL was found on the C7 between 47cM – 88cM (Figure 6.11). One of the global QTL was quite big – covering half of the C7 chromosome, with the increased genotype of Green Duke (the "increasing" term is used to describe the parent line contributing to allele) on this chromosome. This broad existence of Green Duke alleles found on C7 might be due to recombination suppression in that area.

Another Global QTL is located on C5 between 73cM-113cM (Figure 6.10). This QTL is associated with High ROS phenotype regardless of the type of the PAMP and stress treatment as the contributing allele is coming from A12 parental line. In contrast, the Global QTL on C7 is mostly associated with a low flg22-induced ROS response phenotype. Also, Global QTL on C5 may potentially disassociate into 2 different QTL as one region between 70 cM – 90 cM would be associated with high flg22-induced ROS response and the other region between 95cM – 120cM with high elf18-associated ROS response. Improved resolution of the map may be able to separate the flg22 and elf18 response.

Results also showed QTL appearing due to drought stress treatment, which supports the hypothesis for this chapter. Two QTL spanning between 13 cM – 44cM and 68cM – 90 cM on C8 are associated with the traits controlling the ROS response after drought stress (Figure 6.12). Interestingly, they came from Green Duke, and are mostly related to a fold-change in ROS response, showing that the region might be related to stability in response to stress conditions.

Other QTL appeared on C2, C3 and C4 are only associated with the traits under drought stress conditions. The QTL significantly associated with the trait specific to induction in ROS responses named as FC (Fold Change) could be involved in the regulation of this induction event. Furthermore, the regions associated with the increase in QDR against *B. cinerea* trait (named as “delta_all_lesion”) are expected to have genes associated with defence regulations.

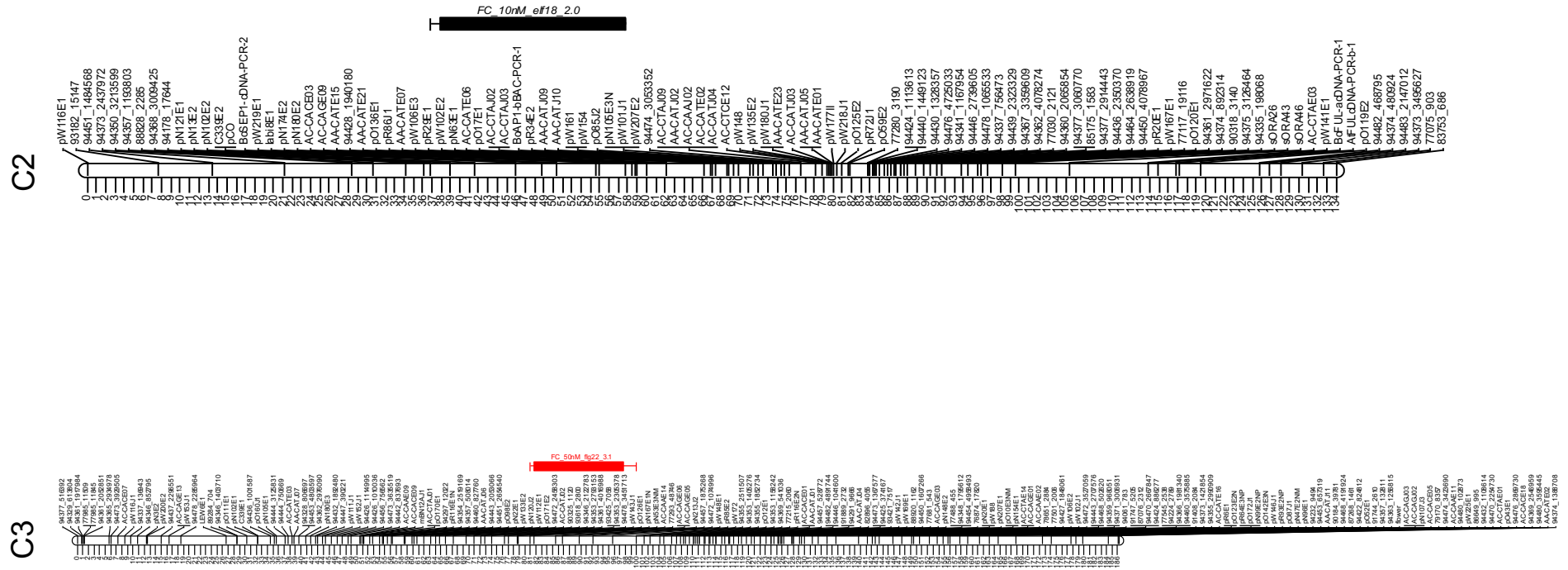


**Figure 6.9** Map Integrating AFLP, RFLP markers on *B. oleracea* chr2, and chr3 with the QTLs on their corresponded locations which are significantly associated with the related trait written on them. The red bars are representing the QTLs related to Green Duke phenotype and black bars are representing the QTLs related to A12 phenotype represented (Genetic map figures are generated by Dr. Peter Walley from Liverpool University with data generated in this PhD study).

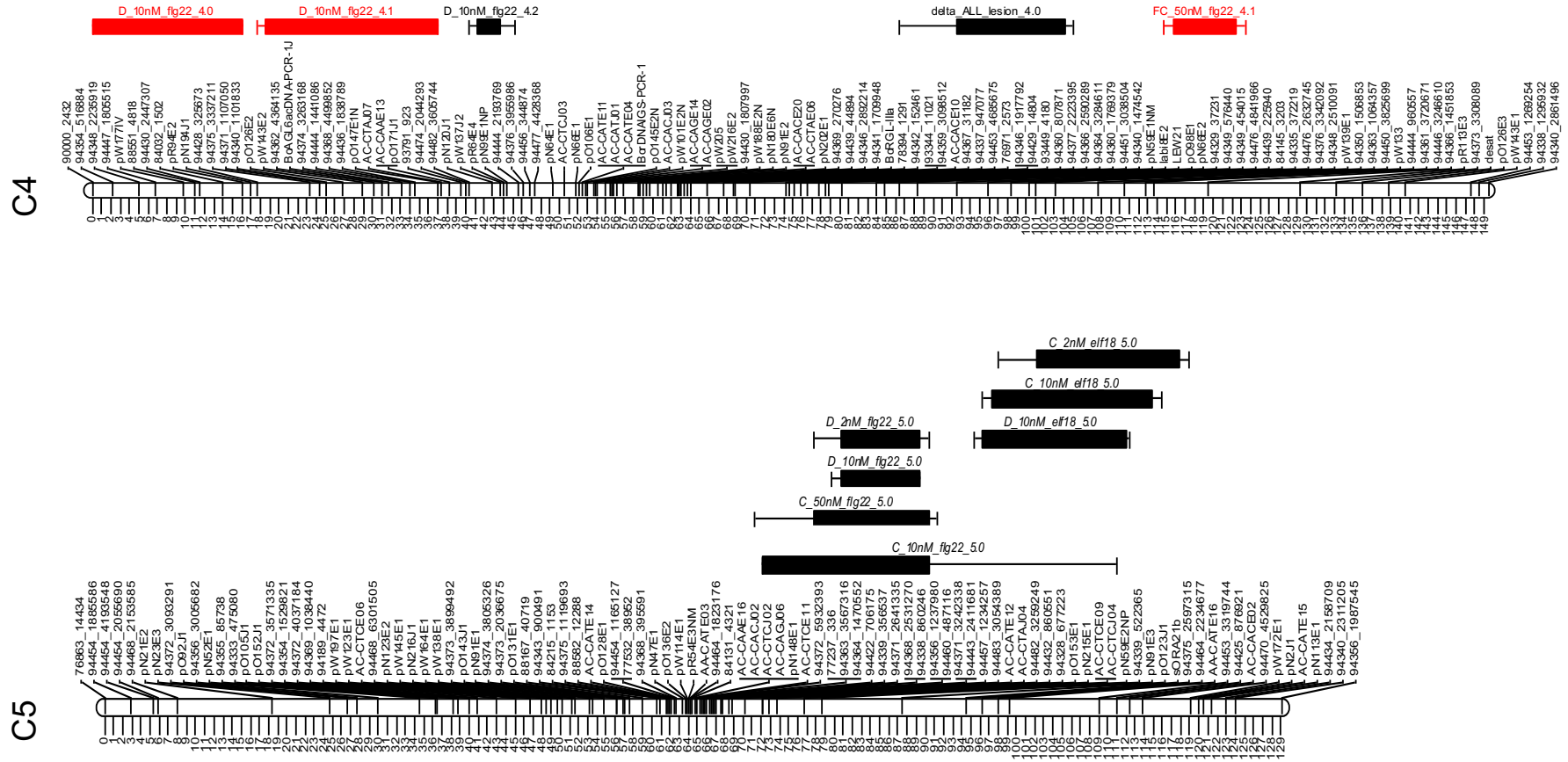


**Figure 6.10** Map Integrating AFLP, RFLP markers on *B. oleracea* chr4, and chr5 with the QTLs on their corresponded locations which are significantly associated with the related trait written on them. The red bars are representing the QTLs related to Green Duke phenotype and black bars are representing the QTLs related to A12 phenotype represented (Genetic map figures are generated by Dr. Peter Walley from Liverpool University with data generated in this PhD study).

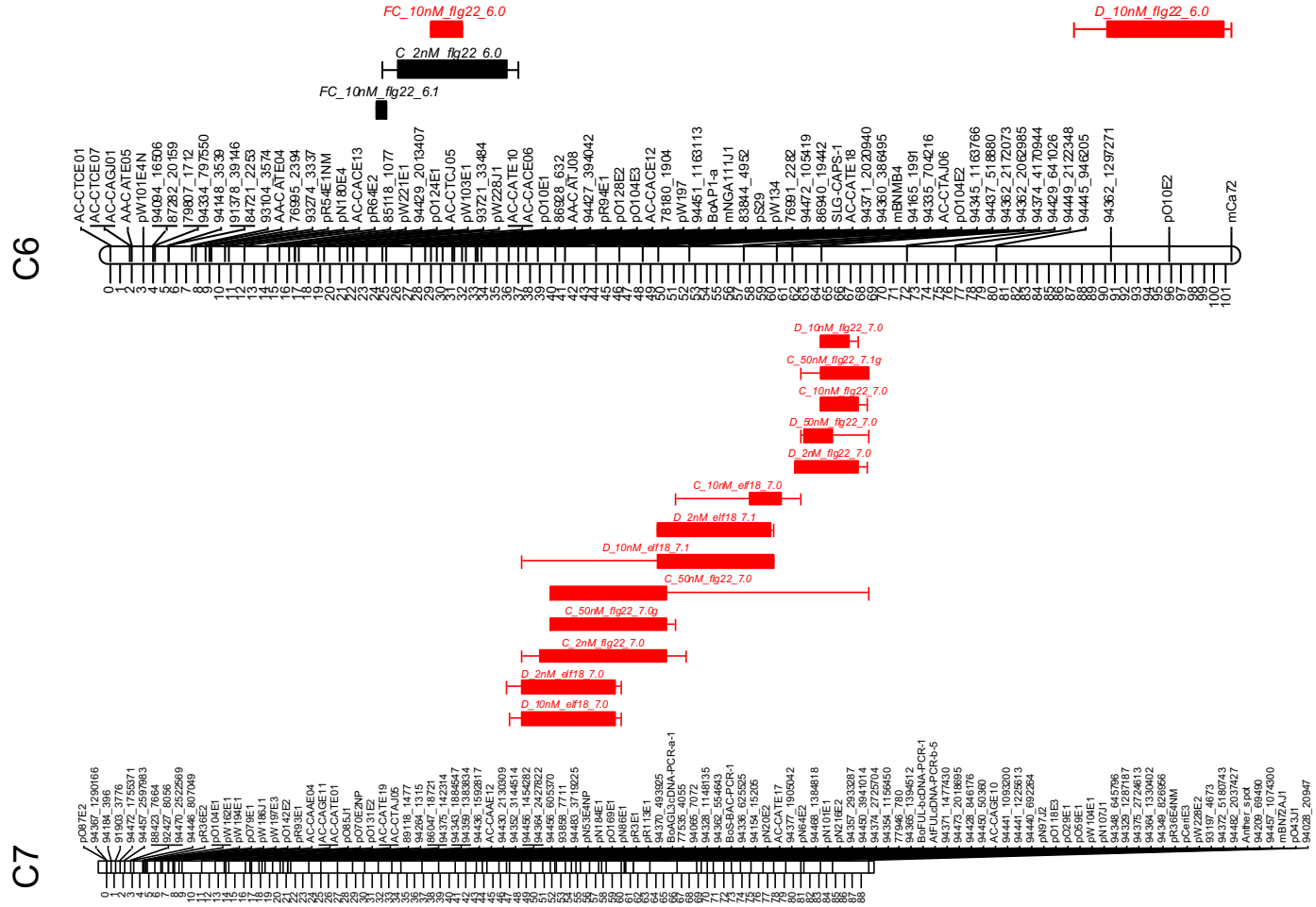


**Figure 6.11** Map Integrating AFLP, RFLP markers on *B. oleracea* chr6, and chr7 with the QTLs on their corresponded locations, which are significantly associated with the related trait written on them. The red bars are representing the QTLs related to Green Duke phenotype, and black bars are representing the QTLs related to A12 phenotype (Genetic map figures are generated by Dr. Peter Walley from Liverpool University with data generated in this PhD study).

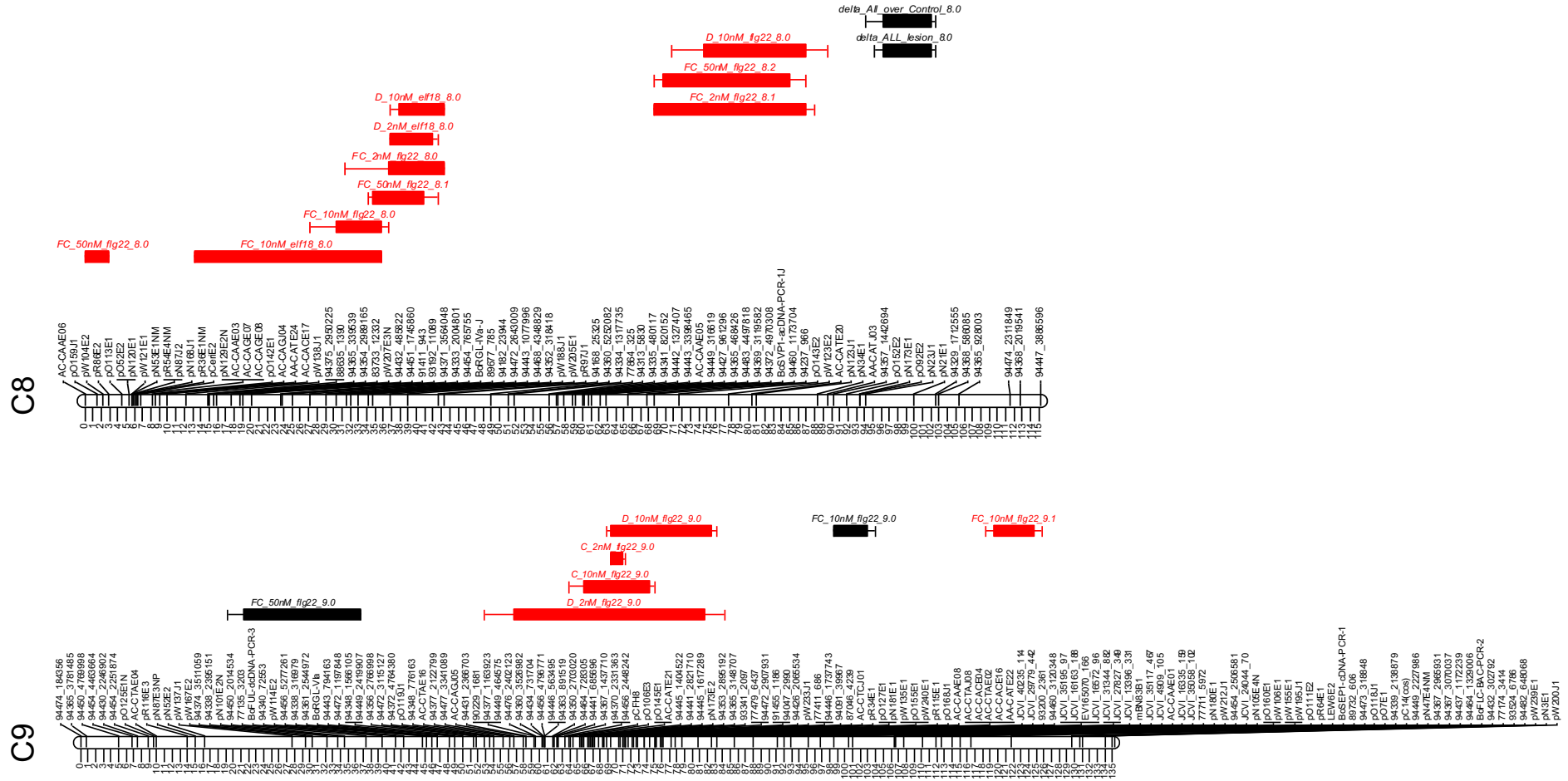


**Figure 6.12** Map Integrating AFLP, RFLP markers on *B. oleracea* chr8, and chr9 with the QTLs on their corresponded locations, which are significantly associated with the related trait written on them. The red bars are representing the QTLs related to Green Duke phenotype, and black bars are representing the QTLs related to A12 phenotype (Genetic map figures are generated by Dr. Peter Walley from Liverpool University with data generated in this PhD study).

### 6.2.6. Transcriptomic Studies

Although the analysis could not be completed before submission of this thesis, lines were selected for a potential transcriptomics study, as shown in Table 6.1. RNA-seq was performed to compare the transcriptional changes between control and drought stress treated plants and revealing the differential regulation between the lines.

Green Duke was selected due to its stability, with the lowest induction levels in ROS burst after the drought treatment (Figure 6.5a). In contrast, A12 always had a high ROS response phenotype and also had more than 2-fold increase in ROS burst when treated with drought stress. Line AG5005 was also selected because it showed the highest induction in ROS response after the stress treatment with more than 16-fold increase.

To be able to eliminate any false positives which might come from any individual plant sample, 3 technical replicates that each consists 3 biological sample bulked inside were prepared for each treatment. After RNA extraction, the samples were run on Agarose gel to visualize any possible degradation (Figure 6.13).

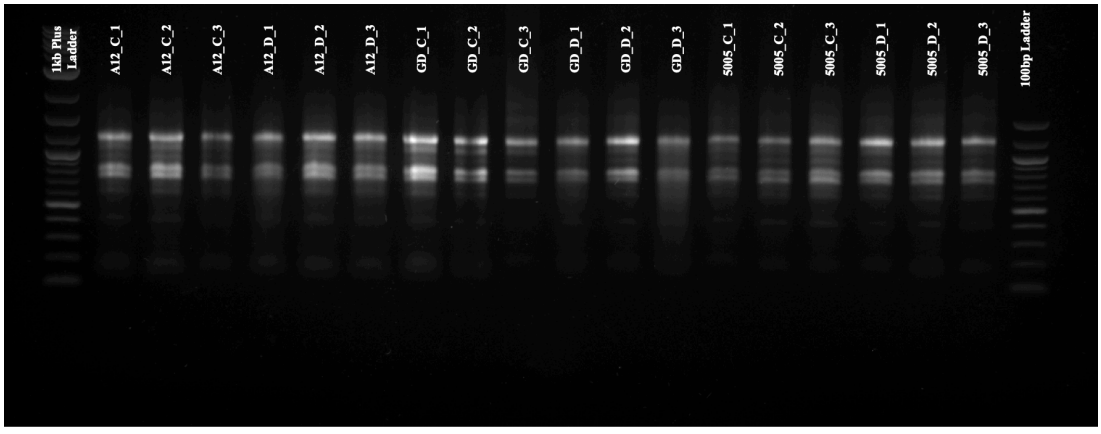


**Figure 6.13** Agarose gel (1%) electrophoresis result of RNA samples sent to sequencing. The name of each sample showed above the image of the bands.

**Table 6.1** Nanodrop results and the RNA Integrity Numbers (RIN) of the RNA libraries created for sequencing. "D" represents Drought stress treated samples, and "C" represents Control samples.

| Name | Species | Tissue | 260/280 | 260/230 | Conc. (ng/µl) | Vol (µl) | Total Amount (ng) | RIN |
|---|---|---|---|---|---|---|---|---|
| A12_C_1 | Brassica oleracea | Leaf | 2.05 | 2.13 | 618.69 | 30 | 18560.7 | 6.8 |
| A12_C_2 | Brassica oleracea | Leaf | 2.06 | 2.08 | 648.68 | 30 | 19460.4 | 7 |
| A12_C_3 | Brassica oleracea | Leaf | 2.08 | 2.12 | 771.96 | 30 | 23158.8 | 5.2 |
| A12_D_1 | Brassica oleracea | Leaf | 2.08 | 2 | 692.09 | 30 | 20762.7 | 6.8 |
| A12_D_2 | Brassica oleracea | Leaf | 2.08 | 1.82 | 709.41 | 30 | 21282.3 | 6 |
| A12_D_3 | Brassica oleracea | Leaf | 2.04 | 1.73 | 371.79 | 30 | 11153.7 | 4.8 |
| GD_C_1 | Brassica oleracea | Leaf | 2.08 | 2.08 | 608.98 | 30 | 18269.4 | 7.1 |
| GD_C_2 | Brassica oleracea | Leaf | 2.04 | 1.95 | 335.4 | 30 | 10062 | 6.9 |
| GD_C_3 | Brassica oleracea | Leaf | 2.01 | 2.15 | 344.36 | 30 | 10330.8 | 7.6 |
| GD_D_1 | Brassica oleracea | Leaf | 2.01 | 1.85 | 300.78 | 30 | 9023.4 | 6.4 |
| GD_D_2 | Brassica oleracea | Leaf | 2.01 | 2.18 | 424.91 | 30 | 12747.3 | 7.6 |
| GD_D_3 | Brassica oleracea | Leaf | 2 | 1.89 | 363.89 | 30 | 10916.7 | 7 |
| 5005_C_1 | Brassica oleracea | Leaf | 2.01 | 2.09 | 425.65 | 30 | 12769.5 | 5 |
| 5005_C_2 | Brassica oleracea | Leaf | 2 | 1.89 | 325.25 | 30 | 9757.5 | 6 |
| 5005_C_3 | Brassica oleracea | Leaf | 2.03 | 2.12 | 471.77 | 30 | 14153.1 | 5.3 |
| 5005_D_1 | Brassica oleracea | Leaf | 2.01 | 2.1 | 454.28 | 30 | 13628.4 | 6.8 |
| 5005_D_2 | Brassica oleracea | Leaf | 2 | 2.09 | 454.44 | 30 | 13633.2 | 6.6 |
| 5005_D_3 | Brassica oleracea | Leaf | 2 | 1.87 | 361.39 | 30 | 10841.7 | 7.2 |

### 6.3. Discussion

In this study, I defined the stress conditions that could be reliably used to investigate the effect of drought stress on PTI and resistance to *B. cinerea*. It was important to define the stress conditions which were sufficient to reveal the induction of ROS yet were not lethal. The results showed that the drought stress conditions caused a specific increase in ROS response, with individual lines behaving similarly for both flg22 and elf18. Thus, drought stress affected PTI induction generally and was not specific to either PAMP. In unstressed condition, there was a significant negative correlation between the magnitude of ROS production and resistance to *B. cinerea*.

In preliminary studies, I also considered using fungal PAMPs, Chitin, and NLP, for this study, However, as explained in Chapter 4, *B. oleracea* does not recognize nlp20 motif, so could not be used. Although chitin is recognized by *B. oleracea,* in the preliminary experiments, I could not measure any response reliably, possibly due to the high level of chitinase activity in leaves. Also, previous experience in the group has shown that there is considerable variation between batches of chitin, which could affect results. On the other hand, there is a strong positive correlation between the magnitude of ROS production in response to BcNEP2 and flg22 in *B. napus* plants (Figure 3.6, correlation coefficient value = 0.58). Thus, 2 different types of PAMP molecules derived from bacterial pathogens were used in this study. And as flg22 is the most well-studied PAMP motif, the flg22 had been used as a model PAMP motif representing the molecule inducing the PTI responses

The experiment has enabled the mapping of QTL associated with ROS production and disease resistance under control and drought-stressed conditions. I provided my phenotype results to Peter Walley at Liverpool University, who had access to sequence data for the population. The mapping defined Global QTL for PAMP-induced ROS that was present in both control and drought stress treatment. One of the Global QTL is located on C9 close to the centromere of the chromosome (Figure

6.12). This was also reported by Simon Lloyd (thesis) and, interestingly, co-locates with the trait related to *Agrobacterium tumefaciens* susceptibility, the alleles coming from Green Duke in the middle of the C9 was determinative for the flg22-induced ROS response phenotype (Sparrow et al., 2004).

Although the parental lines A12 and GD had a significant increase in ROS response and a significant decrease in the *B. cinerea* lesion size, they had distinct phenotypes in response to drought stress when compared with their controls. Green Duke can be classified in the whole population as the most stable line due to the lowest fold change in ROS response following drought treatment. This distinct feature helped to reveal the QTLs with much higher LOD scores.

The results also enabled the identification of suitable lines to compare genes induced under drought stress conditions by RNA-seq, which will be continued in future work. Specific genes are expected to up-regulated due to stress treatment such as ABA and BR related genes (Bürger & Chory, 2019; Fàbregas et al., 2018; Planas-Riverola et al., 2019). The TFs which might have a role in the regulation of the cross-talk between the abiotic and biotic responses will be searched for in the differential gene expression analysis (Chen et al., 2017). It should also be possible to investigate the candidate genes within the QTL intervals as those genes are expected to have a significant difference in their transcript abundance. This will provide robust analysis for the genes differentially induced during drought conditions.

# CHAPTER 7

## General Discussion

This thesis describes a series of investigations into the immune system of Brassicas, and how it is related to quantitative disease resistance. I show that NLP recognition induces resistance in brassicas, and I go on to map genetic loci for NLP-recognition in *B. napus*. I also show that *BSK1* is involved in modulating the NLP-induced ROS response, linking results from the *B. napus* with mechanistic studies from *A. thaliana*. Brassinosteroid hormones are traditionally involved in plant growth and developmental processes, and the involvement of BSK1 in immunity potentially links these two aspects of plant regulatory pathways. I also investigate the effect of environmental stress on PTI and disease resistance. For that investigation, stress conditions were specified and optimized, and progress towards gene identification was made through QTL mapping and RNA-seq analysis. I proved that drought stress is inducing both PTI and disease resistance against *B. cinerea* in *B. oleracea*.

The NLP work in this study advances the results of Albert et al. (2015) demonstrates NLP-recognition is mediated by RLP23-SOBIR1-BAK1 complex in *A.thaliana* and this recognition contributes disease resistance against *S. sclerotiorum* and *P. infestans* in the following ways. Firstly, it applies the findings from the model plant *Arabidopsis* to the crop *B. napus*, and identifies the potential gene loci responsible for the recognition. I also demonstrate the involvement of BSK1 which was not previously reported. The work supports the result that NLP recognition can contribute to QDR, and extends it to a different pathogen, *B. cinerea*, which has a necrotrophic lifestyle. Since the contribution to QDR is based on the recognition of the PAMP, a conserved molecule present in diverse microbial taxa, I would predict that the results would be relevant to other pathogens of brassicas including *L. maculans* and *S. sclerotiorum*.

In previous studies in our group, it has been difficult to demonstrate a direct correlation between PTI and QDR. However, the studies were conducted with diversity sets for which there would be considerable variation in genetic background between individual cultivars. This diversity in the genetic background could mask the effects of PTI in QDR. I was able to overcome this limitation by the selection of individual plants from a population segregating for NLP recognition derived from genetically similar parental lines. This reduced the background genetic diversity and enabled the specific contribution of NLP recognition to QDR to be investigated.

A robust method for assaying infection also contributed to the convincing demonstration that NLP recognition contributes to QDR for *B cinerea*. In some research groups, infection of *B. cinerea* has been conducted by measuring the lesion growth in an exact time frame whereas others measure the time (days/hours) of *B. cinerea* to reach the borders of the leaf discs and completely infect the given leaf sample. In my study, I used the first approach, measuring the lesion size after 3 days of infection. I considered that this approach gave reproducible, high-quality data and also required less labour compared with other protocols, which is a particular advantage when large numbers of samples need to be assayed.

I included control plants to each batch of the experiment to normalise the results, and this enabled me to obtain clear and robust data. Additionally, my research is showing the importance of ensuring consistent environment conditions between the experiments, achieved with Controlled Environment Rooms (CERs), which may not be the case in the previous studies. It has been previously shown that there is cross-talk between hormonal mechanisms, such as the ABA-mediated stress responses and JA-mediated immune pathways, or decrease in PAMP-induced ROS burst mechanisms due to heat stress treatment (Janda et al., 2019). Variation in environmental conditions could, therefore, have a significant effect on ROS response and disease resistance. Since my study is investigating both immunity and effect of the environment, the results obtained from this study will progress understanding of the performance of the plant immunity under field conditions.

## 7.1. Overcoming the challenge of working with polyploids to identify candidate genes for NLP recognition

In my research, I was able to translate a fundamental understanding of the plant immune system to make it relevant to understanding disease resistance in Brassicaceae. There are considerable challenges for working with crop species that have a complicated genomic structure like allotetraploids. *In silico* mapping of the region associated with NLP-recognition on *B. napus* genome was accomplished with an improved BSA pipeline, although the most significant peak identified is on A04 was still spread over 2.5Mbp region. I was able to improve the delimitation of candidate genes using KASP markers for testing $F_2$ individuals of the BSA population to reduce the number of candidate genes (Chapter 4). This combination of BSA and KASP mapping provides a powerful and complementary approach to mapping genes for important traits on crop species.

In the *B. napus* genome, it was assumed that an *AtRLP23* homologue is responsible for recognition of the nlp20 motif, as this gene is from Brassicaceae clade. To map the hypothetical *AtRLP23* homologue on *B. napus* genome, an $F_2$ population segregating for the NLP-recognition was used. At the beginning of this analysis, the most appropriate reference genome was Darmor-*bzh*. Although this was a non-NLP-responsive cultivar, it was the most widely used reference genome in *B. napus* genomic studies with its well-annotated genome (Chalhoub et al., 2014). Another reference genome belonging to an NLP-responsive cultivar was available – ZS11, however, the public version was not assembled to chromosomes (https://www.ncbi.nlm.nih.gov/bioproject/237736). An updated version of the ZS11 genome became available during my studies and was published with improved assembly and annotation at the beginning of 2020 (Song et al., 2020). Therefore, the updated version of the ZS11 genome will be used in the further analysis which will definitely improve the search for the candidate gene since it will enable the possibility to visualize any INDELs occurring in non-responsive cultivars.

After the KASP assay with $F_2$ individuals, the NLP-recognition locus was narrowed down to 240kb interval region on Darmor-*bzh* reference genome and 4 designed markers Nlp_23, Nlp_17, Nlp_18 & Nlp_19 were mapped on the region. This interval contains defence-related genes containing LRR domains, which could potentially be candidate receptor genes. Only 77 $F_2$ plants were used in the test panel for KASP assay, but in total, there are 925 $F_2$ plants available from BSA population derived from Ningyou1 x Ningyou7 crosses. To narrow the region further, it will be necessary to increase the number of plants in the KASP assay. Increasing the number of the $F_2$ individuals tested with those 4 tightly linked markers will be enough to identify new recombination points on the mapped NLP-recognition locus. In future work, firstly to map the region as tight as possible, those 4 markers designed in this study will be surveyed on the population, which is currently frozen and ready to run the analysis. Furthermore, 9 KASP markers generated within this study (including Nlp_17 and Nlp_23), which are co-segregating with NLP-recognition, differentiate other responsive and non-responsive *B. napus* varieties from the diversity set. Improved KASP markers from this PhD study could potentially be directly used in breeding programmes in order to increase the resistance of agronomically important *B. napus* cultivars to *B. cinerea* and other pathogens

Once a candidate gene has been identified, proof will be required to confirm its function in NLP recognition. One approach to achieve this would be through transient expression in *Nicotiana benthamiana*, a method that has been increasingly used for such studies. *N. benthamiana* is *nlp20*-insensitive and was already used in the transient expression study to proof *AtRLP23* is the receptor recognizing the *nlp20* (Albert et al., 2015).

## 7.2. New insight into the competition between NLP- and flg22- recognition at the molecular level

The parallel phenotyping results for BcNEP2 and flg22 using individuals from the Ningyou7 x Ningyou1 $F_2$ population provided an unexpected insight into the competition between the receptors for the two PAMPs. The results showed that the individuals blind to BcNEP2 have significantly higher flg22-induced ROS burst (Chapter 3). Additionally, when the results derived from each NLP-responder $F_2$ individual of the Ningyou7 x Ningyou1 population were examined further, I showed that there is a strong correlation between the BcNEP2 and flg22 induced ROS production (Chapter 3). Based on these results, I hypothesized that each individual plant has a capacity to produce a certain amount of ROS, which is not specific to either PAMP. However, the increased ROS produced by flg22 in NLP-non-responsive $F_2$ individuals suggests that the receptors might compete and occupy the cell membrane to a greater extent if the other receptor is absent.

For example, in the absence of one PAMP receptor, there could be an increased chance of interaction with communal components such as SOBIR1 which has already been shown to form a constitutive ligand-independent complex with stated PRR (RLP23) (Albert et al., 2015). Thus, the superfluity of the shared common co-receptors that different PRRs may operate during signal transduction might result in increased capacity to respond to the flg22 molecule in the absence of the NLP receptor. This hypothesis could be further investigated by quantifying the abundance of the shared components of the NLP and flg22 receptors using cell biology approaches such as the visualisation of fluorescently tagged molecules by confocal microscopy (Loiseau & Robatzek, 2017).

*In silico* mapping of the associated regions for BcNEP2 and flg22-induced ROS production was completed. The results showed similar and distinct regions were associated with the traits (Chapter 4). Additionally, *BnaBSK1.A01* was identified as being associated with NLP-induced ROS burst in *B. napus*, and further verified in *A.*

*thaliana* with ROS and *B. cinerea* disease assays. BSK1 has already been proven to physiologically associate with FLS2 and positively regulates the flg22-induced ROS production. My research has revealed a novel finding that BSK1 might also modulate NLP-induced ROS as well as that induced by flg22.

### 7.3. Progress towards understanding the effects of environmental stress on PTI and Quantitative Disease Resistance

This investigation has made progress towards understanding how environmental conditions affect PTI and has provided the basis for further investigation of the cross-talk between abiotic and biotic stress. I was able to develop a reliable method to create drought stress and used this to map associated QTL and perform an RNA-seq experiment. These investigations should provide insight into the genes involved in the cross-talk between biotic and abiotic stress.

With the guidance of the QTL analysis, the candidate genes locating on the associated intervals will be further investigated in the RNA-seq analysis as they are suspected to be differentially regulated under drought stress conditions. The transcript abundance of the genes associated with increased drought tolerance is expected to evaluated on Green Duke transcripts.

I hypothesise that genes influenced by ABA are likely to be modulated by abiotic stress, as this has already been shown. (Finkelstein, 2013). Recent studies investigating the cross-talk between abiotic and biotic stresses showed that activation in ABA-regulated pathways results in suppression of SA-mediated immune responses (Bürger & Chory, 2019). As ABA increases, it suppresses the SA-mediated immune responses, which then leads to an increase in activation of JA-mediated immune responses. Thus, the antagonistic feature of SA and JA pathways suspected to have a role in this increase in disease resistance.

There are various mechanisms that suppress the SA-meditated pathways to release the antagonist control of the SA over the JA-mediated immune responses. WRKY33 is required for defence responses in *A. thaliana* against the necrotrophs *A. brassicicola* and *B. cinerea* (Zheng et al., 2006) and has a major role in suppression of SA-mediated signalling pathway and consequent enhancement the JA-mediated pathway (Birkenbihl et al., 2012). Interestingly, the cross-talk between the hormones

to regulate the drought stress response is not restricted to the antagonistic relationship between SA and JA since WRKY TFs (WRKY46, WRKY54, and WRKY70) also have a role in BR-regulated growth and drought stress response in *A. thaliana* (Chen et al., 2017). Therefore, I would predict that BR signalling pathway components in *B. oleracea* to be also involved in drought stress response-related pathways.

### 7.4. Conclusion

In order to develop sustainable agriculture, methods need to be developed to support the breeding of new varieties with improved traits of being resistant to diseases and being environmentally stable. In this PhD study, I investigated various aspects of PTI, a fundamental process that is both involved in the recognition of microbes and influenced by abiotic stresses. My investigation contributes novel knowledge about the basis and durability of disease resistance. The work on drought stress is also relevant to improving understanding of crop performance under the changing climatic conditions in the world. Bringing together this knowledge helps in the translation of fundamental research studies so that it can be made relevant crop improvements such as development of new varieties with increased resistance and good performance in challenging environmental conditions.

## *References*


Albert, I., Böhm, H., Albert, M., Feiler, C. E., Imkampe, J., Wallmeroth, N., Brancato, C., Raaymakers, T. M., Oome, S., Zhang, H., Krol, E., Grefen, C., Gust, A. A., Chai, J., Hedrich, R., Van Den Ackerveken, G., & Nürnberger, T. (2015). An RLP23-SOBIR1-BAK1 complex mediates NLP-triggered immunity. *Nature Plants*, *1*(October), 1–9. https://doi.org/10.1038/nplants.2015.140

Alexandratos, N., & Bruinsma, J. (2012). World agriculture towards 2015/2030: The 2012 Revision. *ESA Working Paper*, *No. 12-03*(12), 147. https://doi.org/10.1016/S0264-8377(03)00047-4

Amselem, J., Cuomo, C. A., van Kan, J. A. L., Viaud, M., Benito, E. P., Couloux, A., Coutinho, P. M., de Vries, R. P., Dyer, P. S., Fillinger, S., Fournier, E., Gout, L., Hahn, M., Kohn, L., Lapalu, N., Plummer, K. M., Pradier, J. M., Quévillon, E., Sharon, A., … Dickman, M. (2011). Genomic analysis of the necrotrophic fungal pathogens sclerotinia sclerotiorum and botrytis cinerea. *PLoS Genetics*, *7*(8). https://doi.org/10.1371/journal.pgen.1002230

Azmi, N. S. A., Singkaravanit-Ogawa, S., Ikeda, K., Kitakura, S., Inoue, Y., Narusaka, Y., Shirasu, K., Kaido, M., Mise, K., & Takano, Y. (2018). Inappropriate expression of an NLP effector in Colletotrichum orbiculare impairs infection on cucurbitaceae cultivars via plant recognition of the C-terminal region. *Molecular Plant-Microbe Interactions*, *31*(1), 101–111. https://doi.org/10.1094/MPMI-04-17-0085-FI

Bae, H., Kim, M. S., Sicher, R. C., Bae, H.-J., & Bailey, B. A. (2006). Necrosis- and ethylene-inducing peptide from Fusarium oxysporum induces a complex cascade of transcripts associated with signal transduction and cell death in Arabidopsis. *Plant Physiology*, *141*(3), 1056–1067. https://doi.org/10.1104/pp.106.076869

Bailey, B. A. (1995). Purification of a protein from culture filtrates of Fusarium oxysporum that induces ethylene and necrosis in leaves of Erythroxylum coca. In *Phytopathology* (Vol. 85, Issue 10, pp. 1250–1255). https://doi.org/10.1094/Phyto-85-1250

Bajguz, A., & Hayat, S. (2009). Effects of brassinosteroids on the plant responses to environmental stresses. In *Plant Physiology and Biochemistry* (Vol. 47, Issue 1, pp. 1–8). https://doi.org/10.1016/j.plaphy.2008.10.002

Bancroft, I., Morgan, C., Fraser, F., Higgins, J., Wells, R., Clissold, L., Baker, D., Long, Y., Meng, J., Wang, X., Liu, S., & Trick, M. (2011). Dissecting the genome of the polyploid crop oilseed rape by transcriptome sequencing. *Nature Biotechnology*, *29*(8), 764–768. https://doi.org/10.1038/nbt.1926

Berens, M. L., Wolinska, K. W., Spaepen, S., Ziegler, J., Nobori, T., Nair, A., Krüler, V., Winkelmüller, T. M., Wang, Y., Mine, A., Becker, D., Garrido-Oter, R., Schulze-Lefert, P., & Tsuda, K. (2019). Balancing trade-offs between biotic and abiotic stress responses through leaf age-dependent variation in stress hormone cross-talk. *Proceedings of the National Academy of Sciences of the United States of America*, *116*(6), 2364–2373. https://doi.org/10.1073/pnas.1817233116

Bhatti, A. A., Haq, S., & Bhat, R. A. (2017). Actinomycetes benefaction role in soil and plant health. *Microbial Pathogenesis*, *111*, 458–467. https://doi.org/10.1016/j.micpath.2017.09.036

Bi, G., Liebrand, T. W. H., Cordewener, J. H. G., America, A. H. P., Xu, X., & Joosten, M. H. A. J. (2014). Arabidopsis thaliana receptor-like protein AtRLP23 associates with the receptor-like kinase AtSOBIR1. *Plant Signaling & Behavior*, *9*(2), e27937. https://doi.org/10.4161/psb.27937

Birkenbihl, R. P., Diezel, C., & Somssich, I. E. (2012). Arabidopsis WRKY33 is a key transcriptional regulator of hormonal and metabolic responses toward Botrytis cinerea infection. *Plant Physiology*, *159*(1), 266–285. https://doi.org/10.1104/pp.111.192641

Böhm, H., Albert, I., Oome, S., Raaymakers, T. M., Van den Ackerveken, G., & Nürnberger, T. (2014). A Conserved Peptide Pattern from a Widespread Microbial Virulence Factor Triggers Pattern-Induced Immunity in Arabidopsis. *PLoS Pathogens*, *10*(11), e1004491. https://doi.org/10.1371/journal.ppat.1004491

Bohuon, E. J. R., Keith, D. J., Parkin, I. A. P., Sharpe, A. G., & Lydiate, D. J. (1996).

Alignment of the conserved C genomes of Brassica oleracea and Brassica napus. *Theoretical and Applied Genetics*, *93*(5–6), 833–839. https://doi.org/10.1007/BF00224083

Boller, T., & Felix, G. (2009). A Renaissance of Elicitors: Perception of Microbe-Associated Molecular Patterns and Danger Signals by Pattern-Recognition Receptors. *Annual Review of Plant Biology*, *60*, 379–406. https://doi.org/10.1146/annurev.arplant.57.032905.105346

Boutrot, F., & Zipfel, C. (2017). Function, Discovery, and Exploitation of Plant Pattern Recognition Receptors for Broad-Spectrum Disease Resistance. *Annual Review of Phytopathology*, *55*(1), 257–286. https://doi.org/10.1146/annurev-phyto-080614-120106

Boyd, L. A., Ridout, C., O'Sullivan, D. M., Leach, J. E., & Leung, H. (2013). Plant-pathogen interactions: Disease resistance in modern agriculture. In *Trends in Genetics* (Vol. 29, Issue 4, pp. 233–240). https://doi.org/10.1016/j.tig.2012.10.011

Broman, K. W. (2001). Review of statistical methods for QTL mapping in experimental crosses. *Lab Animal*, *30*(7), 44–52.

Broman, K. W. (2010). Genetic map construction with R/qtl. In *University of Wisconsin-Madison Department of Biostatistics & Medical Informatics Technical Report* (Vol. 214). https://rqtl.org/sampledata,

Brutus, A., Sicilia, F., Macone, A., Cervone, F., De Lorenzo, G., & Lorenzo, G. De. (2010). A domain swap approach reveals a role of the plant wall-associated kinase 1 (WAK1) as a receptor of oligogalacturonides. *Proceedings of the National Academy of Sciences of the United States of America*, *107*(20), 9452–9457. https://doi.org/10.1073/pnas.1000675107

Bürger, M., & Chory, J. (2019). Stressed Out About Hormones: How Plants Orchestrate Immunity. *Cell Host and Microbe*, *26*(2), 163–172. https://doi.org/10.1016/j.chom.2019.07.006

Cai, G., Yang, Q., Yi, B., Fan, C., Edwards, D., Batley, J., & Zhou, Y. (2014). A complex recombination pattern in the genome of allotetraploid Brassica napusas revealed by a high-density genetic map. *PLoS ONE*, *9*(10).

https://doi.org/10.1371/journal.pone.0109910

Chalhoub, B., Denoeud, F., Liu, S., Parkin, I. A. P., Tang, H., Wang, X., Chiquet, J., Belcram, H., Tong, C., Samans, B., Corréa, M., Da Silva, C., Just, J., Falentin, C., Koh, C. S., Le Clainche, I., Bernard, M., Bento, P., Noel, B., … Wincker, P. (2014). Early allopolyploid evolution in the post-neolithic Brassica napus oilseed genome. *Science*, *345*(6199), 950–953. https://doi.org/10.1126/science.1253435

Chen, J., Nolan, T. M., Ye, H., Zhang, M., Tong, H., Xin, P., Chu, J., Chu, C., Li, Z., & Yina, Y. (2017). Arabidopsis WRKY46, WRKY54, and WRKY70 transcription factors are involved in brassinosteroid-regulated plant growth and drought responses. *Plant Cell*, *29*(6), 1425–1439. https://doi.org/10.1105/tpc.17.00364

Cheng, F., Wu, J., Liang, J., & Wang, X. (2015). Genome triplication drove the diversification of Brassica plants. *The Brassica Rapa Genome*, *March*, 115–120. https://doi.org/10.1007/978-3-662-47901-8_10

Chinchilla, D., Shan, L., He, P., de Vries, S., & Kemmerling, B. (2009). One for all: the receptor-associated kinase BAK1. In *Trends in Plant Science* (Vol. 14, Issue 10, pp. 535–541). https://doi.org/10.1016/j.tplants.2009.08.002

Chinchilla, D., Zipfel, C., Robatzek, S., Kemmerling, B., Nürnberger, T., Jones, J. D. G., Felix, G., & Boller, T. (2007). A flagellin-induced complex of the receptor FLS2 and BAK1 initiates plant defence. *Nature*, *448*(7152), 497–500. https://doi.org/10.1038/nature05999

Choi, J., Tanaka, K., Cao, Y., Qi, Y., Qiu, J., Liang, Y., Lee, S. Y., & Stacey, G. (2014). Identification of a plant receptor for extracellular ATP. *Science (New York, N.Y.)*, *343*(6168), 290–294. https://doi.org/10.1126/science.343.6168.290

Choi, J., Tanaka, K., Liang, Y., Cao, Y., Lee, S. Y., & Stacey, G. (2014). Extracellular ATP, a danger signal, is recognized by DORN1 in Arabidopsis. *The Biochemical Journal*, *463*(3), 429–437. https://doi.org/10.1042/BJ20140666

Choudhary, D. K., Prakash, A., & Johri, B. N. (2007). Induced systemic resistance (ISR) in plants: Mechanism of action. *Indian Journal of Microbiology*, *47*(4), 289–297. https://doi.org/10.1007/s12088-007-0054-2

Cingolani, P., Platts, A., Wang, L. Le, Coon, M., Nguyen, T., & Wang, L. (2012). A

program for annotating and predicting the effects of single nucleotide polymorphisms, SnpEff: SNPs in the genome of Drosophila melanogaster strain w1118; iso-2; iso-3. *Fly (Austin)*, *6*(2), 80–92. https://doi.org/10.1016/S1877-1203(13)70353-7

Conrath, U. (2006). Systemic Acquired Resistance. *Plant Signaling and Behavior*, *1*(4), 179–184. https://doi.org/10.1016/0091-3057(88)90118-9

Couto, D., & Zipfel, C. (2016). Regulation of pattern recognition receptor signalling in plants. *Nature Reviews Immunology*, *16*(9), 537–552. https://doi.org/10.1038/nri.2016.77

Cuesta Arenas, Y., Kalkman, E. R. I. C., Schouten, A., Dieho, M., Vredenbregt, P., Uwumukiza, B., Osés Ruiz, M., & van Kan, J. A. L. (2010). Functional analysis and mode of action of phytotoxic Nep1-like proteins of Botrytis cinerea. *Physiological and Molecular Plant Pathology*, *74*(5–6), 376–386. https://doi.org/10.1016/j.pmpp.2010.06.003

Danecek, P., Auton, A., Abecasis, G., Albers, C. A., Banks, E., DePristo, M. A., Handsaker, R. E., Lunter, G., Marth, G. T., Sherry, S. T., McVean, G., & Durbin, R. (2011). The variant call format and VCFtools. *Bioinformatics*, *27*(15), 2156–2158. https://doi.org/10.1093/bioinformatics/btr330

Dangl, J. L., Horvath, D. M., & Staskawicz, B. J. (2013). Pivoting the plant immune system from dissection to deployment. *Science (New York, N.Y.)*, *341*(6147), 746–751. https://doi.org/10.1126/science.1236011

Daudi, A., Cheng, Z., O'Brien, J. A., Mammarella, N., Khan, S., Ausubel, F. M., & Paul Bolwell, G. (2012). The apoplastic oxidative burst peroxidase in Arabidopsis is a major component of pattern-triggered immunity. *Plant Cell*, *24*(1), 275–287. https://doi.org/10.1105/tpc.111.093039

Davière, J. M., & Achard, P. (2013). Gibberellin signaling in plants. *Development (Cambridge)*, *140*(6), 1147–1151. https://doi.org/10.1242/dev.087650

Del Sorbo, G., Schoonbeek, H., & De Waard, M. A. (2000). Fungal transporters involved in efflux of natural toxic compounds and fungicides. *Fungal Genetics and Biology : FG & B*, *30*(1), 1–15. https://doi.org/10.1006/fgbi.2000.1206

Dodds, P. N., & Rathjen, J. P. (2010). Plant immunity: towards an integrated view of

plant–pathogen interactions. *Nature Reviews Genetics*, *11*(8), 539–548. https://doi.org/10.1038/nrg2812

Durinck, S., Moreau, Y., Kasprzyk, A., Davis, S., De Moor, B., Brazma, A., & Huber, W. (2005). BioMart and Bioconductor: A powerful link between biological databases and microarray data analysis. *Bioinformatics*, *21*(16), 3439–3440. https://doi.org/10.1093/bioinformatics/bti525

Durinck, S., Spellman, P. T., Birney, E., & Huber, W. (2009). Mapping identifiers for the integration of genomic datasets with the R/ Bioconductor package biomaRt. *Nature Protocols*, *4*(8), 1184–1191. https://doi.org/10.1038/nprot.2009.97

Ellis, J. G., Lagudah, E. S., Spielmeyer, W., & Dodds, P. N. (2014). The past, present and future of breeding rust resistant wheat. *Front Plant Sci*, *5*(November), 641. https://doi.org/10.3389/fpls.2014.00641

Fàbregas, N., Lozano-Elena, F., Blasco-Escámez, D., Tohge, T., Martínez-Andújar, C., Albacete, A., Osorio, S., Bustamante, M., Riechmann, J. L., Nomura, T., Yokota, T., Conesa, A., Alfocea, F. P., Fernie, A. R., & Caño-Delgado, A. I. (2018). Overexpression of the vascular brassinosteroid receptor BRL3 confers drought resistance without penalizing plant growth. *Nature Communications*, *9*(1). https://doi.org/10.1038/s41467-018-06861-3

Felix, G., & Boller, T. (2003). Molecular sensing of bacteria in plants. The highly conserved RNA-binding motif RNP-1 of bacterial cold shock proteins is recognized as an elicitor signal in tobacco. *The Journal of Biological Chemistry*, *278*(8), 6201–6208. https://doi.org/10.1074/jbc.M209880200

Finkelstein, R. (2013). Abscisic Acid Synthesis and Response. *The Arabidopsis Book*, *11*, e0166. https://doi.org/10.1199/tab.0166

Flor, H. H. (1971). Current status of the Gene-For-Gene concept. *Annual Review of Phytopathology*, *9*(1), 275–296. https://doi.org/10.1146/annurev.py.09.090171.001423

Fonseca, S., Chini, A., Hamberg, M., Adie, B., Porzel, A., Kramell, R., Miersch, O., Wasternack, C., & Solano, R. (2009). (+)-7-iso-Jasmonoyl-L-isoleucine is the endogenous bioactive jasmonate. *Nature Chemical Biology*, *5*(5), 344–350.

https://doi.org/10.1038/nchembio.161

Fradin, E. F., Abd-El-Haliem, A., Masini, L., van den Berg, G. C. M., Joosten, M. H. A. J., & Thomma, B. P. H. J. (2011). Interfamily Transfer of Tomato <em>Ve1</em> Mediates <em>Verticillium</em> Resistance in Arabidopsis. *Plant Physiology*, *156*(4), 2255 LP – 2265. https://doi.org/10.1104/pp.111.180067

Frye, C. A., & Innes, R. W. (1998). An Arabidopsis Mutant with Enhanced Resistance to Powdery Mildew. *The Plant Cell*, *10*(6), 947 LP – 956. https://doi.org/10.1105/tpc.10.6.947

Garrison, E., & Marth, G. (2012). *Haplotype-based variant detection from short-read sequencing*. 1–9. http://arxiv.org/abs/1207.3907

Glawischnig, E. (2007). Camalexin. *Phytochemistry*, *68*(4), 401–406. https://doi.org/10.1016/j.phytochem.2006.12.005

Gómez-Gómez, L., & Boller, T. (2000). FLS2: An LRR Receptor-like Kinase Involved in the Perception of the Bacterial Elicitor Flagellin in Arabidopsis. *Molecular Cell*, *5*(6), 1003–1011. https://doi.org/10.1016/S1097-2765(00)80265-8

Harper, A. L., Trick, M., Higgins, J., Fraser, F., Clissold, L., Wells, R., Hattori, C., Werner, P., & Bancroft, I. (2012). Associative transcriptomics of traits in the polyploid crop species Brassica napus. *Nature Biotechnology*, *30*(8), 798–802. https://doi.org/10.1038/nbt.2302

Hickman, R., Van Verk, M. C., Van Dijken, A. J. H., Mendes, M. P., Vroegop-Vos, I. A., Caarls, L., Steenbergen, M., Van der Nagel, I., Wesselink, G. J., Jironkin, A., Talbot, A., Rhodes, J., De Vries, M., Schuurink, R. C., Denby, K., Pieterse, C. M. J., & Van Wees, S. C. M. (2017). Architecture and Dynamics of the Jasmonic Acid Gene Regulatory Network. *The Plant Cell*, *29*(9), 2086 LP – 2105. https://doi.org/10.1105/tpc.16.00958

Higgins, J., Magusin, A., Trick, M., Fraser, F., & Bancroft, I. (2012). Use of mRNA-seq to discriminate contributions to the transcriptome from the constituent genomes of the polyploid crop species Brassica napus. *BMC Genomics*, *13*(1), 247. https://doi.org/10.1186/1471-2164-13-247

Hind, S. R., Strickler, S. R., Boyle, P. C., Dunham, D. M., Bao, Z., O'Doherty, I. M.,

Baccile, J. A., Hoki, J. S., Viox, E. G., Clarke, C. R., Vinatzer, B. A., Schroeder, F. C., Martin, G. B., Boller, T., Felix, G., Zipfel, C., O'Neill, L. A., Golenbock, D., Bowie, A. G., … Broghammer, A. (2016). Tomato receptor FLAGELLIN-SENSING 3 binds flgII-28 and activates the plant immune system. *Nature Plants*, *2*(9), 16128. https://doi.org/10.1038/nplants.2016.128

Howlett, B. J., Idnurm, A., & Pedras, M. S. C. (2001). Leptosphaeria maculans, the causal agent of blackleg disease of Brassicas. *Fungal Genetics and Biology*, *33*(1), 1–14. https://doi.org/10.1006/fgbi.2001.1274

Hurni, S., Scheuermann, D., Krattinger, S. G., Kessel, B., Wicker, T., Herren, G., Fitze, M. N., Breen, J., Presterl, T., Ouzunova, M., & Keller, B. (2015). The maize disease resistance gene Htn1 against northern corn leaf blight encodes a wall-associated receptor-like kinase. *Proceedings of the National Academy of Sciences*, *112*(28), 8780–8785. https://doi.org/10.1073/pnas.1502522112

Iqbal, N., Khan, N. A., Ferrante, A., Trivellini, A., Francini, A., & Khan, M. I. R. (2017). Ethylene role in plant growth, development and senescence: interaction with other phytohormones. *Frontiers in Plant Science*, *8*(April), 1–19. https://doi.org/10.3389/fpls.2017.00475

Irieda, H., Maeda, H., Akiyama, K., Hagiwara, A., Saitoh, H., Uemura, A., Terauchi, R., & Takano, Y. (2014). Colletotrichum orbiculare secretes virulence effectors to a biotrophic interface at the primary hyphal neck via exocytosis coupled with SEC22-mediated traffic. *Plant Cell*, *26*(5), 2265–2281. https://doi.org/10.1105/tpc.113.120600

Janda, M., Lamparová, L., Zubíková, A., Burketová, L., Martinec, J., & Krčková, Z. (2019). Temporary heat stress suppresses PAMP-triggered immunity and resistance to bacteria in Arabidopsis thaliana. *Molecular Plant Pathology*, *20*(7), 1005–1012. https://doi.org/10.1111/mpp.12799

Jansen, R. C. (1993). Interval mapping of multiple quantitative trait loci. *Genetics*, *135*(1), 205–211.

Jones, J. D. G., & Dangl, J. L. (2006). The plant immune system. *Nature*, *444*(7117), 323–329. https://doi.org/10.1038/nature05286

Jwa, N. S., & Hwang, B. K. (2017). Convergent evolution of pathogen effectors

toward reactive oxygen species signaling networks in plants. *Frontiers in Plant Science*, *8*(September), 1–12. https://doi.org/10.3389/fpls.2017.01687

Kadota, Y., Shirasu, K., & Zipfel, C. (2015). Regulation of the NADPH Oxidase RBOHD during Plant Immunity. *Plant and Cell Physiology*, *56*(8), 1472–1480. https://doi.org/10.1093/pcp/pcv063

Kaku, H., Nishizawa, Y., Ishii-Minami, N., Akimoto-Tomiyama, C., Dohmae, N., Takio, K., Minami, E., & Shibuya, N. (2006). Plant cells recognize chitin fragments for defense signaling through a plasma membrane receptor. *Proceedings of the National Academy of Sciences of the United States of America*, *103*(29), 11086–11091. https://doi.org/10.1073/pnas.0508882103

Kammerhofer, N., Radakovic, Z., Regis, J. M. A., Dobrev, P., Vankova, R., Grundler, F. M. W., Siddique, S., Hofmann, J., & Wieczorek, K. (2015). Role of stress-related hormones in plant defence during early infection of the cyst nematode Heterodera schachtii in Arabidopsis. *New Phytologist*, *207*(3), 778–789. https://doi.org/doi:10.1111/nph.13395

Khot, S. D., Bilgi, V. N., del Río, L. E., & Bradley, C. A. (2011). Identification of Brassica napus Lines with Partial Resistance to Sclerotinia sclerotiorum . *Plant Health Progress*, *12*(1), 15. https://doi.org/10.1094/php-2010-0422-01-rs

Koch, M. A., Haubold, B., & Mitchell-Olds, T. (2000). Comparative evolutionary analysis of chalcone synthase and alcohol dehydrogenase loci in Arabidopsis, Arabis, and related genera (Brassicaceae). *Mol Biol Evol*, *17*(10), 1483–1498. https://doi.org/10.1093/oxfordjournals.molbev.a026248

Lacombe, S., Rougon-Cardoso, A., Sherwood, E., Peeters, N., Dahlbeck, D., van Esse, H. P., Smoker, M., Rallapalli, G., Thomma, B. P. H. J., Staskawicz, B., Jones, J. D. G., & Zipfel, C. (2010). Interfamily transfer of a plant pattern-recognition receptor confers broad-spectrum bacterial resistance. *Nature Biotechnology*, *28*(4), 365–369. https://doi.org/10.1038/nbt.1613

Laurie-Berry, N., Joardar, V., Street, I. H., & Kunkel, B. N. (2006). The Arabidopsis thaliana JASMONATE INSENSITIVE 1 gene is required for suppression of salicylic acid-dependent defenses during infection by Pseudomonas syringae. *Molecular Plant-Microbe Interactions : MPMI*, *19*(7), 789–800.

https://doi.org/10.1094/MPMI-19-0789

Lehti-Shiu, M. D., Zou, C., Hanada, K., & Shiu, S. H. (2009). Evolutionary history and stress regulation of plant receptor-like kinase/pelle genes. *Plant Physiology*, *150*(1), 12–26. https://doi.org/10.1104/pp.108.134353

Li, H., & Durbin, R. (2010). Fast and accurate long-read alignment with Burrows-Wheeler transform. *Bioinformatics*, *26*(5), 589–595. https://doi.org/10.1093/bioinformatics/btp698

Li, H., Handsaker, B., Wysoker, A., Fennell, T., Ruan, J., Homer, N., Marth, G., Abecasis, G., & Durbin, R. (2009). The Sequence Alignment/Map format and SAMtools. *Bioinformatics*, *25*(16), 2078–2079. https://doi.org/10.1093/bioinformatics/btp352

Li, Lixia, Luo, Y., Chen, B., Xu, K., Zhang, F., Li, H., Huang, Q., Xiao, X., Zhang, T., Hu, J., Li, F., & Wu, X. (2016). A genome-wide association study reveals new loci for resistance to clubroot disease in Brassica napus. *Frontiers in Plant Science*, *7*(September2016), 1483. https://doi.org/10.3389/fpls.2016.01483

Li, Lun, Long, Y., Zhang, L., Dalton-Morgan, J., Batley, J., Yu, L., Meng, J., & Li, M. (2015). Genome wide analysis of flowering time trait in multiple environments via high-throughput genotyping technique in Brassica napus L. *PLoS ONE*, *10*(3), e0119425. https://doi.org/10.1371/journal.pone.0119425

Liang, X., & Zhou, J.-M. (2018). Receptor-Like Cytoplasmic Kinases: Central Players in Plant Receptor Kinase–Mediated Signaling. *Annual Review of Plant Biology*, *69*(1), 267–299. https://doi.org/10.1146/annurev-arplant-042817-040540

Liebrand, T. W. H., van den Burg, H. A., & Joosten, M. H. A. J. (2014). Two for all: Receptor-associated kinases SOBIR1 and BAK1. In *Trends in Plant Science* (Vol. 19, Issue 2, pp. 123–132). https://doi.org/10.1016/j.tplants.2013.10.003

Liu, S., Fan, C., Li, J., Cai, G., Yang, Q., Wu, J., Yi, X., Zhang, C., & Zhou, Y. (2016). A genome-wide association study reveals novel elite allelic variations in seed oil content of Brassica napus. *Theoretical and Applied Genetics*, *129*(6), 1203–1215. https://doi.org/10.1007/s00122-016-2697-z

Lloyd, Simon R, Schoonbeek, H.-J., Trick, M., Zipfel, C., & Ridout, C. J. (2014). Methods to study PAMP-triggered immunity in Brassica species. *Molecular*

*Plant-Microbe Interactions : MPMI*, *27*(3), 286–295. https://doi.org/10.1094/MPMI-05-13-0154-FI

Lloyd, Simon Rhys. (2014). *Mapping PAMP Responses and Disease Resistance in Brassicas* (Issue March). University of East Anglia.

Lo Presti, L., Lanver, D., Schweizer, G., Tanaka, S., Liang, L., Tollot, M., Zuccaro, A., Reissmann, S., & Kahmann, R. (2015). Fungal Effectors and Plant Susceptibility. *Annual Review of Plant Biology*, *66*, 513–545. https://doi.org/10.1146/annurev-arplant-043014-114623

Loiseau, J., & Robatzek, S. (2017). Detection and Analyses of Endocytosis of Plant Receptor Kinases. *Methods in Molecular Biology (Clifton, N.J.)*, *1621*, 177–189. https://doi.org/10.1007/978-1-4939-7063-6_17

Lozano-Durán, R., & Zipfel, C. (2015). Trade-off between growth and immunity: Role of brassinosteroids. In *Trends in Plant Science* (Vol. 20, Issue 1, pp. 12–19). Elsevier Ltd. https://doi.org/10.1016/j.tplants.2014.09.003

Lu, K., Peng, L., Zhang, C., Lu, J., Yang, B., Xiao, Z., Liang, Y., Xu, X., Qu, C., Zhang, K., Liu, L., Zhu, Q., Fu, M., Yuan, X., & Li, J. (2017). Genome-wide association and transcriptome analyses reveal candidate genes underlying yield-determining traits in brassica napus. *Frontiers in Plant Science*, *8*, 206. https://doi.org/10.3389/fpls.2017.00206

Lukens, L. N., Quijada, P. A., Udall, J., Pires, J. C., Schranz, M. E., & Osborn, T. C. (2004). Genome redundancy and plasticity within ancient and recent Brassica crop species. *Biological Journal of the Linnean Society*, *82*(4), 665–674. https://doi.org/10.1111/j.1095-8312.2004.00352.x

Lysak, M. A., Koch, M. A., Pecinka, A., & Schubert, I. (2005). Chromosome triplication found across the tribe Brassiceae. *Genome Research*, *15*(4), 516–525. https://doi.org/10.1101/gr.3531105

Macho, A. P., & Zipfel, C. (2014). Plant PRRs and the activation of innate immune signaling. In *Molecular Cell* (Vol. 54, Issue 2, pp. 263–272). https://doi.org/10.1016/j.molcel.2014.03.028

Majhi, B. B., Sreeramulu, S., & Sessa, G. (2019). Brassinosteroid-signaling kinase5 associates with immune receptors and is required for immune responses1.

*Plant Physiology*, *180*(2), 1166–1184. https://doi.org/10.1104/pp.18.01492

Massonnet, C., Vile, D., Fabre, J., Hannah, M. A., Caldana, C., Lisec, J., Beemster, G. T. S., Meyer, R. C., Messerli, G., Gronlund, J. T., Perkovic, J., Wigmore, E., May, S., Bevan, M. W., Meyer, C., Rubio-Díaz, S., Weigel, D., Micol, J. L., Buchanan-Wollaston, V., … Granier, C. (2010). Probing the reproducibility of leaf growth and molecular phenotypes: A comparison of three Arabidopsis accessions cultivated in ten laboratories. *Plant Physiology*, *152*(4), 2142–2157. https://doi.org/10.1104/pp.109.148338

McLoughlin, A. G., Wytinck, N., Walker, P. L., Girard, I. J., Rashid, K. Y., De Kievit, T., Fernando, W. G. D., Whyard, S., & Belmonte, M. F. (2018). Identification and application of exogenous dsRNA confers plant protection against Sclerotinia sclerotiorum and Botrytis cinerea. *Scientific Reports*, *8*(1), 1–14. https://doi.org/10.1038/s41598-018-25434-4

Michelmore, R. W., Paran, I., & Kesseli, R. V. (1991). Michelmore et al 1991. Proc Natl Acad Sci. *Proceedings of the National Academy of Sciences of the United States of America*, *88*(21), 9828–9832. https://doi.org/10.1073/pnas.88.21.9828

Mittler, R. (2017). ROS Are Good. *Trends in Plant Science*, *22*(1), 11–19. https://doi.org/10.1016/j.tplants.2016.08.002

Miya, A., Albert, P., Shinya, T., Desaki, Y., Ichimura, K., Shirasu, K., Narusaka, Y., Kawakami, N., Kaku, H., & Shibuya, N. (2007). CERK1, a LysM receptor kinase, is essential for chitin elicitor signaling in Arabidopsis. *Proceedings of the National Academy of Sciences of the United States of America*, *104*(49), 19613–19618. https://doi.org/10.1073/pnas.0705147104

Nejat, N., & Mantri, N. (2017). Plant Immune System: Crosstalk Between Responses to Biotic and Abiotic Stresses the Missing Link in Understanding Plant Defence. *Current Issues in Molecular Biology*, *23*, 1–16. https://doi.org/10.21775/cimb.023.001

Nguepjop, J. R., Tossim, H. A., Bell, J. M., Rami, J. F., Sharma, S., Courtois, B., Mallikarjuna, N., Sane, D., & Fonceka, D. (2016). Evidence of genomic exchanges between homeologous chromosomes in a cross of peanut with

newly synthetized allotetraploid hybrids. *Frontiers in Plant Science*, *7*(NOVEMBER2016), 1–12. https://doi.org/10.3389/fpls.2016.01635

Nie, H., Wu, Y., Yao, C., & Tang, D. (2011). Suppression of edr2-mediated powdery mildew resistance, cell death and ethylene-induced senescence by mutations in ALD1 in Arabidopsis. *Journal of Genetics and Genomics*, *38*(4), 137–148. https://doi.org/10.1016/j.jgg.2011.03.001

Nolan, T. M., Vukasinović, N., Liu, D., Russinova, E., & Yin, Y. (2020). Brassinosteroids: Multidimensional regulators of plant growth, development, and stress responses. *Plant Cell*, *32*(2), 298–318. https://doi.org/10.1105/tpc.19.00335

OERKE, E.-C. (2006). Crop losses to pests. *The Journal of Agricultural Science*, *144*(01), 31. https://doi.org/10.1017/S0021859605005708

Ooijen, J. W. Van. (2009). Software for the mapping of quantitative trait loci in experimental populations of diploid species. *Genome*, *April*.

Oome, S., Raaymakers, T. M., Cabral, A., Samwel, S., Böhm, H., Albert, I., Nürnberger, T., & Van den Ackerveken, G. (2014). Nep1-like proteins from three kingdoms of life act as a microbe-associated molecular pattern in Arabidopsis. *Proceedings of the National Academy of Sciences of the United States of America*, *111*(47), 16955–16960. https://doi.org/10.1073/pnas.1410031111

Oome, S., & Van den Ackerveken, G. (2014). Comparative and Functional Analysis of the Widely Occurring Family of Nep1-Like Proteins. *Molecular Plant-Microbe Interactions*, *27*(10), 1081–1094. https://doi.org/10.1094/mpmi-04-14-0118-r

Ottmann, C., Luberacki, B., Küfner, I., Koch, W., Brunner, F., Weyand, M., Mattinen, L., Pirhonen, M., Anderluh, G., Seitz, H. U., Nürnberger, T., & Oecking, C. (2009). A common toxin fold mediates microbial attack and plant defense. *Proceedings of the National Academy of Sciences of the United States of America*, *106*(25), 10359–10364. https://doi.org/10.1073/pnas.0902362106

Oxley, S. J. P., & Walters, D. R. (2012). Control of light leaf spot (Pyrenopeziza brassicae) on winter oilseed rape (Brassica napus) with resistance elicitors. *Crop Protection*, *40*, 59–62. https://doi.org/10.1016/j.cropro.2012.04.028

Parkin, I. A. P., Gulden, S. M., Sharpe, A. G., Lukens, L., Trick, M., Osborn, T. C., & Lydiate, D. J. (2005). Segmental structure of the Brassica napus genome based on comparative analysis with Arabidopsis thaliana. *Genetics*, *171*(2), 765–781. https://doi.org/10.1534/genetics.105.042093

Parkin, I. A. P., Koh, C., Tang, H., Robinson, S. J., Kagale, S., Clarke, W. E., Town, C. D., Nixon, J., Krishnakumar, V., Bidwell, S. L., Denoeud, F., Belcram, H., Links, M. G., Just, J., Clarke, C., Bender, T., Huebert, T., Mason, A. S., Chris Pires, J., … Sharpe, A. G. (2014). Transcriptome and methylome profiling reveals relics of genome dominance in the mesopolyploid Brassica oleracea. *Genome Biology*, *15*(6). https://doi.org/10.1186/gb-2014-15-6-r77

Pieterse, C. M., van Wees, S. C., van Pelt, J. A., Knoester, M., Laan, R., Gerrits, H., Weisbeek, P. J., & van Loon, L. C. (1998). A novel signaling pathway controlling induced systemic resistance in Arabidopsis. *The Plant Cell*, *10*(9), 1571–1580. https://doi.org/10.1105/tpc.10.9.1571

Piquerez, S. J. M., Harvey, S. E., Beynon, J. L., & Ntoukakis, V. (2014). Improving crop disease resistance: lessons from research on Arabidopsis and tomato. *Frontiers in Plant Science*, *5*(DEC), 671. https://doi.org/10.3389/fpls.2014.00671

Planas-Riverola, A., Gupta, A., Betegónbetegón-Putze, I., Bosch, N., Iban, M., Es˜, & Can˜ O-Delgado, A. I. (2019). *Brassinosteroid signaling in plant development and adaptation to stress*. https://doi.org/10.1242/dev.151894

Poland, J. A., Balint-Kurti, P. J., Wisser, R. J., Pratt, R. C., & Nelson, R. J. (2009). Shades of gray: the world of quantitative disease resistance. *Trends in Plant Science*, *14*(1), 21–29. https://doi.org/10.1016/j.tplants.2008.10.006

Pritchard, L., & Birch, P. R. J. (2014). The zigzag model of plant-microbe interactions: Is it time to move on? *Molecular Plant Pathology*, *15*(9), 865–870. https://doi.org/10.1111/mpp.12210

Qi, J., Wang, J., Gong, Z., & Zhou, J. M. (2017). Apoplastic ROS signaling in plant immunity. *Current Opinion in Plant Biology*, *38*, 92–100. https://doi.org/10.1016/j.pbi.2017.04.022

Raaymakers, T. M. (2018). *Activation of plant immunity by microbial Nep1-like protein patterns*.

Raman, H., Raman, R., Coombes, N., Song, J., Diffey, S., Kilian, A., Lindbeck, K., Barbulescu, D. M., Batley, J., Edwards, D., Salisbury, P. A., & Marcroft, S. (2016). Genome-wide Association Study Identifies New Loci for Resistance to Leptosphaeria maculans in Canola. *Frontiers in Plant Science*, *7*(October), 1–16. https://doi.org/10.3389/fpls.2016.01513

Ramirez-Gonzalez, R. H., Segovia, V., Bird, N., Fenwick, P., Holdgate, S., Berry, S., Jack, P., Caccamo, M., & Uauy, C. (2015). RNA-Seq bulked segregant analysis enables the identification of high-resolution genetic markers for breeding in hexaploid wheat. *Plant Biotechnology Journal*, *13*(5), 613–624. https://doi.org/10.1111/pbi.12281

Ramirez-Gonzalez, R. H., Uauy, C., & Caccamo, M. (2015). PolyMarker: A fast polyploid primer design pipeline. *Bioinformatics*, *31*(12), 2038–2039. https://doi.org/10.1093/bioinformatics/btv069

Ramsay, L. D., Jennings, D. E., Bohuon, E. J. R., Arthur, A. E., Lydiate, D. J., Kearsey, M. J., & Marshall, D. F. (1996). The construction of a substitution library of recombinant backcross lines in Brassica oleracea for the precision mapping of quantitative trait loci. *Genome*, *39*(3), 558–567. https://doi.org/10.1139/g96-071

Roux, M., Schwessinger, B., Albrecht, C., Chinchilla, D., Jones, A., Holton, N., Malinovsky, F. G., Tör, M., de Vries, S., & Zipfel, C. (2011). The arabidopsis leucine-rich repeat receptor-like kinases BAK1/SERK3 and BKK1/SERK4 are required for innate immunity to Hemibiotrophic and Biotrophic pathogens. *The Plant Cell*, *23*(6), 2440–2455. https://doi.org/10.1105/tpc.111.084301

Santhanam, P., Esse, P. Van, Albert, I., Faino, L., Nürnberger, T., & Thomma, B. P. H. J. (2013). Evidence for Functional Diversification within a Fungal NEP1-Like Protein Family. *Molecular Plant-Microbe Interactions*, *26*(3), 121010102104007. https://doi.org/10.1094/MPMI-09-12-0222-R

Savary, S., Ficke, A., Aubertot, J. N., & Hollier, C. (2012). Crop losses due to diseases and their implications for global food production losses and food security. *Food Security*, *4*(4), 519–537. https://doi.org/10.1007/s12571-012-0200-5

Schmidt, R., Acarkan, A., & Boivin, K. (2001). Comparative structural genomics in

the Brassicaceae family. *Plant Physiology and Biochemistry*, *39*(3–4), 253–262. https://doi.org/10.1016/S0981-9428(01)01239-6

Schoonbeek, H.-J., Wang, H.-H., Stefanato, F. L., Craze, M., Bowden, S., Wallington, E., Zipfel, C., & Ridout, C. J. (2015). Arabidopsis EF-Tu receptor enhances bacterial disease resistance in transgenic wheat. *The New Phytologist*, *206*(2), 606–613. https://doi.org/10.1111/nph.13356

Schoonbeek, H., Raaijmakers, J. M., & De Waard, M. A. (2002). Fungal ABC transporters and microbial interactions in natural environments. *Molecular Plant-Microbe Interactions : MPMI*, *15*(11), 1165–1172. https://doi.org/10.1094/MPMI.2002.15.11.1165

Schwessinger, B., Bahar, O., Thomas, N., Holton, N., Nekrasov, V., Ruan, D., Canlas, P. E., Daudi, A., Petzold, C. J., Singan, V. R., Kuo, R., Chovatia, M., Daum, C., Heazlewood, J. L., Zipfel, C., & Ronald, P. C. (2015). Transgenic Expression of the Dicotyledonous Pattern Recognition Receptor EFR in Rice Leads to Ligand-Dependent Activation of Defense Responses. *PLOS Pathogens*, *11*(3), e1004809. https://doi.org/10.1371/journal.ppat.1004809

Schwessinger, B., Bart, R., Krasileva, K. V, & Coaker, G. (2015). Focus issue on plant immunity: from model systems to crop species. *Frontiers in Plant Science*, *6*(March), 195. https://doi.org/10.3389/fpls.2015.00195

Seidl, M. F., & Van den Ackerveken, G. (2019). Activity and Phylogenetics of the Broadly Occurring Family of Microbial Nep1-Like Proteins. *Annual Review of Phytopathology*, *57*(1), 367–386. https://doi.org/10.1146/annurev-phyto-082718-100054

Seo, P. J., & Park, C. M. (2010). MYB96-mediated abscisic acid signals induce pathogen resistance response by promoting salicylic acid biosynthesis in Arabidopsis. *New Phytologist*, *186*(2), 471–483. https://doi.org/10.1111/j.1469-8137.2010.03183.x

Shi, H., Shen, Q., Qi, Y., Yan, H., Nie, H., Chen, Y., Zhao, T., Katagiri, F., & Tang, D. (2013). BR-signaling kinase1 physically associates with flagellin SENSING2 and regulates plant innate immunity in Arabidopsis. *Plant Cell*, *25*(3), 1143–1157. https://doi.org/10.1105/tpc.112.107904

Shi, H., Yan, H., Li, J., & Tang, D. (2013). BSK1, a receptor-like cytoplasmic kinase, involved in both BR signaling and innate immunity in Arabidopsis. *Plant Signaling & Behavior*, *8*(8), e24996. https://doi.org/10.4161/psb.24996

Shi, Q., Febres, V. J., Jones, J. B., & Moore, G. A. (2015). Responsiveness of different citrus genotypes to the Xanthomonas citri ssp. citri-derived pathogen-associated molecular pattern (PAMP) flg22 correlates with resistance to citrus canker. *Molecular Plant Pathology*, *16*(5), 507–520. https://doi.org/10.1111/mpp.12206

Sonah, H., Zhang, X., Deshmukh, R. K., Borhan, M. H., Fernando, W. G. D., & Bélanger, R. R. (2016). Comparative Transcriptomic Analysis of Virulence Factors in Leptosphaeria maculans during Compatible and Incompatible Interactions with Canola. *Frontiers in Plant Science*, *7*, 1784. https://doi.org/10.3389/fpls.2016.01784

Song, J. M., Guan, Z., Hu, J., Guo, C., Yang, Z., Wang, S., Liu, D., Wang, B., Lu, S., Zhou, R., Xie, W. Z., Cheng, Y., Zhang, Y., Liu, K., Yang, Q. Y., Chen, L. L., & Guo, L. (2020). Eight high-quality genomes reveal pan-genome architecture and ecotype differentiation of Brassica napus. *Nature Plants*, *6*(1), 34–45. https://doi.org/10.1038/s41477-019-0577-7

Sparrow, P. A. C., Townsend, T. M., Arthur, A. E., Dale, P. J., & Irwin, J. A. (2004). Genetic analysis of Agrobacterium tumefaciens susceptibility in Brassica oleracea. *Theoretical and Applied Genetics*, *108*(4), 644–650. https://doi.org/10.1007/s00122-003-1473-z

Staswick, P. E., Tiryaki, I., & Rowe, M. L. (2002). Jasmonate response locus JAR1 and several related Arabidopsis genes encode enzymes of the firefly luciferase superfamily that show activity on jasmonic, salicylic, and indole-3-acetic acids in an assay for adenylation. *The Plant Cell*, *14*(6), 1405–1415. https://doi.org/10.1105/tpc.000885

Stefanato, F. L., Abou-Mansour, E., Buchala, A., Kretschmer, M., Mosbach, A., Hahn, M., Bochet, C. G., Métraux, J. P., & Schoonbeek, H. J. (2009). The ABC transporter BcatrB from Botrytis cinerea exports camalexin and is a virulence factor on Arabidopsis thaliana. *Plant Journal*, *58*(3), 499–510.

https://doi.org/10.1111/j.1365-313X.2009.03794.x

Stotz, H. U., Mitrousia, G. K., de Wit, P. J. G. M., & Fitt, B. D. L. (2014). Effector-triggered defence against apoplastic fungal pathogens. In *Trends in Plant Science* (Vol. 19, Issue 8, pp. 491–500). https://doi.org/10.1016/j.tplants.2014.04.009

Suza, W. P., & Staswick, P. E. (2008). The role of JAR1 in Jasmonoyl-L: -isoleucine production during Arabidopsis wound response. *Planta*, *227*(6), 1221–1232. https://doi.org/10.1007/s00425-008-0694-4

Takagi, H., Abe, A., Yoshida, K., Kosugi, S., Natsume, S., Mitsuoka, C., Uemura, A., Utsushi, H., Tamiru, M., Takuno, S., Innan, H., Cano, L. M., Kamoun, S., & Terauchi, R. (2013). QTL-seq: Rapid mapping of quantitative trait loci in rice by whole genome resequencing of DNA from two bulked populations. *Plant Journal*, *74*(1), 174–183. https://doi.org/10.1111/tpj.12105

Takken, F. L., Albrecht, M., & Tameling, W. Il. (2006). Resistance proteins: molecular switches of plant defence. In *Current Opinion in Plant Biology* (Vol. 9, Issue 4, pp. 383–390). https://doi.org/10.1016/j.pbi.2006.05.009

Tang, D., Ade, J., Frye, C. A., & Innes, R. W. (2005). Regulation of plant defense responses in Arabidopsis by EDR2, a PH and START domain-containing protein. *The Plant Journal*, *44*(2), 245–257. https://doi.org/doi:10.1111/j.1365-313X.2005.02523.x

Tang, D., Ade, J., Frye, C. A., & Innes, R. W. (2006). A mutation in the GTP hydrolysis site of Arabidopsis dynamin-related protein 1E confers enhanced cell death in response to powdery mildew infection. *The Plant Journal : For Cell and Molecular Biology*, *47*(1), 75–84. https://doi.org/10.1111/j.1365-313X.2006.02769.x

Tang, D., & Zhou, J.-M. (2015). PEPRs spice up plant immunity. *The EMBO Journal*, *35*(1), 4–5. https://doi.org/10.15252/embj.201593434

Tekaia, F., & Latgé, J. P. (2005). Aspergillus fumigatus: Saprophyte or pathogen? *Current Opinion in Microbiology*, *8*(4), 385–392. https://doi.org/10.1016/j.mib.2005.06.017

Tian, S., Wang, X., Li, P., Wang, H., Ji, H., Xie, J., Qiu, Q., Shen, D., & Dong, H. (2016).

Plant aquaporin AtPIP1;4 links apoplastic H2O2 induction to disease immunity pathways. *Plant Physiology*, *171*(3), 1635–1650. https://doi.org/10.1104/pp.15.01237

Tian, Y., Fan, M., Qin, Z., Lv, H., Wang, M., Zhang, Z., Zhou, W., Zhao, N., Li, X., Han, C., Ding, Z., Wang, W., Wang, Z. Y., & Bai, M. Y. (2018). Hydrogen peroxide positively regulates brassinosteroid signaling through oxidation of the BRASSINAZOLE-RESISTANT1 transcription factor. *Nature Communications*, *9*(1). https://doi.org/10.1038/s41467-018-03463-x

Ton, J., Van Pelt, J. A., Van Loon, L. C., & Pieterse, C. M. J. (2002). Differential effectiveness of salicylate-dependent and jasmonate/ethylene-dependent induced resistance in Arabidopsis. *Molecular Plant-Microbe Interactions*, *15*(1), 27–34. https://doi.org/10.1094/MPMI.2002.15.1.27

Trick, M., Adamski, N. M., Mugford, S. G., Jiang, C. C., Febrer, M., & Uauy, C. (2012). Combining SNP discovery from next-generation sequencing data with bulked segregant analysis (BSA) to fine-map genes in polyploid wheat. *BMC Plant Biology*, *12*. https://doi.org/10.1186/1471-2229-12-14

Tripathy, B. C., & Oelmüller, R. (2012). Reactive oxygen species generation and signaling in plants. *Plant Signaling & Behavior*, *7*(12), 1621–1633. https://doi.org/10.4161/psb.22455

Tudor, E. H., Jones, D. M., He, Z., Bancroft, I., Trick, M., Wells, R., Irwin, J. A., & Dean, C. (2020). QTL-seq identifies BnaFT.A02 and BnaFLC.A02 as candidates for variation in vernalization requirement and response in winter oilseed rape ( Brassica napus ) . *Plant Biotechnology Journal*, 0–2. https://doi.org/10.1111/pbi.13421

Untergasser, A., Nijveen, H., Rao, X., Bisseling, T., Geurts, R., & Leunissen, J. A. M. (2007). Primer3Plus, an enhanced web interface to Primer3. *Nucleic Acids Research*, *35*(SUPPL.2), 71–74. https://doi.org/10.1093/nar/gkm306

Veluchamy, S., Hind, S. R., Dunham, D. M., Martin, G. B., & Panthee, D. R. (2014). Natural variation for responsiveness to flg22, flgII-28, and csp22 and Pseudomonas syringae pv. tomato in heirloom tomatoes. *PLoS ONE*, *9*(9), 1–12. https://doi.org/10.1371/journal.pone.0106119

Vermeulen, T., Schoonbeek, H., & De Waard, M. A. (2001). The ABC transporter BcatrB from Botrytis cinerea is a determinant of the activity of the phenylpyrrole fungicide fludioxonil. *Pest Management Science*, *57*(5), 393–402. https://doi.org/10.1002/ps.309

Voorrips, R. E. (2002). Mapchart: Software for the graphical presentation of linkage maps and QTLs. *Journal of Heredity*, *93*(1), 77–78. https://doi.org/10.1093/jhered/93.1.77

Vorwerk, S., Schiff, C., Santamaria, M., Koh, S., Nishimura, M., Vogel, J., Somerville, C., & Somerville, S. (2007). EDR2 negatively regulates salicylic acid-based defenses and cell death during powdery mildew infections of Arabidopsis thaliana. *BMC Plant Biology*, *7*, 35. https://doi.org/10.1186/1471-2229-7-35

Walley, P. G., Carder, J., Skipper, E., Mathas, E., Lynn, J., Pink, D., & Buchanan-Wollaston, V. (2012). A new broccoli × broccoli immortal mapping population and framework genetic map: Tools for breeders and complex trait analysis. *Theoretical and Applied Genetics*, *124*(3), 467–484. https://doi.org/10.1007/s00122-011-1721-6

Wan, W. L., Zhang, L., Pruitt, R., Zaidem, M., Brugman, R., Ma, X., Krol, E., Perraki, A., Kilian, J., Grossmann, G., Stahl, M., Shan, L., Zipfel, C., van Kan, J. A. L., Hedrich, R., Weigel, D., Gust, A. A., & Nürnberger, T. (2019). Comparing Arabidopsis receptor kinase and receptor protein-mediated immune signaling reveals BIK1-dependent differences. *New Phytologist*, *221*(4), 2080–2095. https://doi.org/10.1111/nph.15497

Wang, H., Cheng, H., Wang, W., Liu, J., Hao, M., Mei, D., Zhou, R., Fu, L., & Hu, Q. (2016). Identification of BnaYUCCA6 as a candidate gene for branch angle in Brassica napus by QTL-seq. *Scientific Reports*, *6*(December), 1–10. https://doi.org/10.1038/srep38493

Wang, X., Long, Y., Wang, N., Zou, J., Ding, G., Broadley, M. R., White, P. J., Yuan, P., Zhang, Q., Luo, Z., Liu, P., Zhao, H., Zhang, Y., Cai, H., King, G. J., Xu, F., Meng, J., & Shi, L. (2017). Breeding histories and selection criteria for oilseed rape in Europe and China identified by genome wide pedigree dissection. *Scientific Reports*, *7*(1), 1916. https://doi.org/10.1038/s41598-017-02188-z

Wang, X. X., Wang, H. H. H., Wang, J. J. J., Sun, R., Wu, J., Liu, S., Bai, Y., Mun, J.-H., Bancroft, I., Cheng, F., Huang, S. S., Li, X., Hua, W., Wang, J. J. J., Wang, X. X., Freeling, M., Pires, J. C., Paterson, A. H., Chalhoub, B., … Zhang, Z. (2011). The genome of the mesopolyploid crop species Brassica rapa. *Nature Genetics*, *43*(10), 1035–1039. https://doi.org/10.1038/ng.919

Wang, Z.-Y. (2012). Brassinosteroids modulate plant immunity at multiple levels. *Proceedings of the National Academy of Sciences*, *109*(1), 7–8. https://doi.org/10.1073/pnas.1118600109

Warnke, S. E., Douches, D. S., & Branham, B. E. (1998). Isozyme analysis supports allotetraploid inheritance in tetraploid creeping bentgrass (Agrostis palustris Huds.). *Crop Science*, *38*(3), 801–805. https://doi.org/10.2135/cropsci1998.0011183X003800030030x

Wasternack, C. (2007). Jasmonates: An Update on Biosynthesis, Signal Transduction and Action in Plant Stress Response, Growth and Development. *Annals of Botany*, *100*(4), 681–697. https://doi.org/10.1093/aob/mcm079

Wei, L., Jian, H., Lu, K., Filardo, F., Yin, N., Liu, L., Qu, C., Li, W., Du, H., & Li, J. (2016). Genome-wide association analysis and differential expression analysis of resistance to Sclerotinia stem rot in Brassica napus. *Plant Biotechnology Journal*, *14*(6), 1368–1380. https://doi.org/10.1111/pbi.12501

Wells, R., Trick, M., Soumpourou, E., Clissold, L., Morgan, C., Werner, P., Gibbard, C., Clarke, M., Jennaway, R., & Bancroft, I. (2014). The control of seed oil polyunsaturate content in the polyploid crop species Brassica napus. *Molecular Breeding*, *33*(2), 349–362. https://doi.org/10.1007/s11032-013-9954-5

Wickham, H. (2016). ggplot2: elegant graphics for data analysis. In *Journal of the Royal Statistical Society: Series A (Statistics in Society)* (Vol. 174, Issue 1). Springer International Publishing. https://doi.org/10.1007/978-3-319-24277-4

Williamson, B., Tudzynski, B., Tudzynski, P., & Van Kan, J. A. L. (2007). Botrytis cinerea: The cause of grey mould disease. In *Molecular Plant Pathology* (Vol. 8, Issue 5, pp. 561–580). https://doi.org/10.1111/j.1364-3703.2007.00417.x

Wu, L., Chen, H., Curtis, C., & Fu, Z. Q. (2014). Go in for the kill. How plants deploy effector-triggered immunity to combat pathogens. *Virulence*, *5*(7), 710–721.

https://doi.org/10.4161/viru.29755

Xia, X. J., Zhou, Y. H., Shi, K., Zhou, J., Foyer, C. H., & Yu, J. Q. (2015). Interplay between reactive oxygen species and hormones in the control of plant development and stress tolerance. *Journal of Experimental Botany*, *66*(10), 2839–2856. https://doi.org/10.1093/jxb/erv089

Yasuda, M., Ishikawa, A., Jikumaru, Y., Seki, M., Umezawa, T., Asami, T., Maruyama-Nakashita, A., Kudo, T., Shinozaki, K., Yoshida, S., & Nakashita, H. (2008). Antagonistic interaction between systemic acquired resistance and the abscisic acid-mediated abiotic stress response in Arabidopsis. *Plant Cell*, *20*(6), 1678–1692. https://doi.org/10.1105/tpc.107.054296

Yunde Zhao. (2010). Auxin biosynthesis and its role in development. *Annu Rev Plant Biol.*, *2*(61), 49–64. https://doi.org/10.1146/annurev-arplant-042809-112308.Auxin

Zhang, X., Peng, G., Kutcher, H. R., Balesdent, M. H., Delourme, R., & Fernando, W. G. D. (2016). Breakdown of Rlm3 resistance in the Brassica napus–Leptosphaeria maculans pathosystem in western Canada. *European Journal of Plant Pathology*, *145*(3), 659–674. https://doi.org/10.1007/s10658-015-0819-0

Zheng, Z., Qamar, S. A., Chen, Z., & Mengiste, T. (2006). Arabidopsis WRKY33 transcription factor is required for resistance to necrotrophic fungal pathogens. *Plant Journal*, *48*(4), 592–605. https://doi.org/10.1111/j.1365-313X.2006.02901.x

Zipfel, C. (2014). Plant pattern-recognition receptors. *Trends in Immunology*, *35*(7), 345–351. https://doi.org/10.1016/j.it.2014.05.004

Zipfel, C., Kunze, G., Chinchilla, D., Caniard, A., Jones, J. D. G., Boller, T., & Felix, G. (2006). Perception of the Bacterial PAMP EF-Tu by the Receptor EFR Restricts Agrobacterium-Mediated Transformation. *Cell*, *125*(4), 749–760. https://doi.org/10.1016/j.cell.2006.03.037

Zipfel, C., Robatzek, S., Navarro, L., Oakeley, E. J., Jones, J. D. G., Felix, G., & Boller, T. (2004). Bacterial disease resistance in Arabidopsis through flagellin perception. *Nature*, *428*(6984), 764–767. https://doi.org/10.1038/nature02485

Zou, C., Wang, P., & Xu, Y. (2016). Bulked sample analysis in genetics, genomics and crop improvement. *Plant Biotechnology Journal*, *14*(10), 1941–1955. https://doi.org/10.1111/pbi.12559

Zou, J., Mao, L., Qiu, J., Wang, M., Jia, L., Wu, D., He, Z., Chen, M., Shen, Y., Shen, E., Huang, Y., Li, R., Hu, D., Shi, L., Wang, K., Zhu, Q., Ye, C., Bancroft, I., King, G. J., … Fan, L. (2019). Genome-wide selection footprints and deleterious variations in young Asian allotetraploid rapeseed. *Plant Biotechnology Journal*, *17*(10), 1998–2010. https://doi.org/10.1111/pbi.13115

## *Appendix*

**Appendix A**

Data quality summary table – Sequencing data information.

**Appendix B**

Genotyping results of KASP markers.

**Appendix C**

Variations have effect on *BnaA01g02190D* with computed BFR values

**Table C -** Annotation and Effect prediction of 106 variations on ChrA01 have predicted effect on BnaA01g02190D with their corresponding locations on Darmor-*bzh* genome and computed bulk frequency ratio (BFR AO & BFR RO) values for High NLP and High flg22 phenotype (AO: counts of Alternative (Alt) variation, RO: counts of Reference (Ref) variation).

**Appendix D**

QTLs obtained with Multiple QTL Mapping (MQM) analysis that significantly associated with interested traits on *B. oleracea* genome

**Table D -** QTLs associated with ROS responses against various concentrations of flg22 & elf18 PAMP molecules in control and drought conditions and QTLs associated with the induced traits – Fold Change (FC) in ROS response and difference between the lesion sizes of B. cinerea infection (delta) in comparison to control with genome-wide $\alpha \leq 0.05$. The locations of the QTLs with increased genotype and linked amplified fragment length polymorphism (AFLP) and restriction fragment length polymorphism (RFLP) markers are represented. LOD scores are coloured in Green – Yellow -Red colour scale according to their decreasing values from Green to Red. (Tables are generated by Dr. Peter Walley from Liverpool University with data generated in this PhD study).